

AD-A086 112

TECHNICAL
LIBRARY

AD-A086 112

MEMORANDUM REPORT ARBRL-MR-03013

INERTIAL DESPIN MOMENT MEASUREMENTS
OF A CANTED LOOSE RING DURING
SPIN AND NUTATION

Clarence C. Bush

April 1980



US ARMY ARMAMENT RESEARCH AND DEVELOPMENT COMMAND
BALLISTIC RESEARCH LABORATORY
ABERDEEN PROVING GROUND, MARYLAND

Approved for public release; distribution unlimited.

DTIC QUALITY INSPECTED 3

Destroy this report when it is no longer needed.
Do not return it to the originator.

Secondary distribution of this report by originating
or sponsoring activity is prohibited.

Additional copies of this report may be obtained
from the National Technical Information Service,
U.S. Department of Commerce, Springfield, Virginia
22151.

The findings in this report are not to be construed as
an official Department of the Army position, unless
so designated by other authorized documents.

*The use of trade names or manufacturers' names in this report
does not constitute indorsement of any commercial product.*

REPORT DOCUMENTATION PAGE		READ INSTRUCTIONS BEFORE COMPLETING FORM
1. REPORT NUMBER MEMORANDUM REPORT ARBRL-MR-03013	2. GOVT ACCESSION NO.	3. RECIPIENT'S CATALOG NUMBER
4. TITLE (and Subtitle) INERTIAL DESPIN MOMENT MEASUREMENTS OF A CANTED LOOSE RING DURING SPIN AND NUTATION		5. TYPE OF REPORT & PERIOD COVERED Final
		6. PERFORMING ORG. REPORT NUMBER
7. AUTHOR(s) Clarence C. Bush		8. CONTRACT OR GRANT NUMBER(s)
9. PERFORMING ORGANIZATION NAME AND ADDRESS U.S. Army Ballistic Research Laboratory (ATTN: DRDAR-BLL) Aberdeen Proving Ground, Maryland 21005		10. PROGRAM ELEMENT, PROJECT, TASK AREA & WORK UNIT NUMBERS RDT&E 1L662618AH80
11. CONTROLLING OFFICE NAME AND ADDRESS U.S. Army Armament Research & Development Command U.S. Army Ballistic Research Laboratory (ATTN: DRDAR-BL) Aberdeen Proving Ground, MD 21005		12. REPORT DATE April 1980
		13. NUMBER OF PAGES 88
14. MONITORING AGENCY NAME & ADDRESS (if different from Controlling Office)		15. SECURITY CLASS. (of this report) UNCLASSIFIED
		15a. DECLASSIFICATION/DOWNGRADING SCHEDULE
16. DISTRIBUTION STATEMENT (of this Report) Approved for public release, distribution unlimited.		
17. DISTRIBUTION STATEMENT (of the abstract entered in Block 20, if different from Report)		
18. SUPPLEMENTARY NOTES		
19. KEY WORDS (Continue on reverse side if necessary and identify by block number) Internal component looseness Projectiles <i>trajectory</i> Stability (Gyroscopic) <i>spin</i>		
20. ABSTRACT (Continue on reverse side if necessary and identify by block number) Experiments were made on a loose ring model in a spin fixture to check the validity of the theory that predicts the effect of a loose internal component on the flight behavior of spinning and nutating projectiles. The inertial despin moment of the loose ring was obtained by recording the spin rate versus time. During the test, the complete model was allowed to decelerate freely in spin while it was held at discrete coning angles between		

20. ABSTRACT (Continued).

zero and 20 degrees and discrete nutation rates between zero and 600 RPM. The anticipated spin rate at the start of each spin-down was 6,500 RPM; however, sufficient spin power was not always available.

Four loose rings, having 0.004, 0.012, 0.0225 and 0.040 radian cant angle clearance, were tested. The important polar angle relationship between the cant plane of the loose ring and the yaw plane of the projectile during spin-downs could not be measured. This experimental inadequacy resulted in an insufficient validation of the theory.

Initially, in the absence of the cant-plane phase angle measurement, the correlation between theory and experiment was made by assuming a phase angle of 45 degrees. This correlation, made at a spin rate of 3,000 RPM, indicated a general support of the theory by the experiments. The test results, in conjunction with the spin theory, were also used for computation of the loose ring phase angles that existed during the spin-downs. These results indicate an average phase lag angle of approximately 30 degrees, although large variations were observed with spin rate during the spin downs. Averaged phase angles from three flight tests were 34.0, 29.0, and 24.4 degrees.

TABLE OF CONTENTS

	<u>Page</u>
LIST OF ILLUSTRATIONS	5
LIST OF TABLES	6
I. BACKGROUND	7
II. THEORY	8
III. THEORETICAL MODEL	8
IV. EXPERIMENTAL APPROACH TO VERIFYING THE THEORY	9
V. TEST FIXTURE	10
VI. SPIN MODEL	10
VII. INSTRUMENTATION	11
VIII. TEST PROCEDURE	12
IX. TEST RESULTS	12
X. DATA REDUCTION	12
XI. RESULTS	13
XII. DATA ANALYSIS	15
XIII. EXPERIMENTAL ACCURACY	18
XIV. EXPERIMENTAL PROBLEMS	19
XV. CONCLUSIONS	21
ACKNOWLEDGEMENT	21
REFERENCES	61
LIST OF SYMBOLS	63
APPENDIX A: COMPUTED CANT-PLANE PHASE ANGLES DURING SPIN-DOWNS	65
APPENDIX B: CONCEPT TECHNIQUE FOR MEASURING THE CANT- PLANE PHASE ANGLE	79
DISTRIBUTION LIST	87

LIST OF ILLUSTRATIONS

<u>Figure</u>		<u>Page</u>
1	Measured Spin History of the T317	22
2	Projectile with Canted Loose Ring	23
3	Computed Angular Motion of the T317 ($\gamma = 0$)	24
4	Computed Angular Motion of the T317 ($\gamma = .004$)	25
5	Computed Spin History of the T317	26
6	Spin Model and Fixture's Nutation Frame	27
	Photo 1. Spin Fixture	28
	Photo 2. Spin Hardware	29
7	Test Results from L.R. 1	30
	a. At 5 Degrees Coning Angle	30
	b. At 10 Degrees Coning Angle	31
	c. At 15 Degrees Coning Angle	32
	d. At 20 Degrees Coning Angle	33
8	Test Results from L.R. 2	34
	a. At 5 Degrees Coning Angle	34
	b. At 10 Degrees Coning Angle	35
	c. At 15 Degrees Coning Angle	36
	d. At 20 Degrees Coning Angle	37
9	Test Results from L.R. 3	38
	a. At 5 Degrees Coning Angle	38
	b. At 10 Degrees Coning Angle	39
	c. At 15 Degrees Coning Angle	40
	d. At 20 Degrees Coning Angle	41
10	Test Results from L.R. 4	42
	a. At 5 Degrees Coning Angle	42
	b. At 10 Degrees Coning Angle	43

LIST OF ILLUSTRATIONS (Continued)

<u>Figure</u>	<u>Page</u>
c. At 15 Degrees Coning Angle	44
d. At 20 Degrees Coning Angle	45
11 Example of Effect of Spin Coupling	46
12 Example of Effect of Loose Ring Axial Position	47
13 Example of Presumed Aberrant Test Results	48
14 Example of Presumed Limitation of Combined Variables	49
15 Example Spin-Down Showing Zero Spin Anomaly	50
16 Zero Coning Angle Test Results Conflict with Theory	51
a. At Coupled L.R. 1	51
b. At Coupled L.R. 2	52
c. At Coupled L.R. 3	53
d. At Coupled L.R. 4	54
e. At Uncoupled L.R. 1 Position 4 Inches Below Intersection of Axes	55
17 Computed Cant Plane Phase Angle vs. Cant Angle	56

LIST OF TABLES

<u>Table</u>	<u>Page</u>
1 Aerodynamic Coefficients for T317	57
2 Computed Flight Motions of T317	58
3 Physical Characteristics of Rings	59
4 Physical Characteristics of Complete Spin Models	59
5 Spin Rate vs. Inertial Despin Rate and Moment	60

I. BACKGROUND

Murphy¹ has presented a theory for predicting the dynamic flight behavior and range loss of projectiles having loose internal components. This author is indebted to Reference 1 for the following background information, which is intended to refresh the reader on the important features of that theory and to indicate the basis for assuming 45 degrees as the polar orientation angle, ϕ_γ , for the cant plane of the loose ring.

In 1955 four shell types exhibited unusual flight behavior which involved the movement of their internal parts. One of these projectiles, the 8-inch T-317, had several rings held by a central column. The rings were free to move with small but finite clearances and were not spin-coupled to remain in phase with the spin of the parent projectile. This shell showed large spin decays and significant range losses. In all cases small amplitude motions of the internal parts had significant effect on the parent shell's motion.

The actual spin histories of several T317's are given in Figure 1, which also shows the spin history for three T347's. The T347 shell has the same external shape, mass and moments of inertia as the T317, but has no movable internal components. In all observed cases, the T317, with its loose parts, had a greater spin loss and flew to a lesser range. The relative decrements between the range of each T317 shell and the average range of the T347's is shown in the figure. Thus, a spin loss of almost 4200 rpm was observed for a projectile that flew 11% short of its proper range.

Unfortunately, in-flight measurements of the yawing motion were not made. A range loss of 11% would, however, require an angular motion amplitude of 10-15 degrees.

The shell's internal construction is fairly complicated, but can be theoretically approximated by a single ring that is permitted to slide freely on a central shaft. The clearance is quite small but sufficient to allow the ring to cant to an angle as large as 0.004 radian. When the ring is fully canted, its center-of-mass is on the axis of the shell as shown in Figure 2. Hence, the ring exhibits zero eccentricity when fully canted. For theoretical purposes, the ring is assumed to spin without slippage. Also shown in Figure 2 are the sign conventions for the loose ring angular motions and moments.

1. C. H. Murphy, "Angular Motion of Projectiles with a Moving Internal Part", BRL Memorandum Report No. 2731, U.S. Army Ballistic Research Laboratory, Aberdeen Proving Ground, Maryland, February 1977. AD A037338.

II. THEORY

A means of predicting the effect of loose internal parts was seen as necessary for improving the predictability of the flight dynamics of those spinning projectiles that require a finite looseness of internal parts. With this predictability, the performance of new designs would become more reliable, and limiting clearances could then be specified with improved assurance.

A theory for the prediction of the influence of moving internal parts on the angular motion of spinning projectiles was developed at the U.S. Army Ballistic Research Laboratory by Charles H. Murphy in 1976. Several influencing parameters, governing the generation of the inertial despin moment, were proposed; the working relationship of Murphy's theory is the following spin equation:

$$I_x \dot{p}_b = A_{\ell_p} p_b - \dot{\phi}_1 \sin K_1 (I_{xc} p_b - I_{tc} \dot{\phi}_1) \gamma \sin \phi_\gamma$$

where

$I_x \dot{p}_b$ = the total despin moment of the projectile, ft lb

$A_{\ell_p} p_b$ = the aerodynamic despin moment of the projectile, ft lb

$\dot{\phi}_1 \sin K_1 (I_{xc} p_b - I_{tc} \dot{\phi}_1) \gamma \sin \phi_\gamma$ = the despin moment due to the inertial effect of the loose internal component, ft lb

III. THEORETICAL MODEL

When the spin theory was being developed it was predicted that the coning angle, K_1 , would grow to some equilibrium value early in the projectile's flight and this equilibrium value could then be used to give the spin moment. A theoretical model of the T317 was based on the assumption that it has values of γ and ϕ_γ , such that its fast-mode motion grows to 10-15 degrees and causes the observed spin-down and range loss.

Computer runs were made and, although the complete set of aerodynamic coefficients were not well known for this shell, nominal values were used. These nominal values, indicated in Table 1 for $\gamma = 0$, produced the usual small-amplitude, slow-mode, limit-cycle yawing motion which is frequently observed. A typical result of this computation is shown in Figure 3.

Computer runs were then made for $\gamma = 0.004$ radian and $\phi_\gamma = 45$ degrees. The result was a rapid growth of the fast-mode angular motion to about 18 degrees and a decay on the down-leg of the trajectory. A range loss of 11% was computed. The computer spin-down was as large as the observed spin-down, but different in detail. Thus, it is assumed that the actual angular motion grew slower than computed, but reached a larger maximum value. These results are shown in Figures 4 and 5 and are summarized in Table 2.

IV. EXPERIMENTAL APPROACH TO VERIFYING THE THEORY

A projectile payload simulation was tested in a spin fixture to measure the effect of a loose ring on the despin rate over the anticipated ranges of the dependent variables of the theory. The difference between the spin-down rates of the loose ring configurations and the corresponding rigid model configuration was used for computing the inertial despin moment resulting from an internal component being loosely held.

We also computed the theoretical inertial despin moment for the corresponding configurations for comparison with the inertial despin moments from the spin fixture experiments. This is a first effort at verifying Murphy's theory by ground-based experimental means.

In the free-flight projectile case, the kinetic energy from the loss of spin is translated into an increased magnitude of the coning angle and eventually into increased drag and reduced range.

The test fixture, however, holds the spinning model at constant coning angle and nutation rate during the spin-downs. Thus, without strain gage or other types of force and moment measurements being available for measurement of the gyroscopic force that is developed on the support shaft by the loose ring, the only useful measurements were the spin and nutation rates versus time as the model was permitted to coast down in spin.

The experiments were designed to individually investigate the influence of all the theory's variables on the inertial despin moment; e.g., cant angle, coning angle, spin rate, and nutation rate. The phase lag angle of the loose ring's cant plane was also to be measured but this was found to be too costly in time and effort. Additional tests were made on the effect of a spin decoupling of the loose ring and on the effect of the axial position of the loose ring relative to the intersection of the fixture's spin and coning axes. The ratio of the axial to the transverse moments of inertia of the loose ring was not investigated. This ratio will vary as the shape of the loose rings ranges from more tubular to more washer-like and the suggestion is made that such shape variations could influence the phase lag angle of the cant plane of the loose ring. Another possible influence on

the phase angle is whether the loose ring is positioned ahead of or behind (above or below in the fixture) the intersection of the spin and coning axes. For this test the loose rings were designed to have nearly the same moment of inertia in both the axial and the transverse planes.

No significance was placed on the relative orientations of the support shaft between the fixture test, where the shift is nearly vertical, and real life, where the projectile is more horizontal. This is to say that the effect of gravity on the loose rings motion is considered to be negligible. Also, for moment of inertia considerations, the loose ring was assumed not to cant.

V. TEST FIXTURE

A spin fixture² at the Weapon Systems Concepts Team's facility at Aberdeen Proving Ground-Edgewood Area has the capability for spin down testing of 8-inch diameter projectiles.

The end-bells of the subject spin model are held by cylindrical clevises which are separated from the fixture's nutation frame by ball-bearinged races. An air turbine is used to spin the model up to in excess of 6,000 rpm and an electric motor is used to rotate the model-holding frame at nutation rates up to 600 rpm. When zero coning angle is present, the model's spin axis is oriented vertically. The fixture can also be adjusted to hold the spin model for coning angles of 5, 10, 15, and 20 degrees, as shown in Figure 6 and Photograph 1. Sensors in the fixture measure the spin and nutation rates and provide inputs to the readout instrumentation.

A strain gage attached to the fixture's upper beam provides a measure of its load oscillations and was useful in indicating resonance conditions and the precision of the dynamic balancing adjustments made to the nutation frame each time the model configuration was changed.

The angular motion of the spin and nutation were both counter-clockwise when viewed from above, to agree with the standard angular motions developed by a projectile.

VI. SPIN MODEL

The simulated projectile hardware was designed to be extremely rigid and wear resistant. The solid support shaft was 21.75 inches long and 2.000 inches in diameter, as shown in Figure 6 and Photograph 2.

2. M. C. Miller, "Flight Stability Test Fixture for Non-Rigid Payloads", presented at the Chemical Systems Laboratory Technical Conference, 23-24 May 1978.

All parts were made from 4130 alloy steel heat-treated to 37-38 on Rockwell "C" scale. All surfaces were finely finished. Four each, $\frac{1}{4}$ -20 dog-ended set screws, that entered snugly into recesses in the shaft, were used to fix each part rigidly to the shaft. The loose rings, of course, were not rigidly anchored to the shaft in any way.

One rigid ring (tare ring) and four loose rings were fabricated. The physical characteristics of these rings are shown in Table 3.

The complete model physicals, including the shaft, end bells, base ring, anti-climb stop, and tare ring (or with any of the loose rings) are shown in Table 4.

The center-of-mass of the loose rings was positioned at the intersection of the fixture's spin and coning axes during most of the spin-downs to minimize the spin weight and tare moments of inertia and to encourage a full canting of the loose rings. An anti-climb stop was positioned on the shaft above the loose ring. Its vertical location was adjustable so that the clearance between the loose ring and the stop was only slightly greater than that required by the various loose rings when they were fully canted. Bending of the shaft was determined to be negligible.

For a limited number of spin-downs, loose ring number one was positioned with its center-of-mass 4 inches below the intersection of the fixture's spin and coning axes to investigate the possibility of the loose ring being inhibited from canting by the asymmetric centrifugal force distribution acting on it. It was then necessary to add a rigidly fixed balance ring, equal in all respects to the combination of the tare ring and the base ring. To attain a proper balance of the fixture, the center-of-mass of this balance ring was positioned $4\frac{1}{2}$ inches above the intersection of the spin and coning axes.

For the purpose of keeping the loose rings spinning at the same rate as the remainder of the spin model, a ball-ended dowel was anchored into one face of the base ring to connect with a cylindrical recess in each of the loose rings. Progressively larger diameter recesses were used in the loose rings, as the ring-to-shaft clearance increased, to preclude inhibiting the canting development. Reversing the base ring on the shaft permitted the spin drive to the loose ring to be disconnected. During these limited number of spin-downs, the spin of the loose ring was dependent upon only a frictional coupling.

VII. INSTRUMENTATION

The data acquisition and fixture control station was located behind a safety shield several feet from the spin fixture. The spin and nutation rates were recorded on a GOULD Model 2400 3-channel strip chart oscillograph. Angular velocity versus time traces resulted.

VIII. TEST PROCEDURE

During the experiments, after the model's configuration was established, the model was spun-up to approximately 6,500 rpm and then the nutation rate was brought up to the desired value. As the model was given nutation, the spin rate invariably experienced some decay because the spin motor had insufficient power to maintain the initial spin rate in the presence of the additional despin moment that was now being developed. Nutation rates were maintained constant at 600, 500, 400, 200, and zero rpm by manual control of the electric motor. When the test data were being acquired, the air supply to the spin motor was valved-off and the model was permitted to decelerate in spin. Spin-down runs were made with the tare ring and with each of the several loose rings. The loose ring runs were made between the tare ring runs and later repetitions of the tare ring runs.

IX. TEST RESULTS

Typically, the spin-down tare and loose ring results were smooth traces asymptotically approaching zero. The nutation rate traces were constant value during the 30 to 180 second spin-downs, with the loose ring configurations taking the shorter time to despin.

The deceleration data were locally averaged spin-versus-time slopes tangential at each 500 rpm increment in the spin rate. Identical manual data reading processes were used for the tare and related loose ring runs. The manually read slope data were plotted versus spin rate to insure reasonable slope measurements. However, in all cases, the unfaired data were used for the computation of the experimental despin moments to preclude any tendency to bias the raw data.

Early in the test it was discovered that reruns of identical configurations did not repeat very well. The reruns generally resulted in a more rapid spin-down to indicate a gradual degradation of the fixture's performance. Therefore the tare runs were repeated after the completion of the loose ring runs to provide a bracketing of the loose ring runs by the tare runs. This permitted a weighted-average technique to be used for the tare runs when the test results were reduced. A total of 285 spin-downs were made, but some were problem investigations or photographic attempts and thus did not contribute to the test results.

X. DATA REDUCTION

A FORTRAN program was devised for computing the despin rate at each 500 rpm increment of spin, for computing the resulting experimental tare and loose ring despin moments, for weight-averaging

selected tare despin moments, for computing the predicted theoretical inertial despin moments, and for taking the difference between the predicted and experimental inertial despin moments. The theoretical predictions were based on the theory as described previously and the computation of the experimental data followed the formulation shown below:

$$M_{I_{LR}} = M_{LR} - M_R ;$$

at spin rates of 6000, 5500, 5000, 4500, 4000 0 rpm.

Computations were made for all selected conditions of spin, coning angle, nutation rate, cant angle, coupled and uncoupled loose rings and for two axial positions of the center-of-mass of the loose ring relative to the intersection of the fixture's spin and coning axes. (In one case the center-of-mass of the loose ring was at the intersection of the fixture's spin and coning axes. In the other case it was 4 inches below.)

Subsequently, hand-made multi-colored cross-plot families of various kinds were made. The theoretical and experimental data were plotted on the same page to improve the visualization of the complete body of results. The patterns formed by these cross-plotted results showed the influence of the specific variables and, in some instances, indicated the limiting extent of their useful range.

XI. RESULTS

The raw despin data, in the form of traces of spin rate versus time, are too extensive for presentation. Somewhat less voluminous are the computed individual spin-down runs of tare despin moment, total despin moment, and inertial despin moment versus spin rate. Because of the variety and magnitudes of the experimental digressions from the theoretical predictions, and without an adequate means available for properly describing those variations, the computed results of the individual spin-downs are presented as an LFD Internal Memorandum with limited distribution. The computed results for the individual runs, having been converted to inertial despin moment, are readily available there for comparison with other experimental results, if additional testing is done. These individual run tabulated results are organized in the format of four related runs on each page. The corresponding graphs are presented in similar fashion.

The body of the report shows cross-plot data for the four loose rings at various configurations and test conditions. An arbitrary selected spin rate of 3000 rpm was used for this presentation as a means of reducing the number of plots presented. While considerably less than the average spin rate of the T317 projectile, this

selection of 3,000 rpm appeared to be the highest spin rate suitable to all the test configurations, without a requirement for certain extrapolations of the test results. However, the selection of a single representative spin rate does imply a linear variation of the experimental inertial despin moment with spin rate; a condition that existed only approximately.

The theoretical predictions of inertial despin moment and the corresponding experimental results for each of the four coupled loose rings are plotted versus nutation rate at each of four coning angles in Figures 7a through 10d for the case where the center-of-mass of the loose ring is at the intersection of the fixture's spin and coning axes. These sixteen plots are the condensed version of the main body of the effort at verifying the theory by experimental means. Coupled loose ring number two produced the experimental results that agreed closest with the theoretical predictions. Some cross-plots, using faired values of the inertial despin moment versus spin rate, were made to see if a substantial improvement in the appearance of the cross-plots would ensue. Since this trial exercise did not indicate a substantial improvement, the unfaired results are the only ones presented.

The T317 projectile originally did not have a spin coupling between its loose rings and the body of the shell. Later, the projectile was modified to incorporate that coupling, so a limited number of tests were made with an uncoupled loose ring configuration. One of these tests is shown in Figure 11 for loose ring number two at a coning angle of 20 degrees for the coupled and uncoupled loose rings both positioned at the intersecting axes of the fixture. This presentation of inertial despin moment versus nutation rate indicates a smaller inertial despin moment when the loose ring is uncoupled.

Figure 12 compares a case where the center-of-mass of the uncoupled loose ring is at the intersection of the fixture's spin and coning axes and another case where it is axially displaced 4 inches down the shaft. This presentation is for uncoupled loose ring number one at a coning angle of 20 degrees.

One of the most striking anomalies of the test occurred with coupled loose ring number one. The spin-downs at all nutation rates at a coning angle of five degrees invariably produced excessive inertial despin moments, while at a coning angle of 15 degrees essentially zero inertial despin moment was developed at all nutation rates. A particularly graphic example is shown in Figure 13 for the coupled loose ring number one at a nutation rate of 500 rpm.

Figure 14, inertial despin moment versus cant angle, is presented to demonstrate the loss of agreement between theory and experiment that can result as the nutation rate is increased.

Table 5 and Figure 15 are presented to show an example of the computation format and the machine graphs that were made for all the spin-down runs.

Many spin-down runs were made at zero coning angle on each of the loose rings in an effort to investigate the resulting unexpected inertial despin moment statistically. These results at nutation rates of 600, 500, 400, and 200 rpm evidenced large inertial despin moment with increased nutation rate and increases in the magnitude of the cant angle. The inertial despin moment versus the spin rate, with all the nutation rate data, is presented in Figures 16a through 16e for the coupled and uncoupled loose rings positioned both at the axes intersection and 4 inches below.

A different kind of data presentation is made in Figure 17, where test results from the spin fixture are compared with results from free-flight tests through the medium of the computed phase angle, using the theoretical spin equation as the basis for the computations. The detailed test results from all the useful spin-downs are shown in Appendix A in the form of the computed cant plane phase angle.

XII. DATA ANALYSIS

The ground-based experiments, in a general way, reflect the theoretical predictions and provide a qualitative support of the loose ring theory. Since the cant-plane phase angle could not be measured during the spin-downs, it is not possible to make a rigorous analysis of the results of the spin fixture tests and to produce an accurate assessment of the quality of the verification. What can be done is to discuss the useful results and point out certain abnormal circumstances and experimental problem areas.

When it was decided that it would be too costly in time and effort to attempt to obtain a direct measurement of the cant-plane phase angle during the spin-downs, the decision was made to assume 45 degrees for that angle so that there would be some theoretical predictions for comparison with the experimental results. This comparison would be made through the medium of the inertial despin moment.

Some examples of reasonable agreement between theory and experiment are shown in Figures 8a through 8d, but the correlations shown in Figures 7a through 7d and 9a through 10d are less satisfactory. Postulations are made in the following paragraphs of this section concerning possible reasons for the less satisfactory results.

Among the four loose rings, coupled loose ring number two, with its three-times-normal cant angle, was found to provide the most orderly results. This is probably because, compared to loose ring number one, it produced a larger difference between the loose ring

despin results and the tare ring despin results without encountering the problems of excess associated with rings three and four with their much larger shaft clearances. That the loose ring two results also appeared to have the best agreement with the theoretical predictions could have been due to a fortunate relationship between the assumed 45 degree cant-plane phase angle, used for making the inertial despin moment predictions, and the average cant-plane phase angle actually experienced by that loose ring during the tests. See Figure B3.

The phase angle is determined by the detailed interaction between the projectile and its loose ring(s) and these detailed interactions are not known for the model loose rings that were tested. The cant angle was expected to range from 30 to 45 degrees, varying with configurational changes of the model and with test conditions.

The smaller inertial despin moment by the uncoupled loose ring of Figure 11 is considered to result from the relatively ineffective frictional spin coupling between the loose ring and the base ring. This ineffective coupling would not guarantee the loose ring reaching full spin before the coast-down is begun. Also, the uncoupled loose ring may encounter periods of super-spin later in the spin-down. Subspin is expected to result in a reduced inertial despin moment and super-spin is expected to produce an excessive inertial despin moment, unless the phase angle also changes sufficiently to disrupt the results.

The Figure 12 results for loose ring number one show a particularly low experimental inertial despin moment for an uncoupled loose ring positioned at the axes intersection of the fixture and a much larger experimental inertial despin moment for the same ring when it is axially displaced by 4 inches. In both cases the coning angle is 20 degrees and the spin rate is 3,000 rpm. Only a limited amount of experimental data were acquired to study the effect of the axial position of the loose ring and none of the experiments included loose rings that were spin-coupled. The data of Figure 12, while not conclusive, indicate a larger inertial despin moment when the ring is axially displaced. This suggests that some loose ring activity other than full canting could exist when the center-of-mass of the loose ring is not at the intersection of the spin and coning axes. The gyroscopic force acting on a loose ring, positioned with its center-of-mass at the intersection of its spin and coning axes, produces a pure couple on the loose ring which tends to make it cant. When the loose ring is axially displaced, a radially outward force distribution is added to the couple. This outward-directed force may inhibit the canting of the loose ring and a planetary type motion (probably "hula hooping") could result. Figure 12 indicates that a 4 inch displacement of the 4 inch height loose ring does in fact alter the motion of the ring and suggests that a "hula hoop" type loose ring motion, if present, is more effective than canting in the generation of inertial despin moment.

The reason for the gross divergence between prediction and experiment shown in Figure 13 is not known. It appears that the loose ring motion and its resulting effect is damped at a coning angle of 15 degrees and reinforced at a coning angle of 5 degrees. This suggests that a resonance interaction exists between the fixture and the loose ring. In this worst case result, it would have been particularly interesting to have been able to make spin-downs at, say, 4, 6, 14, and 16 degree coning angles. That experiment could have provided the clues necessary for determining the reason for the poor correlation between theory and experiment at those conditions. However, the test was over before the discrepancy was known. Also, the fixture does not have provisions for small coning angle variations, so it was not possible to investigate further.

Figure 14 indicates a loss of correlation between theory and experiment as the nutation rate is increased. This change appears to be gradual. Similar results sometimes occur when the coning angle or cant angle (in the presence of larger magnitudes of the other variables) is increased beyond some limiting value. When a "critical combination" of the magnitudes of the variables exists, a theoretical motion of the loose ring is established that the loose ring is unable to follow. The spin and nutation rates appear to have more influence than the coning and cant angles on this hypothesized limitation of the motion amplitude of the loose ring.

Figure 15 shows an anomaly at a spin rate of zero. The predicted inertial despin moment goes negative while the experimental inertial despin moment must always be zero at zero spin rate. No significance should be given this discrepancy with the theory because spin stabilized projectiles will never reach the zero spin rate conditions during their flight.

A final discrepancy between the theory and the experiments is indicated in Figures 16a through 16e where the inertial despin moment is presented versus the spin rate for the four loose rings at a coning angle of zero. These data are presented as the limiting experimental values from despin runs at 200, 400, 500, and 600 rpm nutation rate. According to the theory, no inertial despin moment should be developed when the coning angle is zero. Again, no emphasis should be placed on this anomalous result, even though the indicated inertial despin moment can be quite large, because a coning angle of zero would never be encountered by a real-life projectile. It would have been interesting to have fabricated a tare ring with the hole off-center so that a measure of the despin effect from a known spin unbalance could have been obtained to see how it might compare with the despin effect from suspected "hula-hooping".

Table 2, developed from measurements made by on-board sunsondes and relayed to ground-based data acquisition equipment by on-board telemetry units, presents the computed phase angle developed by loose

rings of known geometry. Guns of different twist were used in these 8-inch projectile tests and the three projectiles included two different loose ring cant angle configurations. A useful technique for assessing the validity of the free flight results of these projectile firings was to make the spin, coning angle and nutation rate histories and insert that information into the theoretical spin equation for computation of the phase lag angles of the loose ring cant plant (assuming all rings of one projectile canted at the same phase angle as the flight progressed). Data were available for this purpose at five-second intervals.

Now, if the computed phase angles were found to fall between zero and 90 degrees ($\sin \phi_\gamma$ between zero and +1), then the results would be considered reasonable. That the sine of the phase angle was determined to range from 0.38 to 0.62 (between 22 and 38 degrees) while the spin rate was ranging from 8100 down to 1560 rpm and the coning angle from 3 up to 42 degrees was indeed encouraging.

If the ground-based experiments could be determined to provide similar results, a further substantiation of the theory would be obtained. The ground-based experiments included results at coning angles of from 5 to 20 degrees and nutation rates of from 200 to 600 rpm and cant angles of from 0.004 to 0.040 radian. The resulting average phase angles were computed for a spin rate of 3000 rpm and they were found to range from 53 down to 17 degrees over the range of cant angles shown in Figure 17. While this is a larger spread of phase angle than occurred in the flight experiments, both excursions center about approximately a 30 degree phase angle. This result further substantiates the credibility of the spin theory and both the free flight and spin fixture experimental techniques are supported.

XIII. EXPERIMENTAL ACCURACY

The accuracy of the experiments is not known. The inability to reproduce properly the despin measurements in the spin fixture indicates fundamental inaccuracy. Because the results of at least two runs must be compared for isolation of the inertial effect, a tare run was made before and after each loose ring run but the format for doing this was not orderly. Weighted average tare values were used in the data reduction but the weighting depended, without assurance, on a linear variation of the fixtures performance with use. However, when tare spin-downs were made without much separation by other runs, the results were reproduced to within 5%. The loose ring runs were not repeated because of insufficient time. It was thought confidence in the quality of the experimental results would be ensured through the large quantity of test results. However, because of some disorder in the results, this large quantity of test data did little to define the test accuracy.

If the inertial despin moments had been accurate well-established values and if it had been possible to measure the crucial cant plane phase angle during the spin-downs, then it would have been possible to make a rigorous overall assessment of the combined accuracy of the experimental despin technique and the particular test hardware being used. Furthermore, if the despin technique was well established as providing accurate results, then the accuracy limits of the spin fixture could be isolated. These pre-conditions could not be met because of the fixture's performance problems and the fact that the inertial despin moments, with which the test correlation was desired, were only the predictions of an unproven theory and were based on an assumed cant-plane phase angle.

The best indication of the accuracy of the test comes from the correlation of the computed phase angles of the loose ring's cant plane with similar computations from projectile firings. The results from these two distinctly different tests show the computed phase angle, based on the theoretical spin equation, to be centered about approximately 30 degrees.

XIV. EXPERIMENTAL PROBLEMS

The experimental problem areas are given specific attention below as an aid to any plans for an additional validation experiment.

A fixture with improved spin bearings should be used for any future experiment. This fixture should also have the capability for additional discrete coning angle settings; or preferably for a continuous variation of the coning angle during a test (at no loss of fixture rigidity). Thus, the result should be smaller and more stable tares and increased flexibility of application. Additionally, the fixture should have more power for spin to insure acquisition of test results at higher spin conditions and compatibility with actual projectile conditions. Also, a means of providing vibration damping between the spin model and the nutation frame would be useful in isolating the spin model from vibrational excitement by the fixture. (During these experiments, resonance conditions usually precluded obtaining useful results at 5,000 rpm spin.)

The model should have provisions for measuring the polar angle of the cant plane of the loose component relative to the yaw plane of the projectile. This capability would also include the ability to determine between canting and "hula-hooping", unless the loose ring did not fully cant. In that case, it would not be possible to distinguish between the two motion modes by the following electrical technique and motion photographics could be employed for that purpose.

An electrical commutator technique is seen as being capable of resolving the phase angle to within $\pm 2\frac{1}{2}$ degrees when 72 commutator

segments are used. These electrically conducting strips would be placed at 5 degree intervals around the inside of an electrically insulated shell that would surround the loose ring. Seventy-two slip rings would be required to complete the individual circuits to "ground based" instrumentation. Also, the model should have its loose rings fabricated by composite construction, i.e., the rings should have heavy metal (tungsten alloy or depleted uranium) rims, their intermediate radius structure made of magnesium or aluminum alloy (hollowed out for additional lightness) and with hardened alloy steel inner bushings (for wear resistance and dimensional stability). All other rotating parts should be lightened as much as possible to minimize the despin tares. This combination of improvements would promote accuracy by increasing the magnitude of the inertial despin moments while producing a reduction in the magnitude of the tares. These proposed model modifications are presented in more detail in Appendix B.

The data acquisition instrumentation should be improved to include automatic acquisition of the despin rate at each 500 rpm increment of the despin record as a means of improving the on-site management of the test. It would also eliminate the tedious manual retrieval of the despin rate data encountered during this test.

The test sequence should be modified to call for a tare run to be followed by a loose ring run, followed by a repeat of the loose ring run, followed by a repeat of the tare run. This test sequence would be time-consuming due to the additional model changes but would tend to optimize the experimental accuracy since the tare and loose ring runs would be close together, the loose ring runs as well as the tare runs would be systematically repeated, and the tare runs would closely bracket the loose ring runs. One of the problems of the subject test was that the loose ring runs were not usually repeated and those tare runs that were repeated were sometimes made long after the corresponding loose ring runs. Another shortcoming of this test was that data acquisition was sometimes stopped before the 500 rpm spin-down point was reached and it was later observed that a break in the spin rate was encountered at about that point.

Consideration should be given to an entirely new approach to the measurement of inertial despin moments. Ideally, a large spherical air bearing, to hold the spinning projectile or simulated model while permitting three degrees of angular freedom, would be capable of providing more accurate results. In this concept a retractable motor would induce model spin, a magnetic yaw inducer would then start the model gyrating and motion data could be acquired by a digital-type system of on-board light sources, discrete apertures and ground-based photo-detectors. This system would employ fiber optics as necessary in the confined space and would be similar to sting-mounted dynamic stability systems already developed for wind tunnel purposes. Other data acquisition techniques might also be feasible; e.g., orthogonal motion photogramatics or on-board sun-sensor type instrumentation. If

this spherical air-bearing fixture had provisions for magnetically developing a gravity compensating force and if it was enclosed in a vacuum chamber, it could be useful for satellite dynamic experiments.

XV. CONCLUSIONS

The loose ring theory is generally supported by these ground-based tests that use the despin technique. Verification, however, was not possible because the phase angle of the cant plane could not be measured during the spin-downs.

The quality of the test results were adversely influenced by both the experimental technique and the performance of the spin fixture.

a. The necessity for making despins with both a loose ring and a corresponding tare ring (rigidly fixed to the shaft), for isolation of the inertial effect, required the extraction of a relatively small number from the difference of two large numbers and those numbers could not be acceptably reproduced.

b. The spin fixture had other performance and design deficiencies.

(1) Greater spin power was desired.

(2) Additional coning angle settings, or a continuously variable coning angle excursion, would have been useful.

More tests, based on improved fixture performance, experimental technique, and model design, are required and the phase angle of the loose ring's cant plane will have to be measured before the theory can be adequately verified.

ACKNOWLEDGEMENT

The author is indebted to Mr. Owen Smith and Mr. Jack Molnar of the Weapon Systems Concepts Team for their efficiency and cooperation during the spin-down experiments at their facility, and to Mr. Donald Mylin for his development of the computer program and other assistance during the computing and plotting operations. Appreciation is also expressed for the text review by Mr. James Bradley.

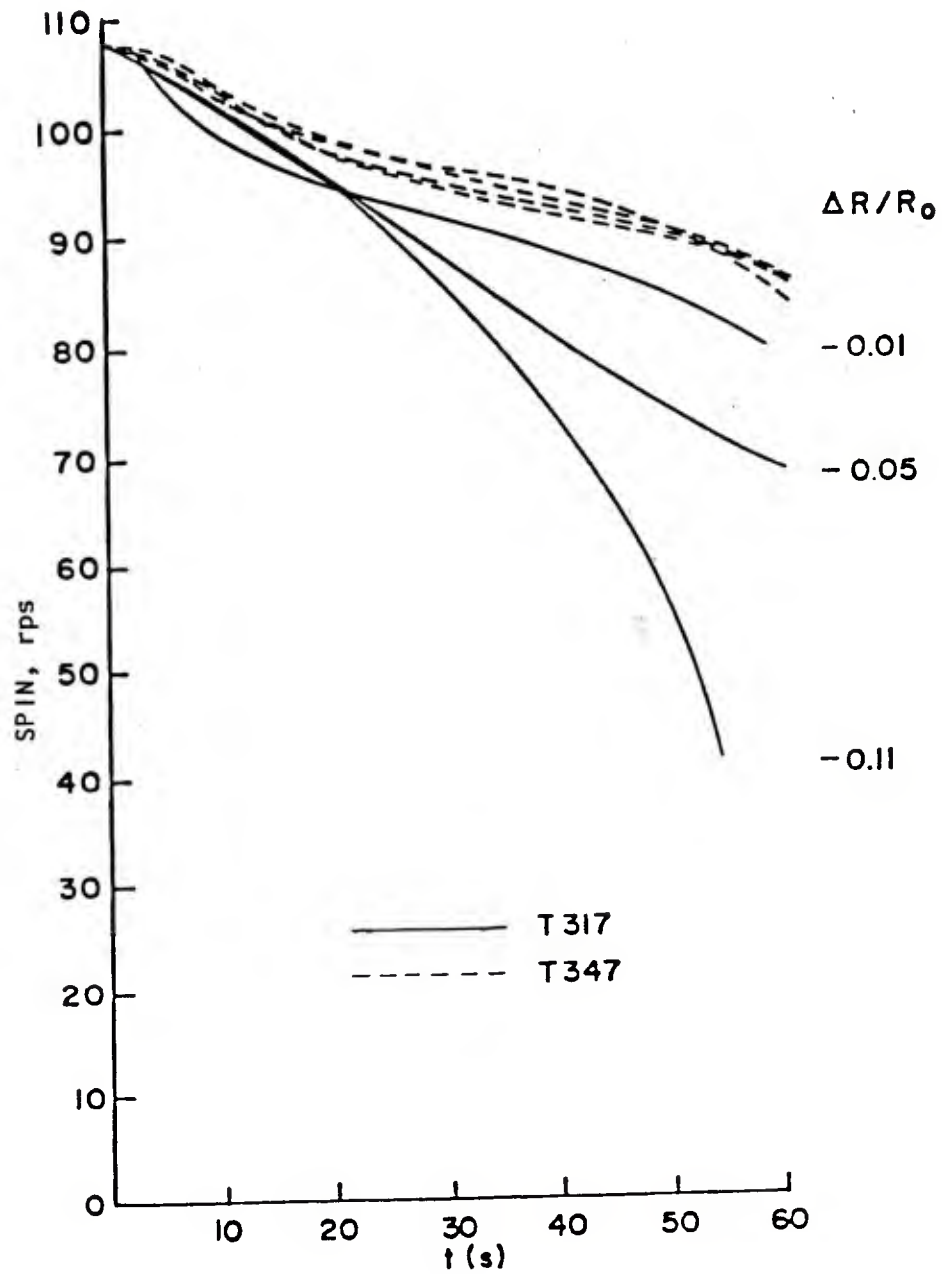


Figure 1. Measured Spin History of the T317

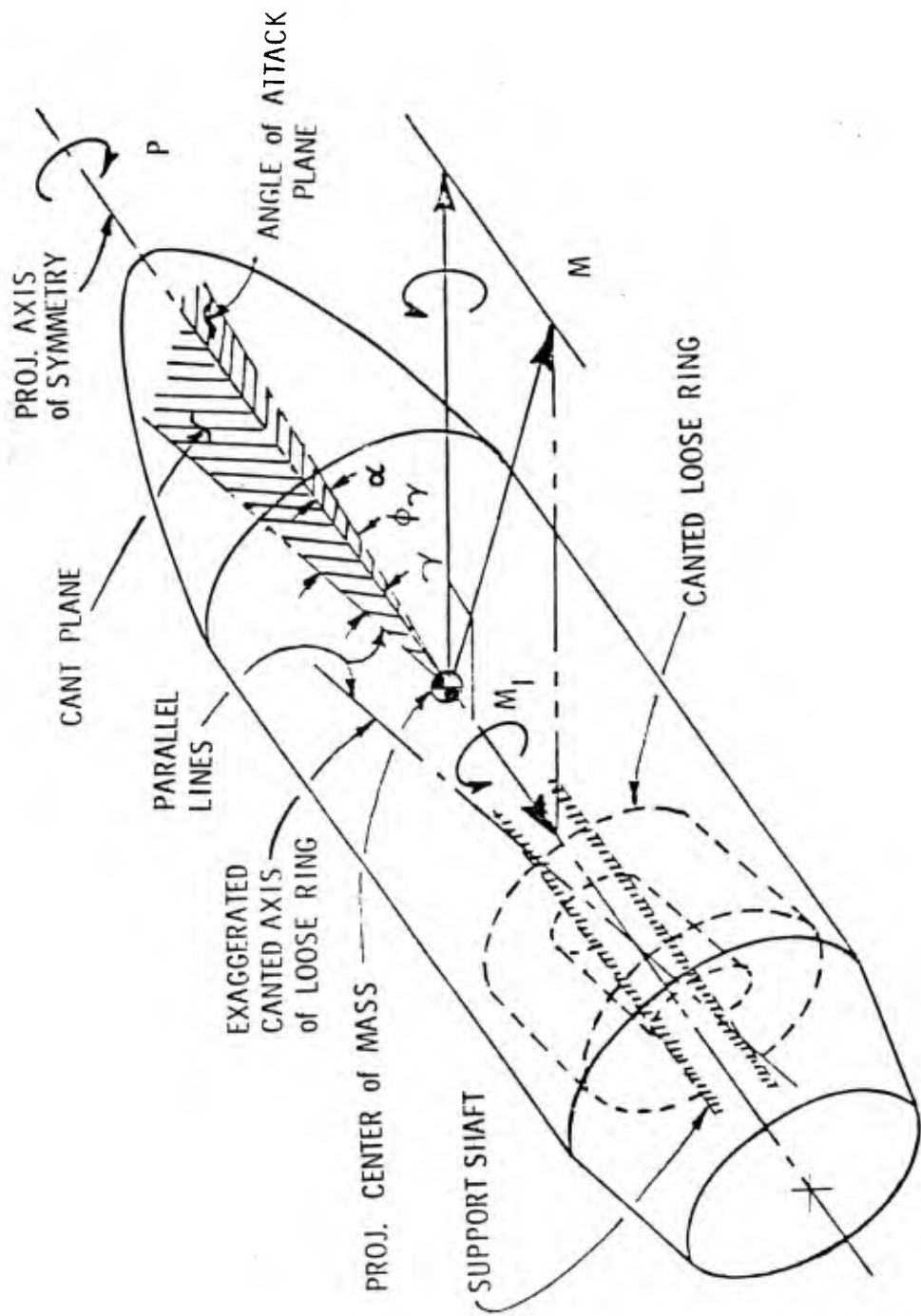


Figure 2. Projectile with Canted Loose Ring

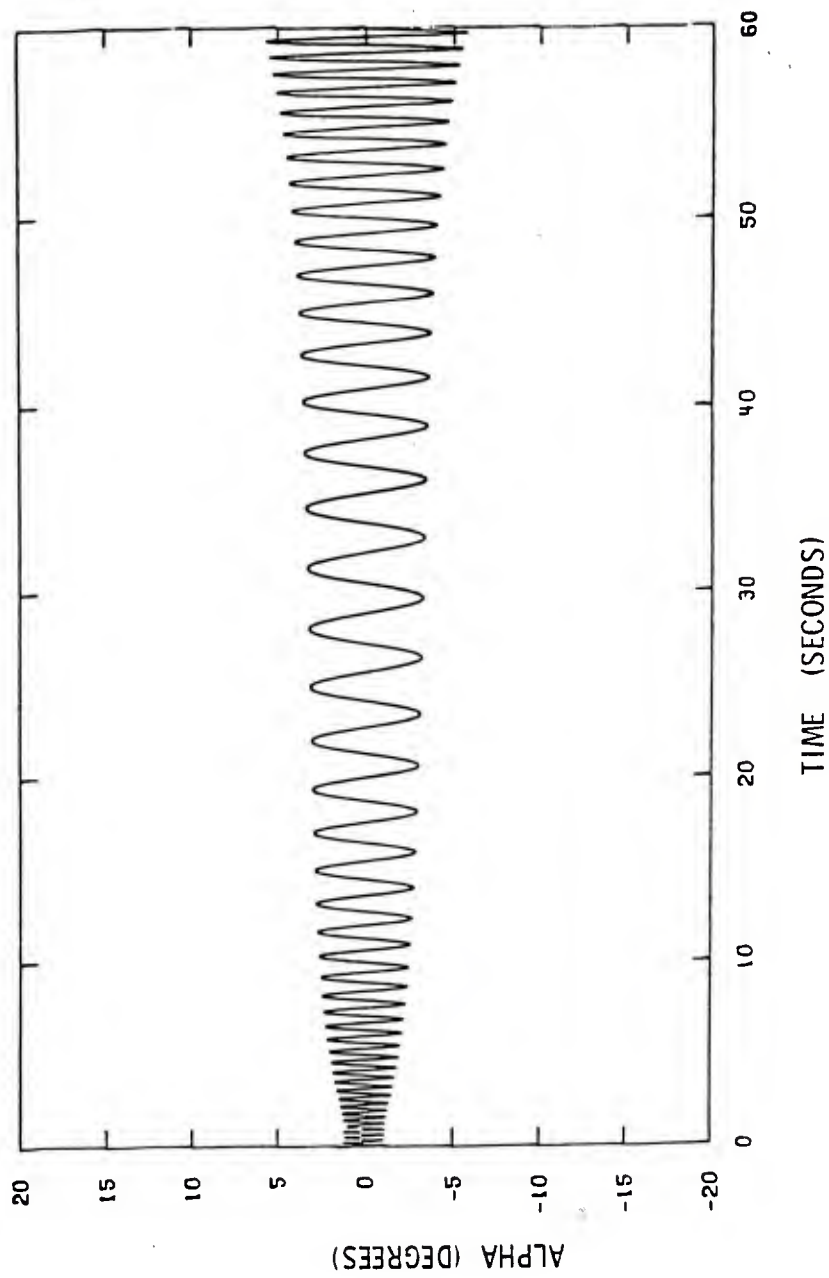


Figure 3. Computed Angular Motion of the T317 ($\gamma = 0$)

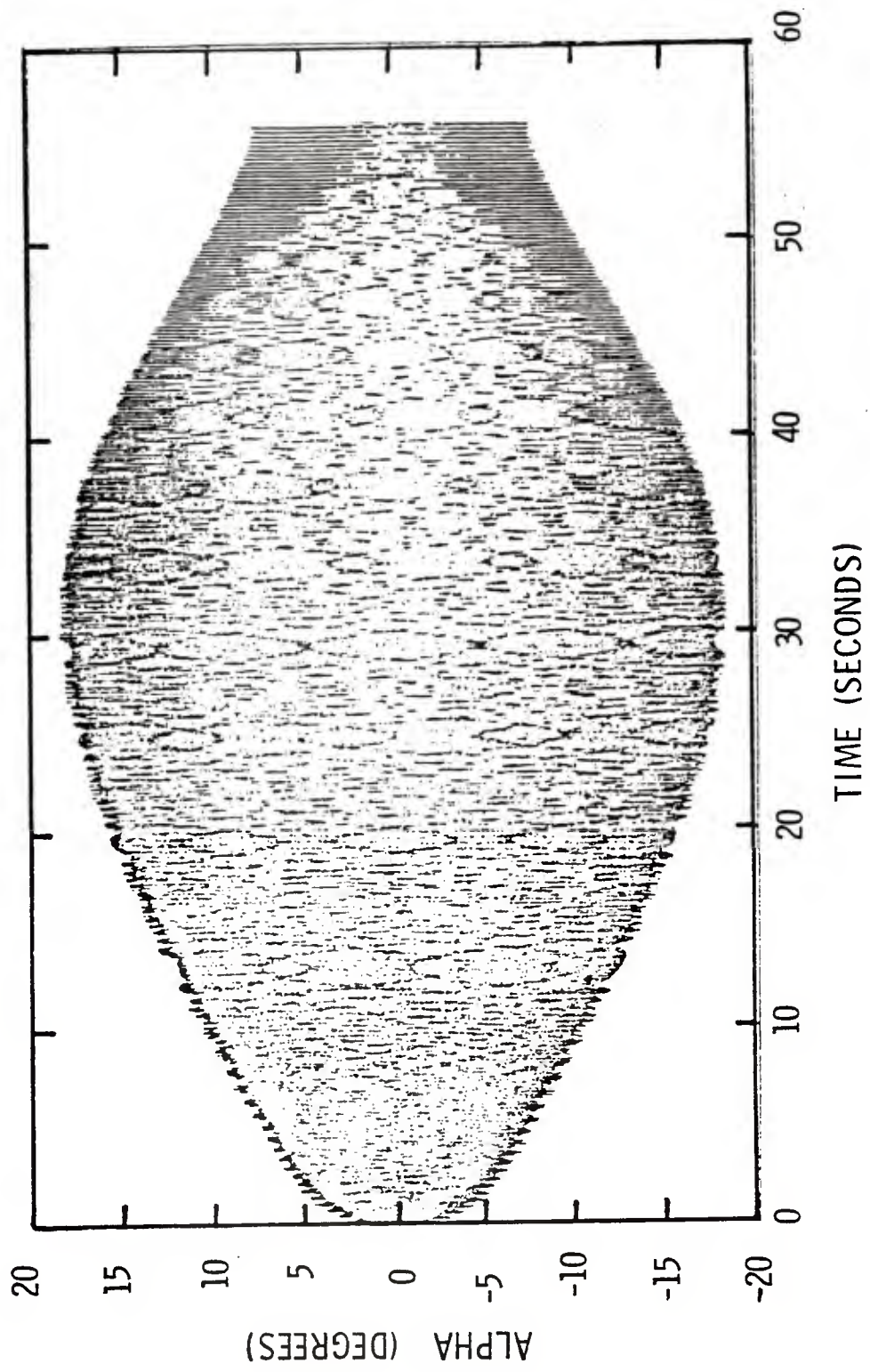


Figure 4. Computed Angular Motion of the T317 ($\gamma = .004$)

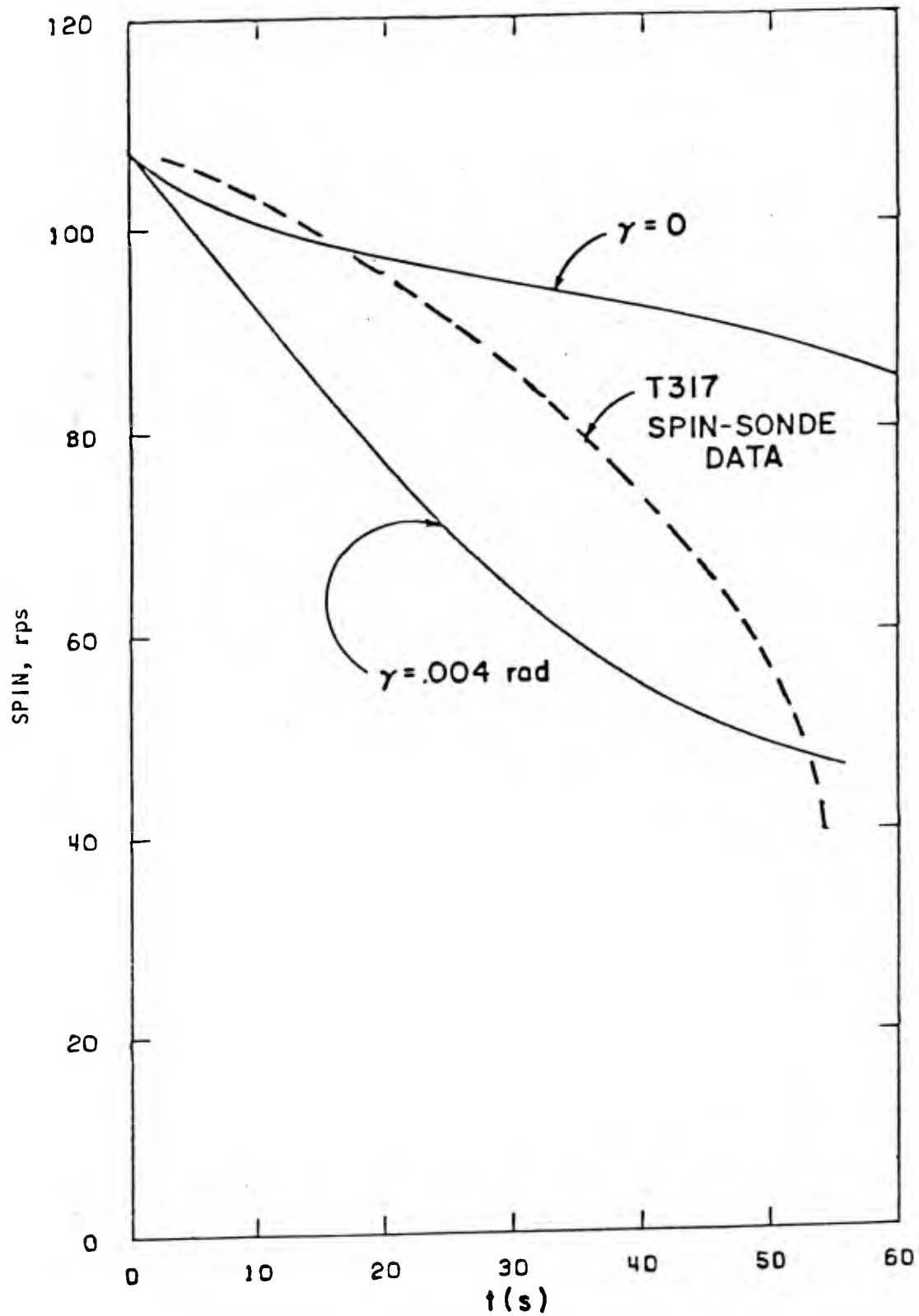
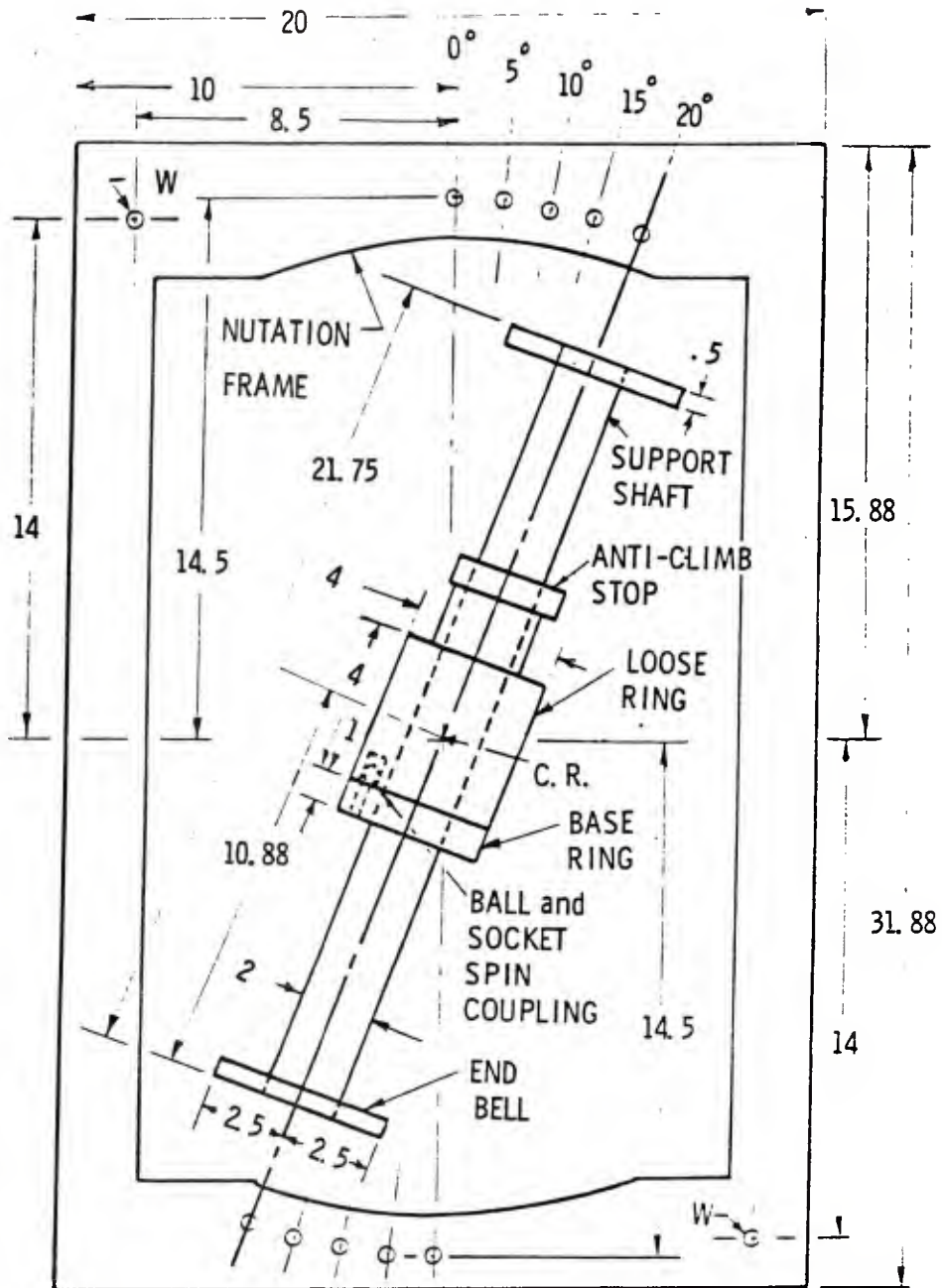


Figure 5. Computed Spin History of the T317



ALL DIMENSIONS in INCHES
 W = FIXTURE BALANCING POINT
 C. R. = INTERSECTION of FIXTURE SPIN and CONING AXES

Figure 6. Spin Model and Fixture's Nutation Frame

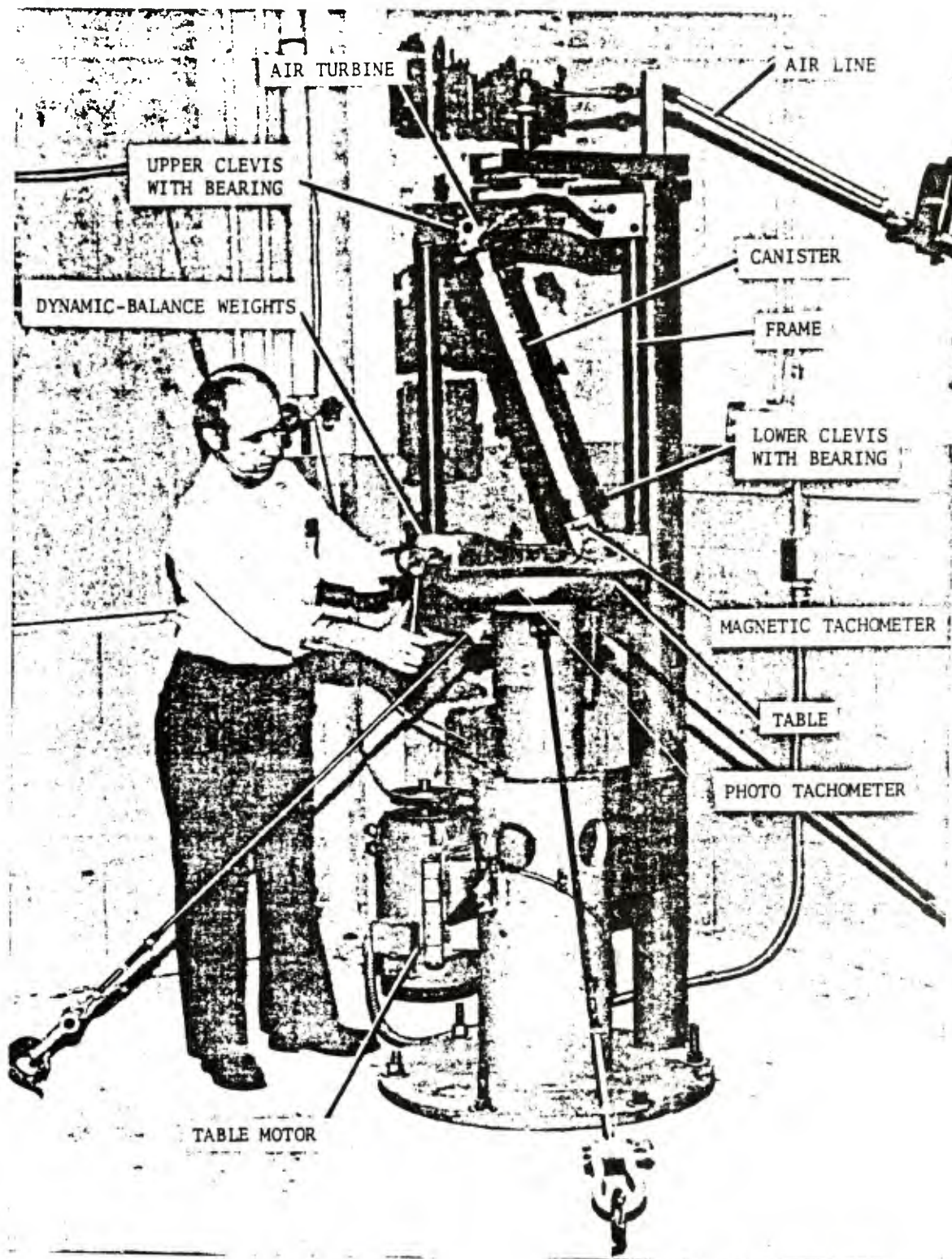


Photo 1. Spin Fixture

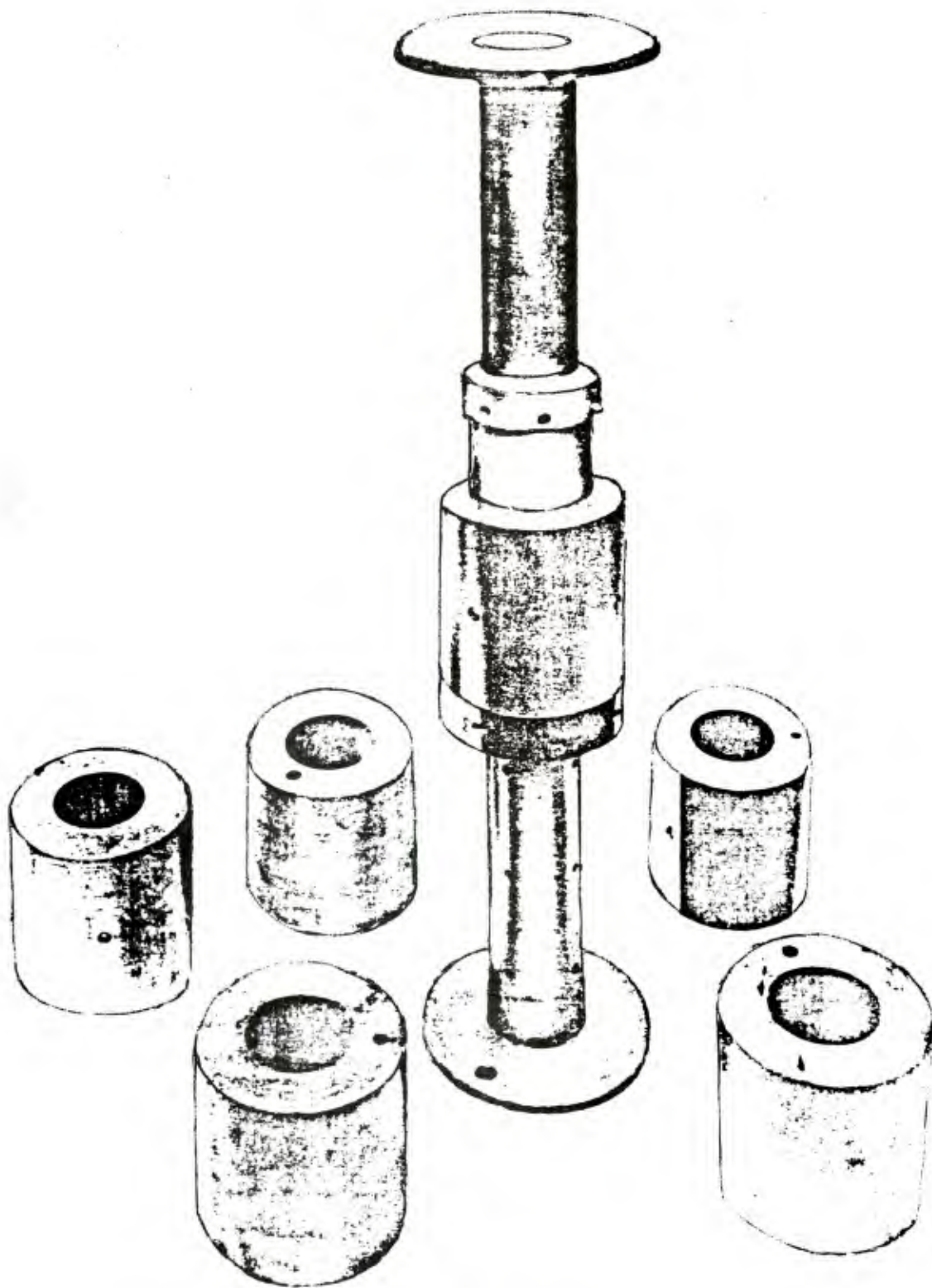


Photo 2. Spin Hardware

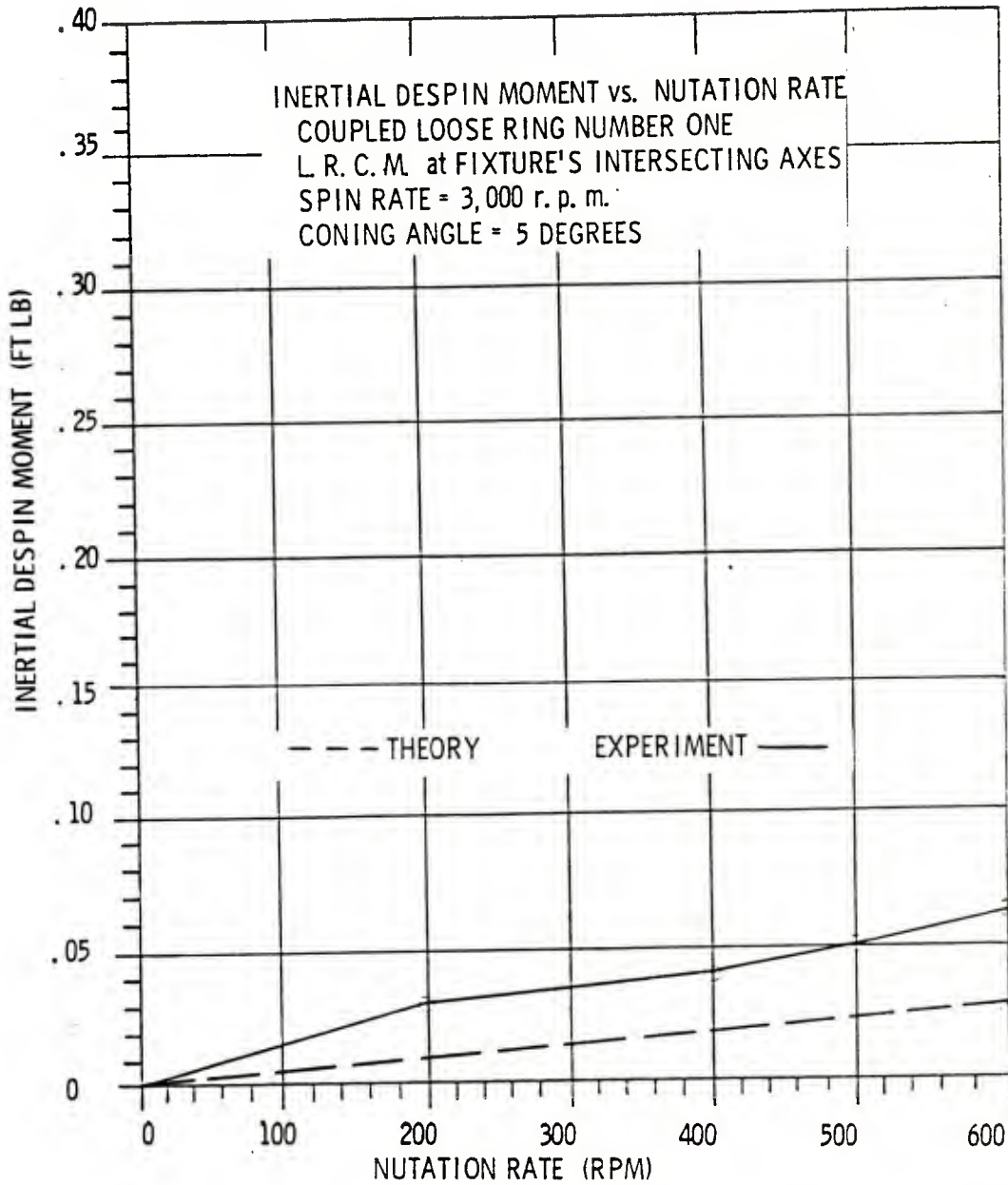


Figure 7a. Test Results from L.R. 1 at 5 Degrees Coning Angle

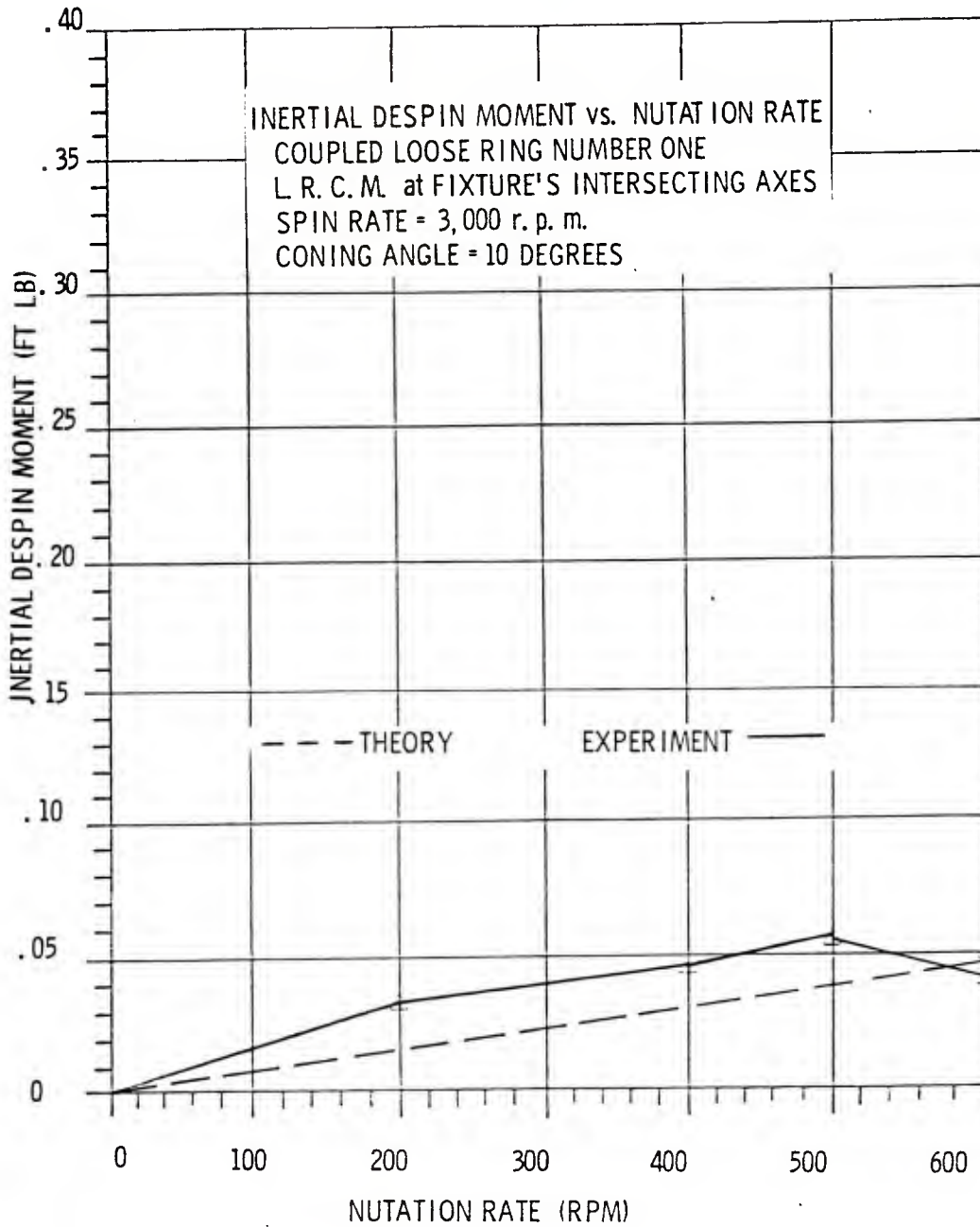


Figure 7b. Test Results from L.R. 1 at 10 Degrees Coning Angle

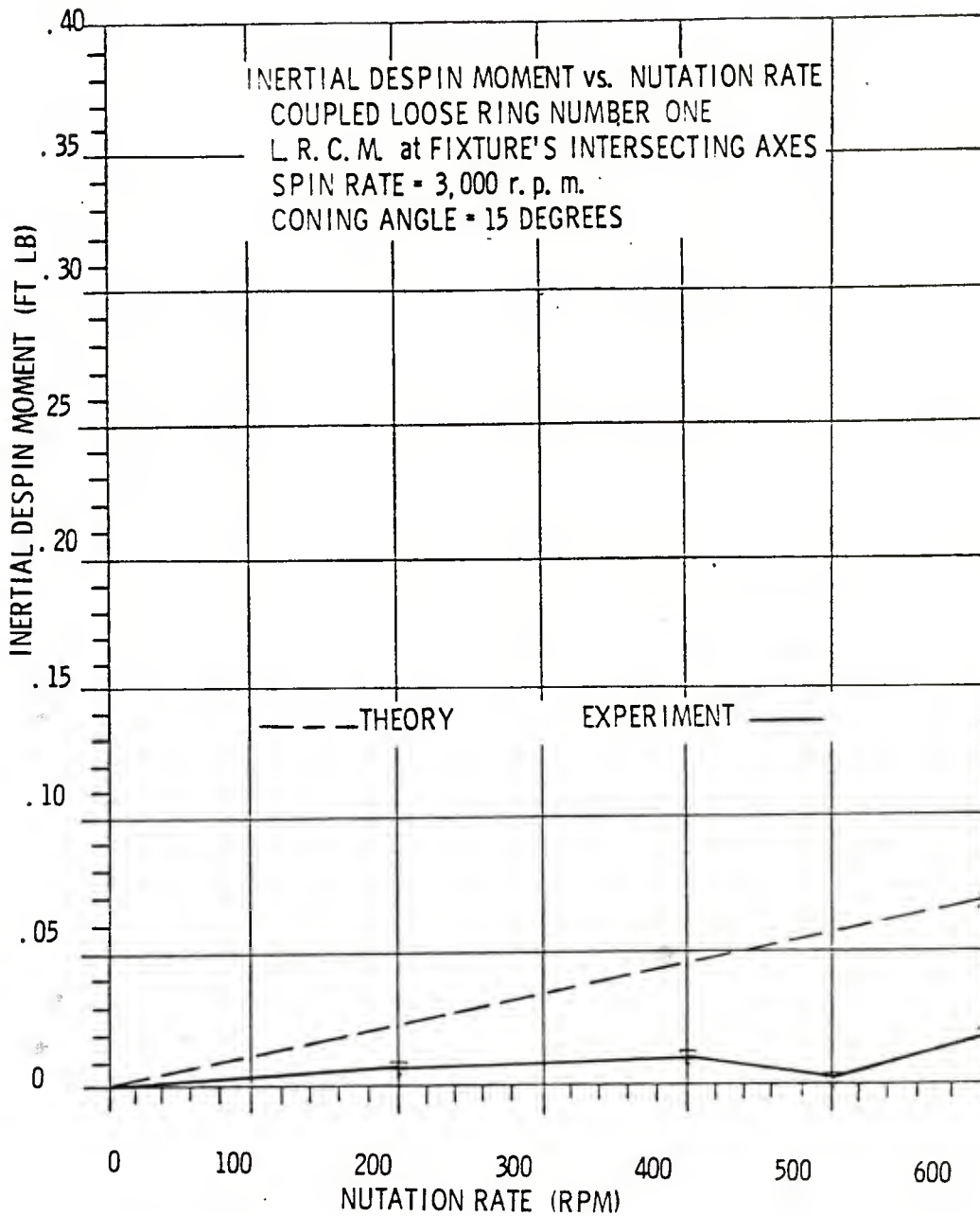


Figure 7c. Test Results from L.R. 1 at 15 Degrees Coning Angle

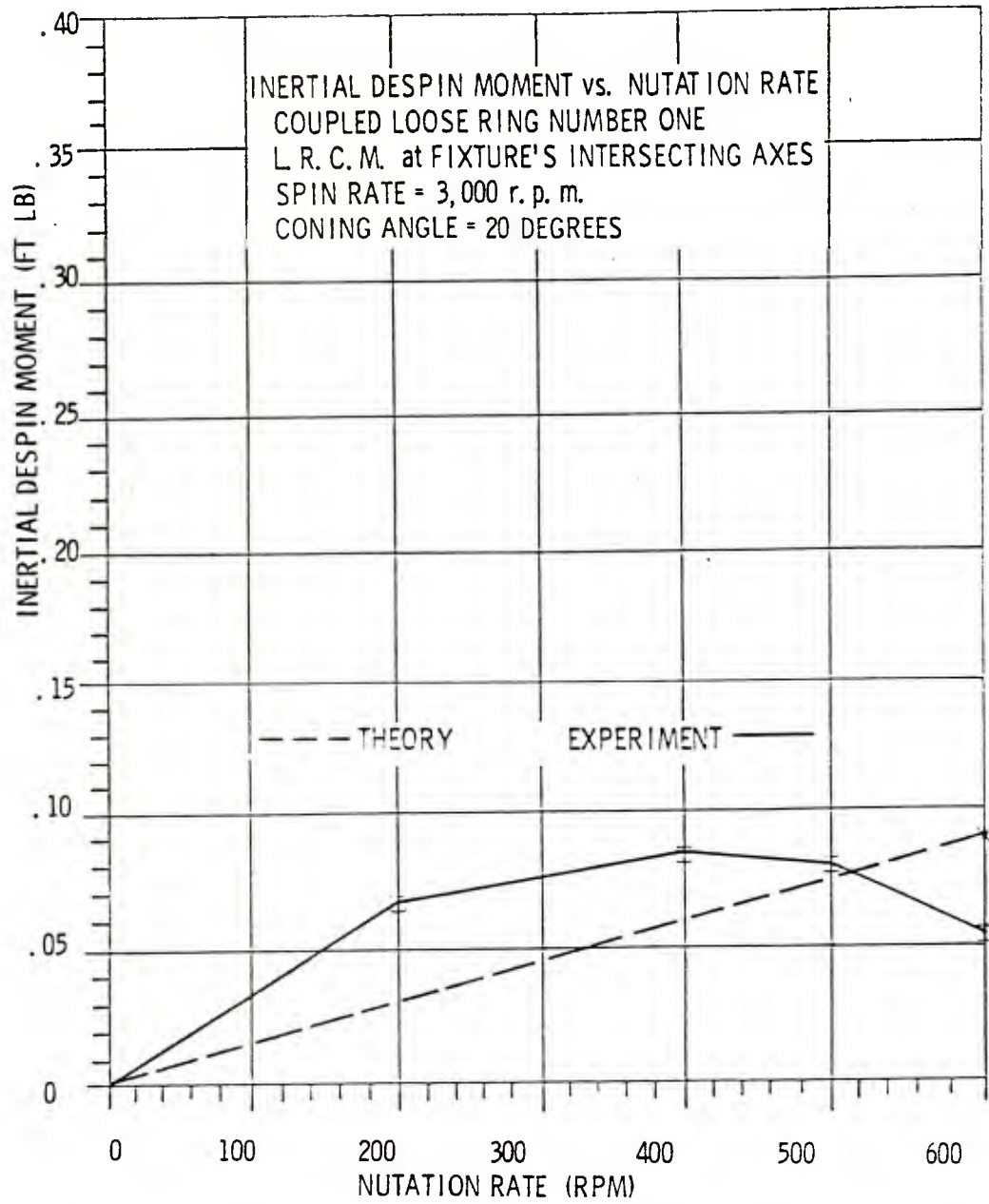


Figure 7d. Test Results from L.R. 1 at 20 Degrees Coning Angle

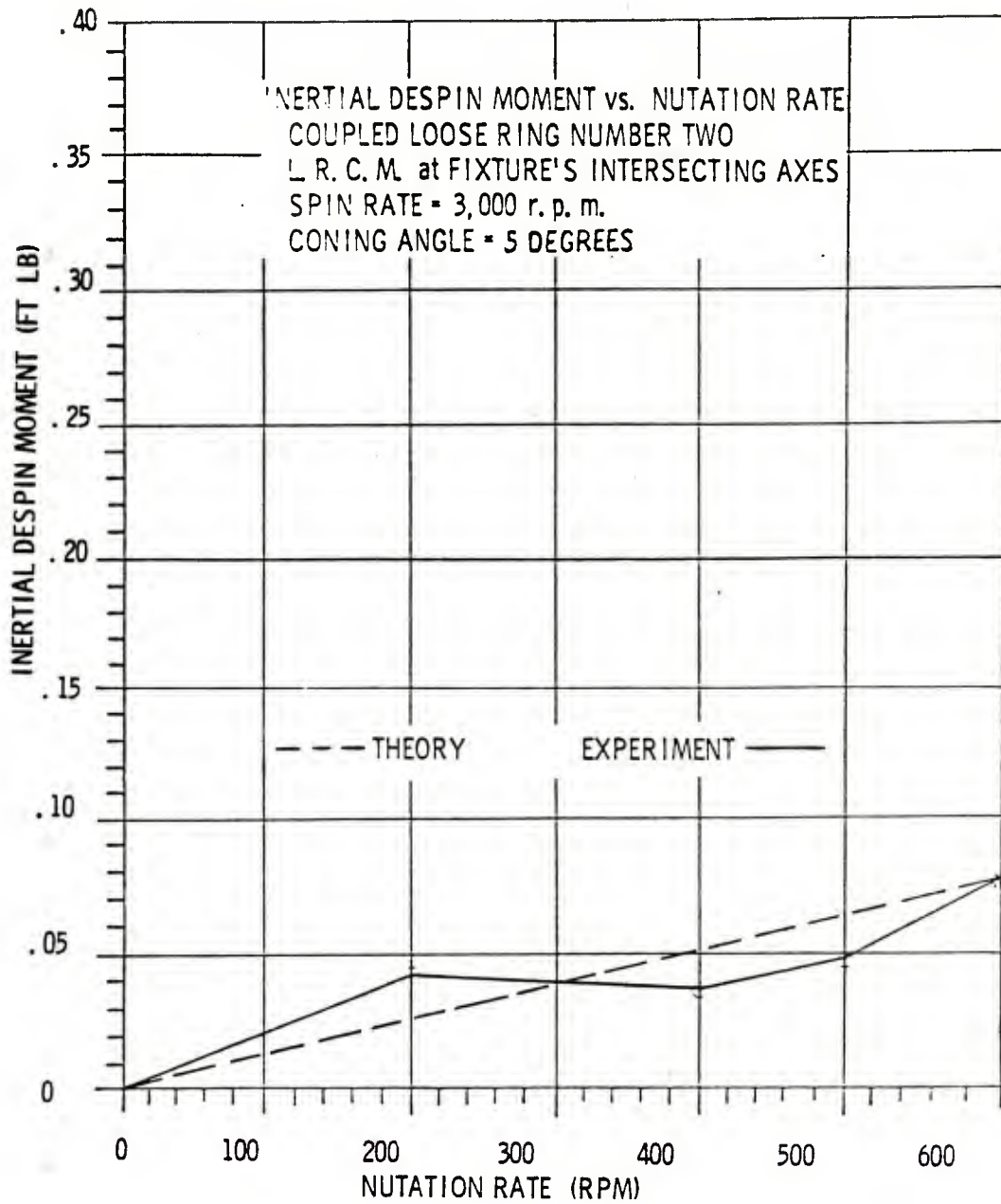


Figure 8a. Test Results from L.R. 2 at 5 Degrees Coning Angle

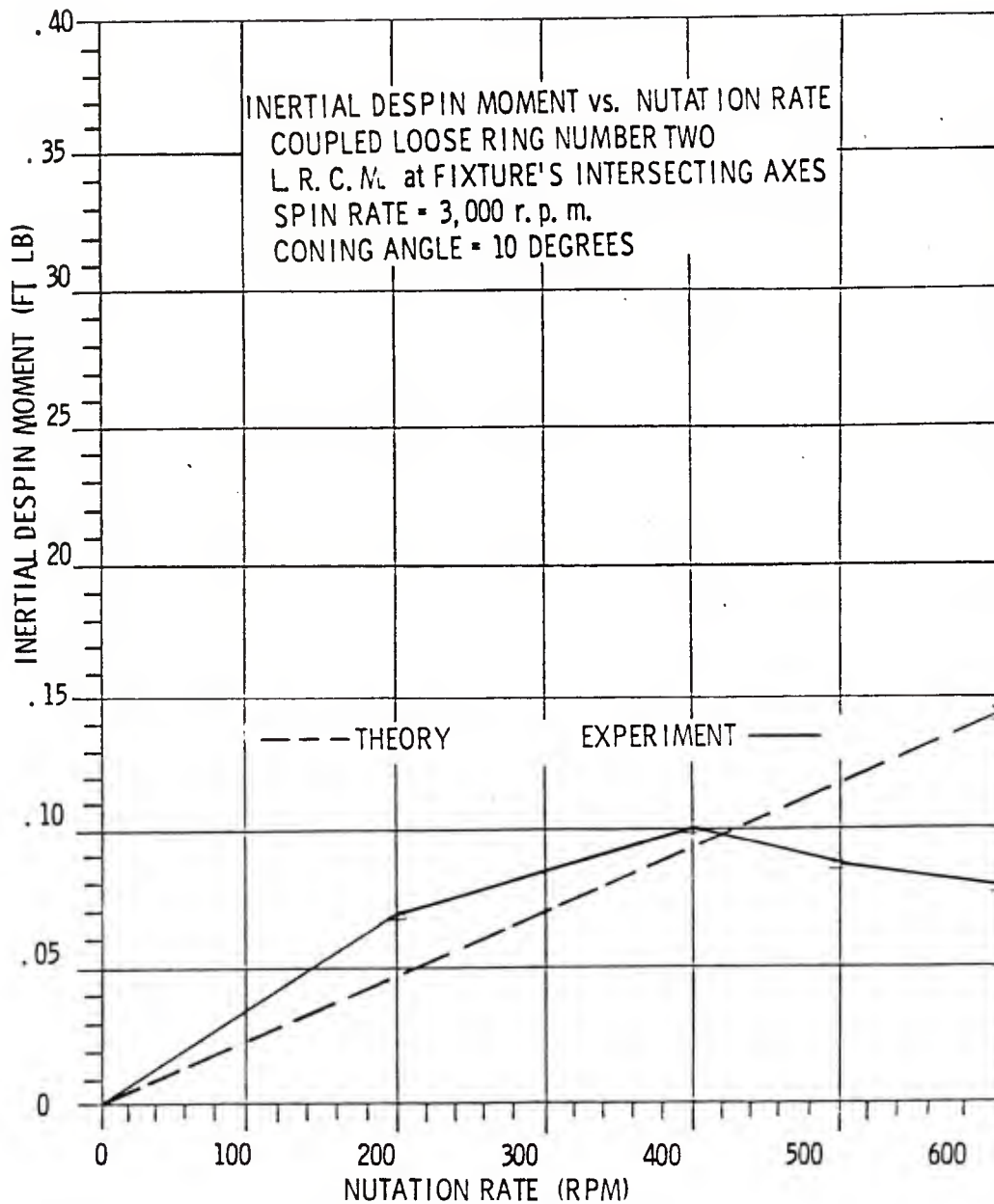


Figure 8b. Test Results From L.R. 2 at 10 Degrees Coning Angle

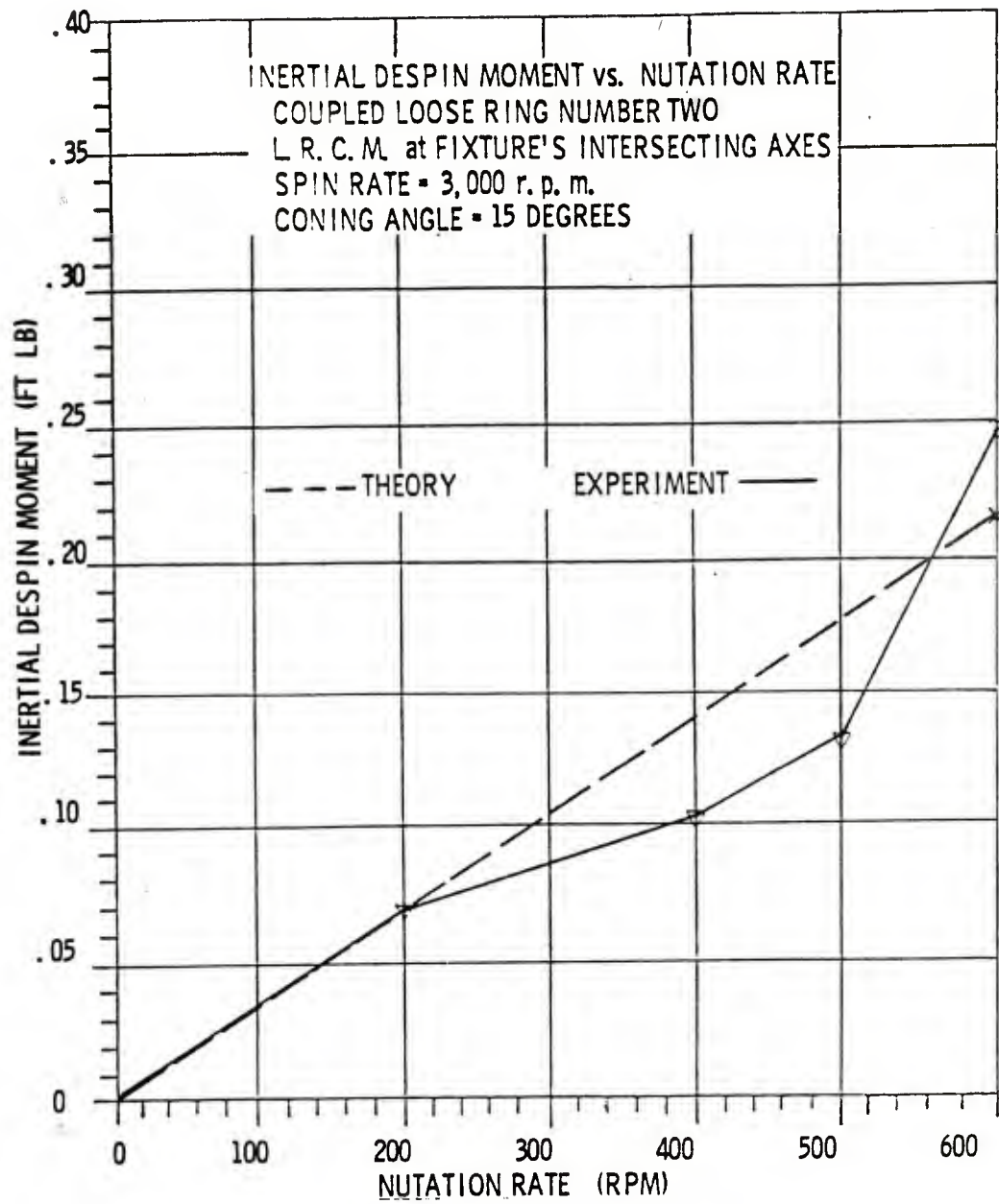


Figure 8c. Test Results from L.R. 2 at 15 Degrees Coning Angle

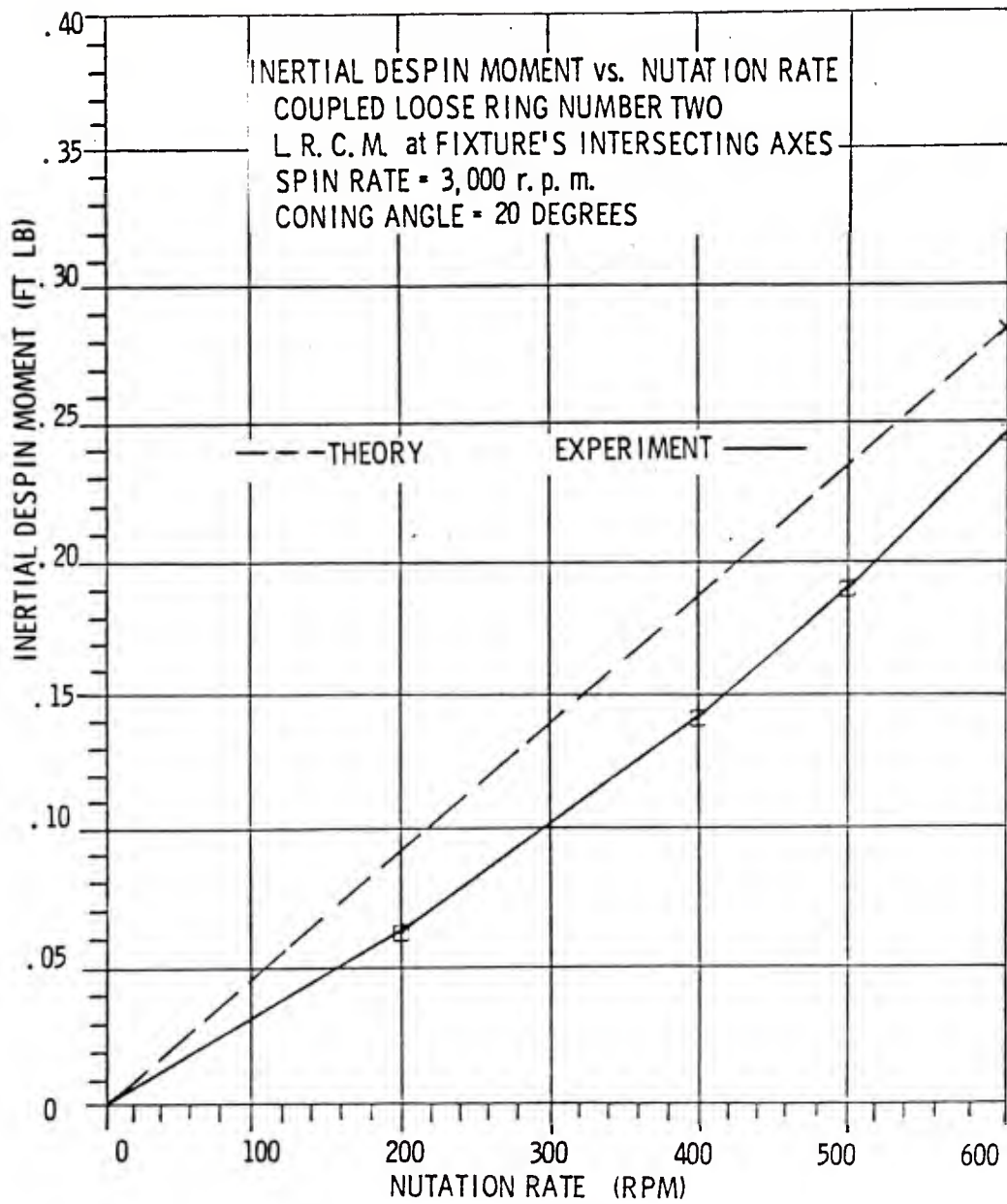


Figure 8d. Test Results from L.R. 2 at 20 Degrees Coning Angle

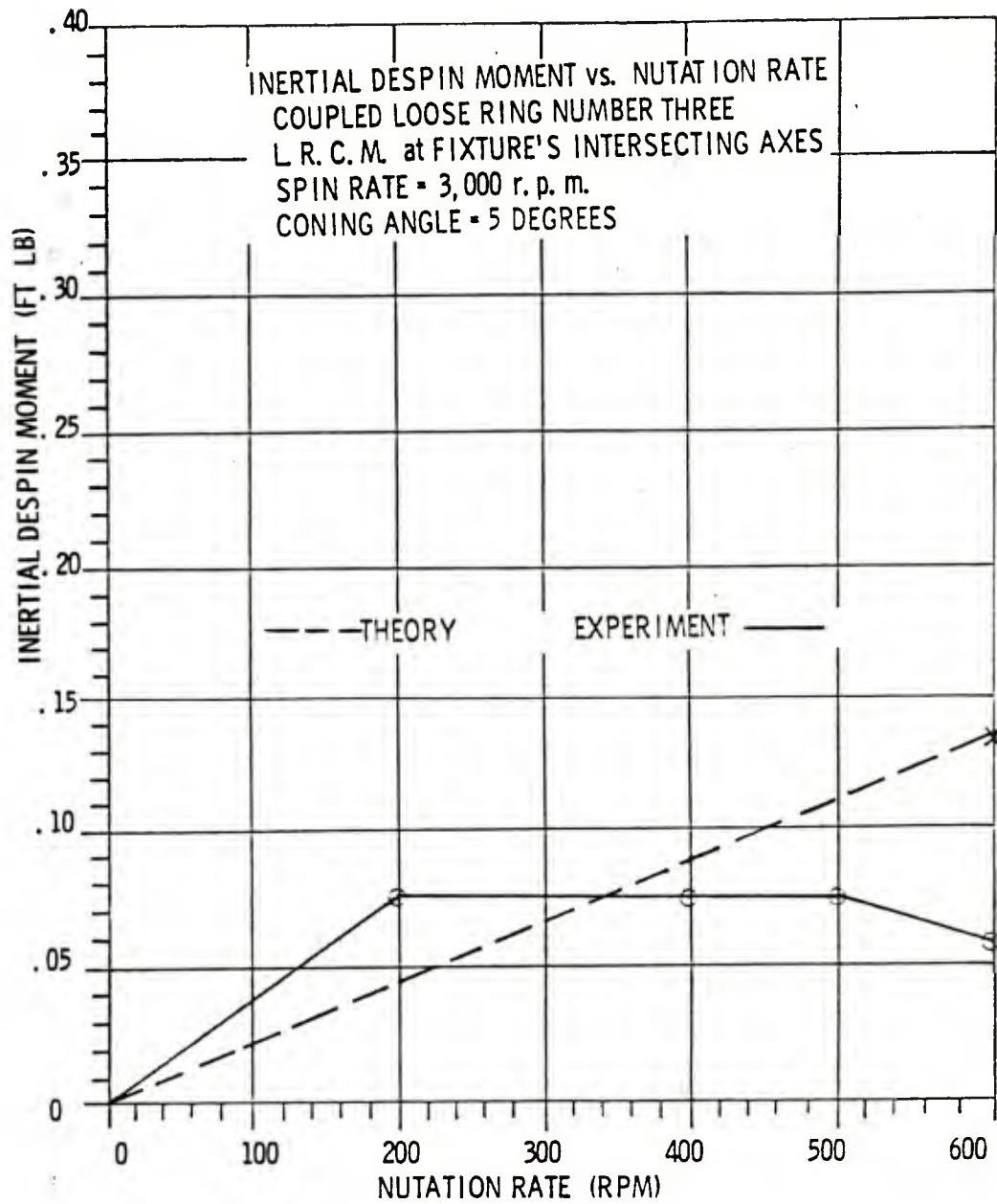


Figure 9a. Test Results from L.R. 3 at 5 Degrees Coning Angle

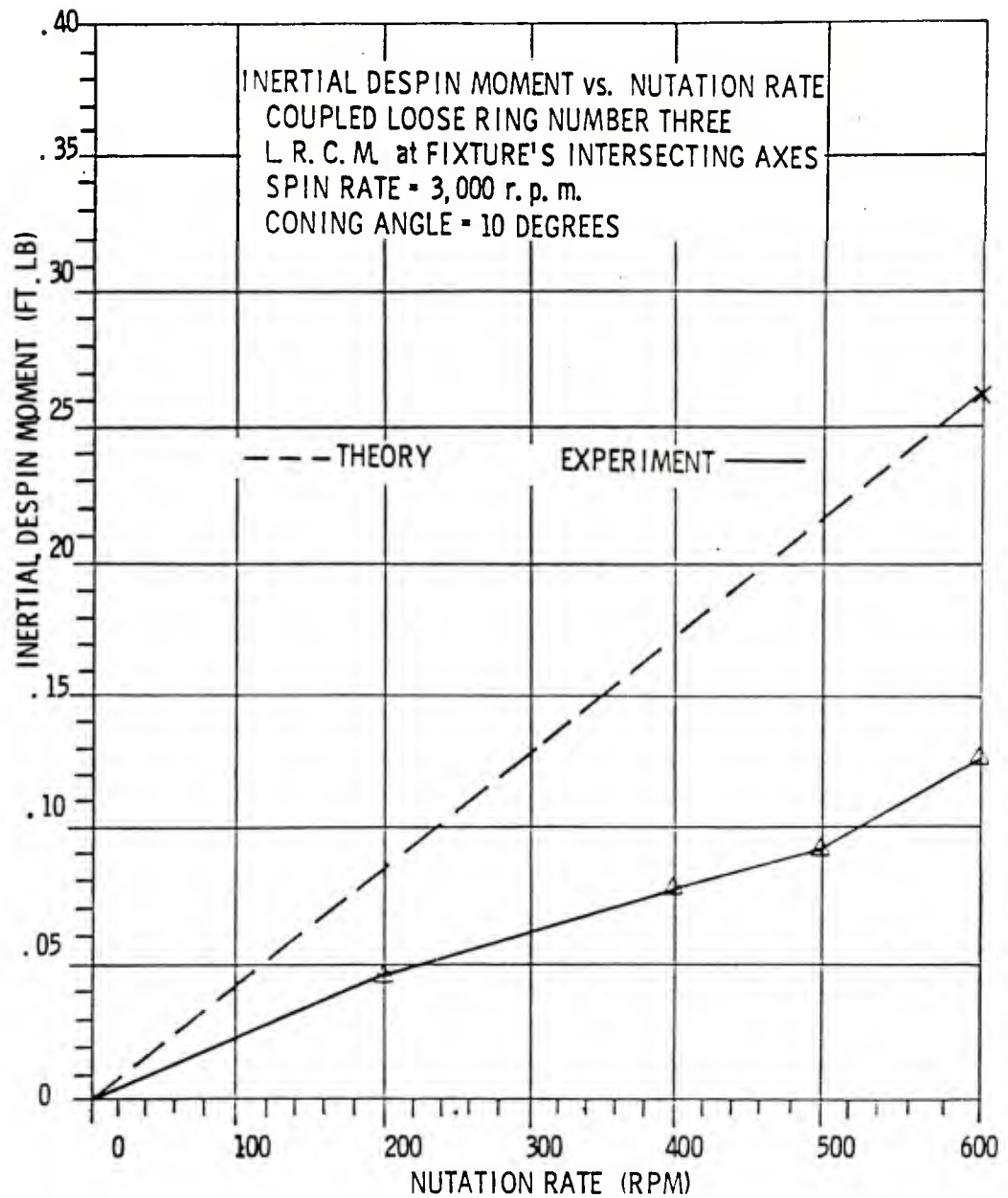


Figure 9b. Test Results from L.R. 3 at 10 Degrees Coning Angle

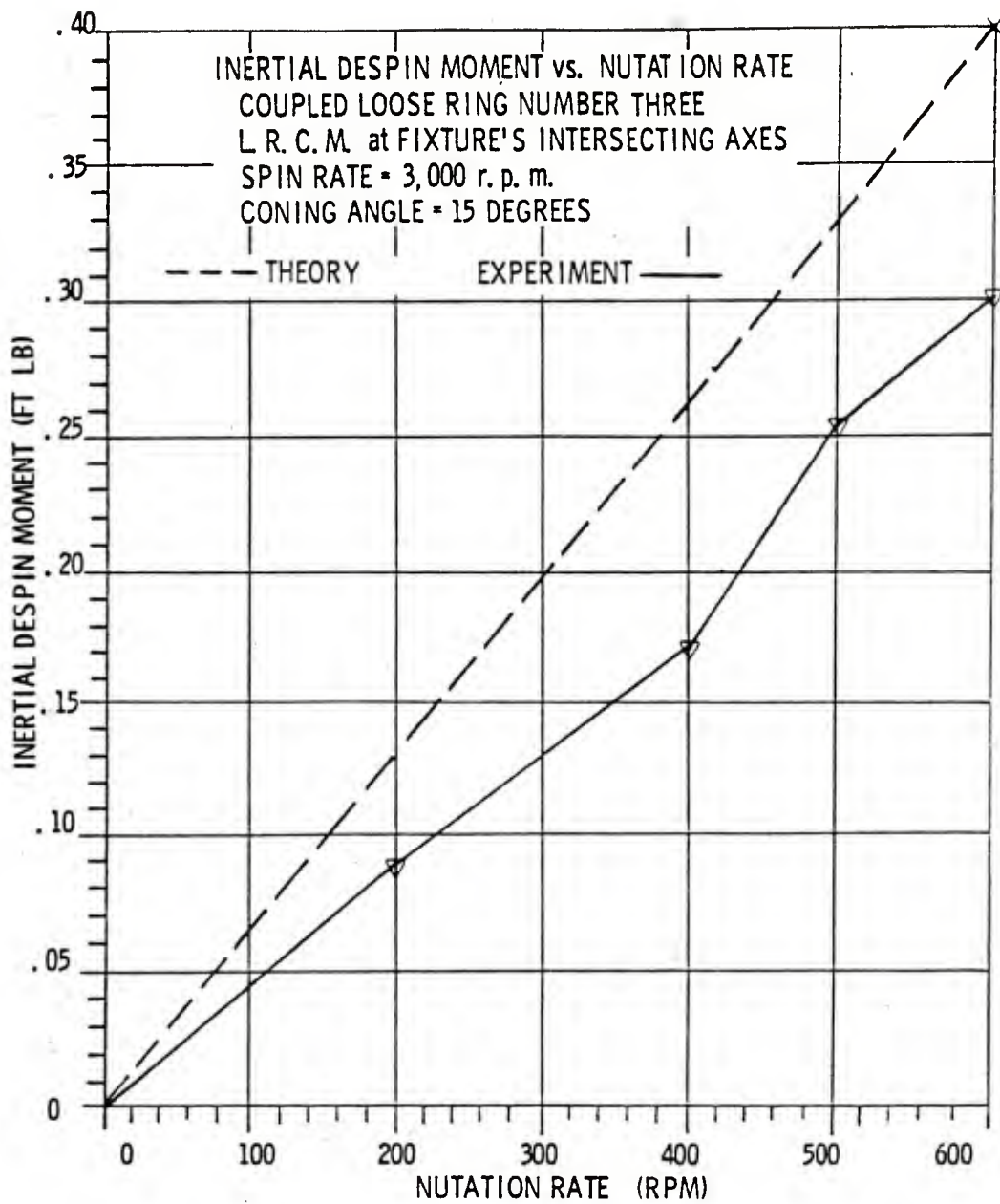


Figure 9c. Test Results from L.R. 3 at 15 Degrees Coning Angle

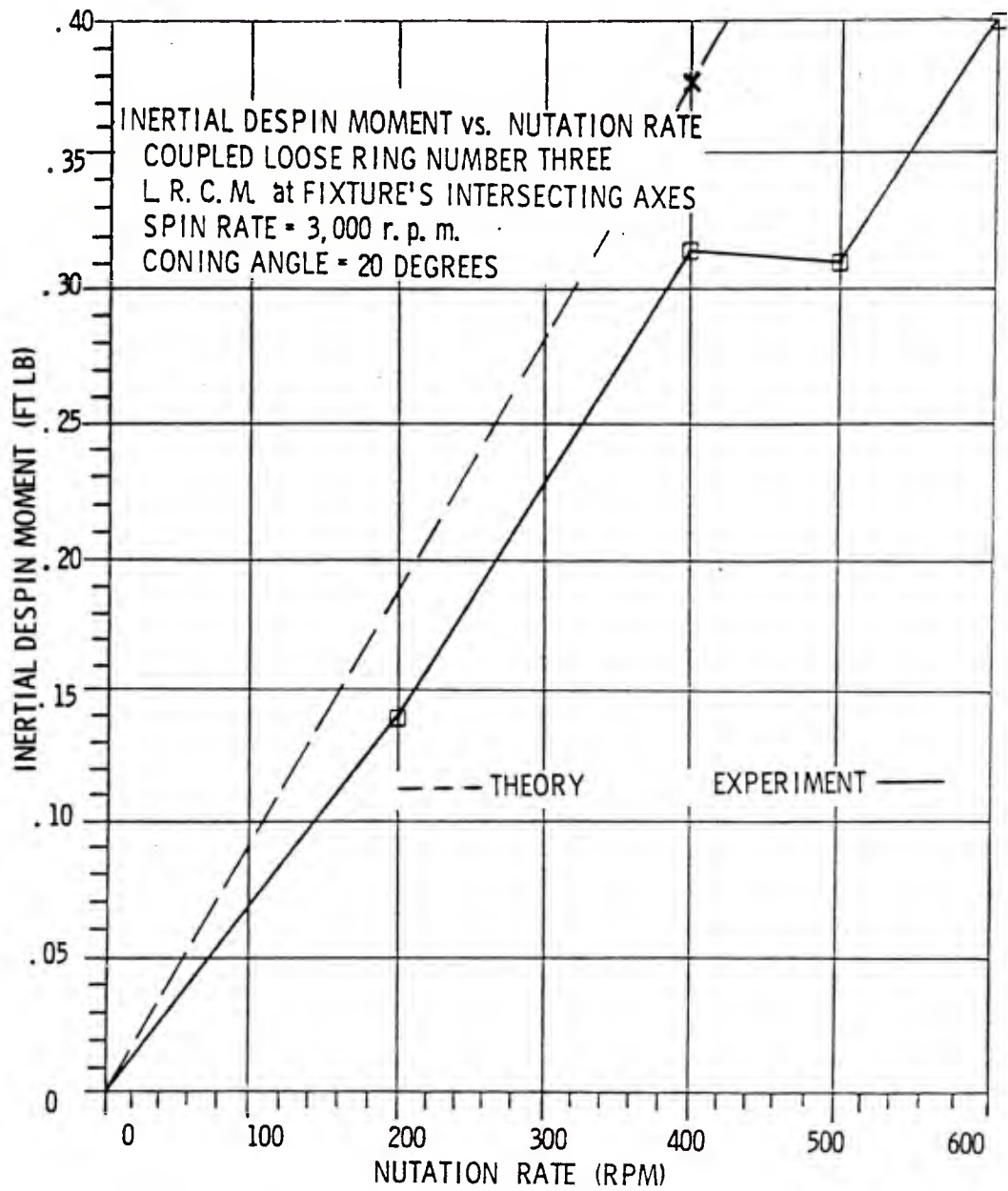


Figure 9d. Test Results from L.R. 3 at 20 Degrees Coning Angle

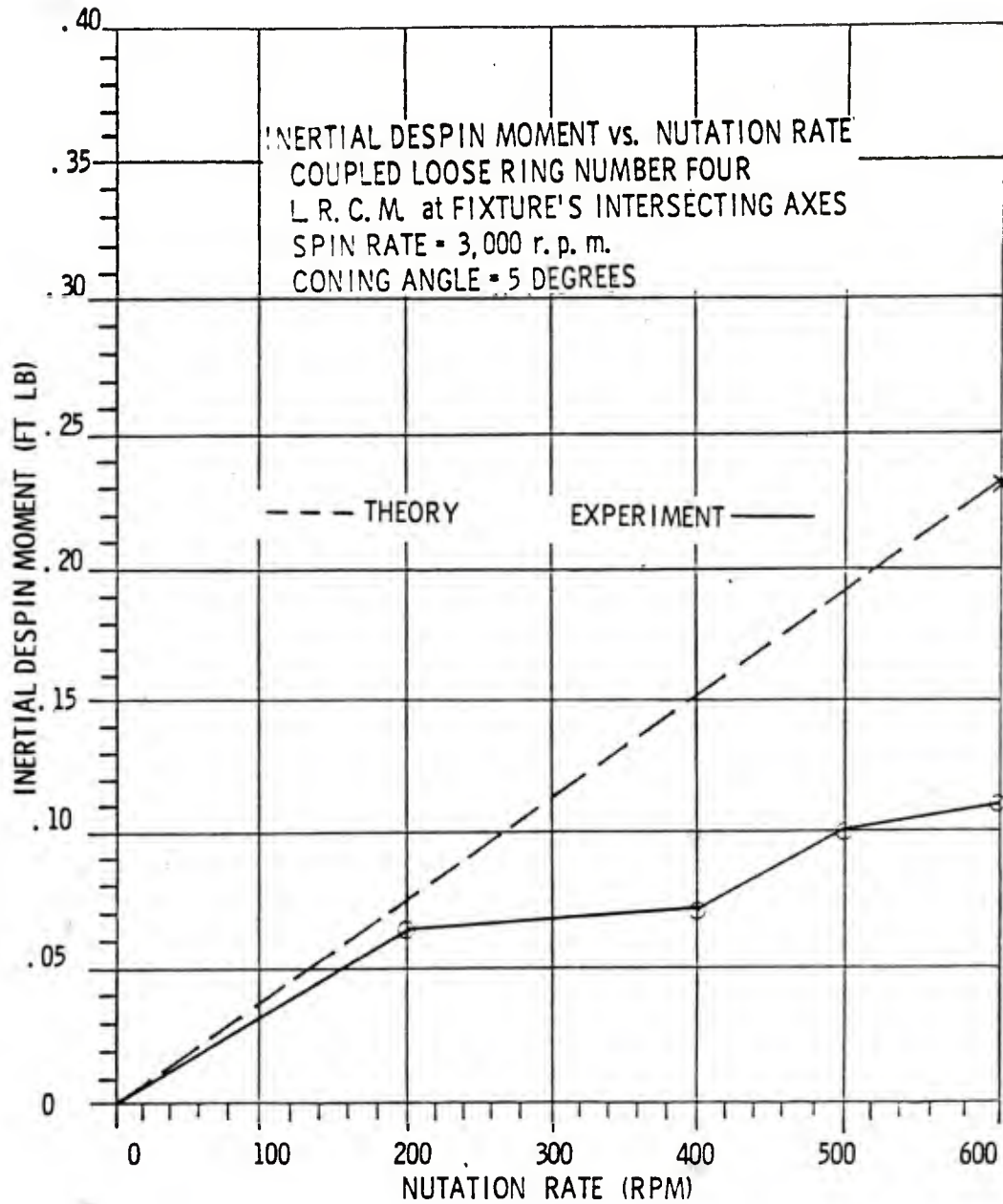


Figure 10a. Test Results from L.R. 4 at 5 Degrees Coning Angle

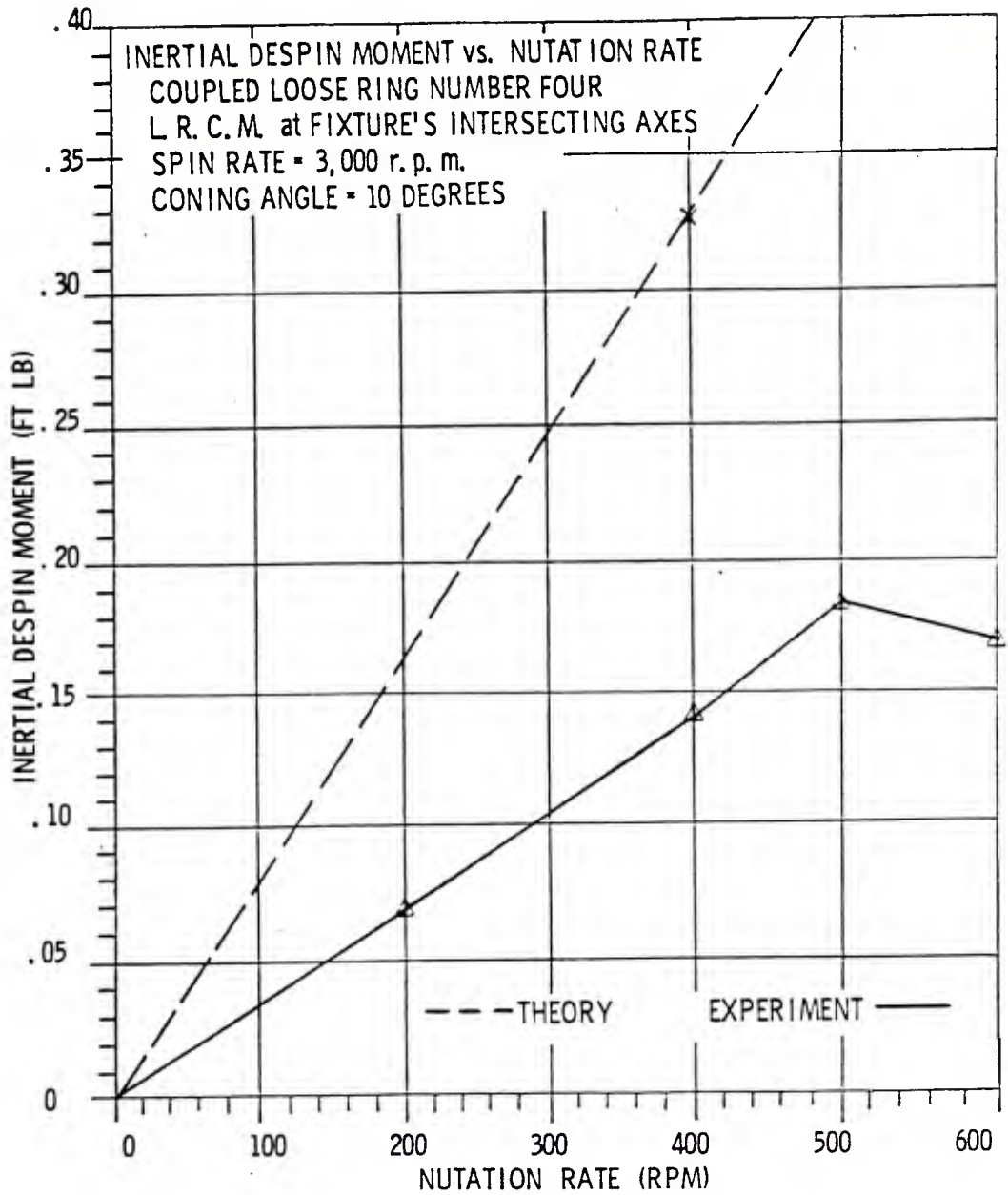


Figure 10b. Test Results from L.R. 4 at 10 Degrees Coning Angle

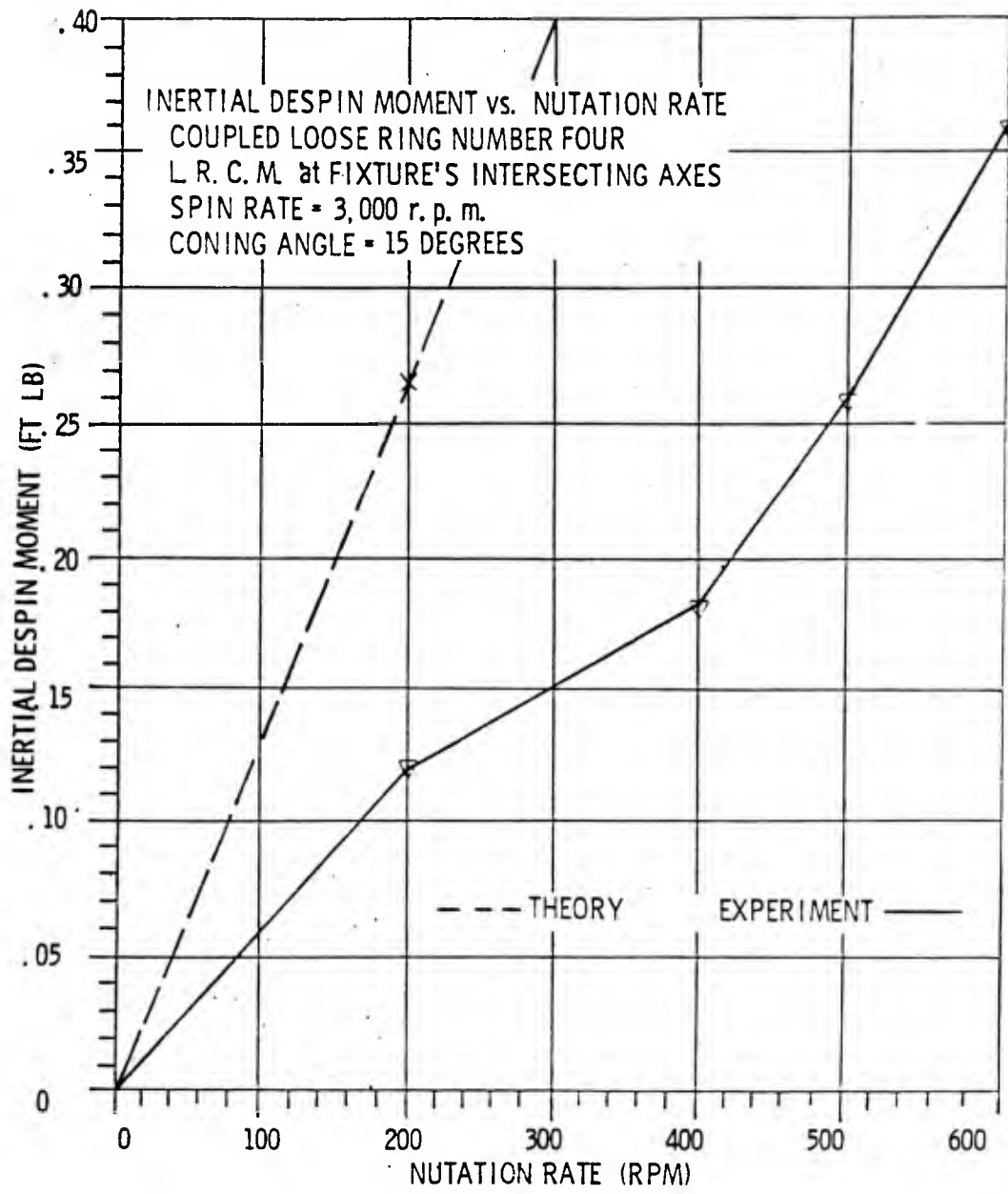


Figure 10c. Test Results from L.R. 4 at 15 Degrees Coning Angle

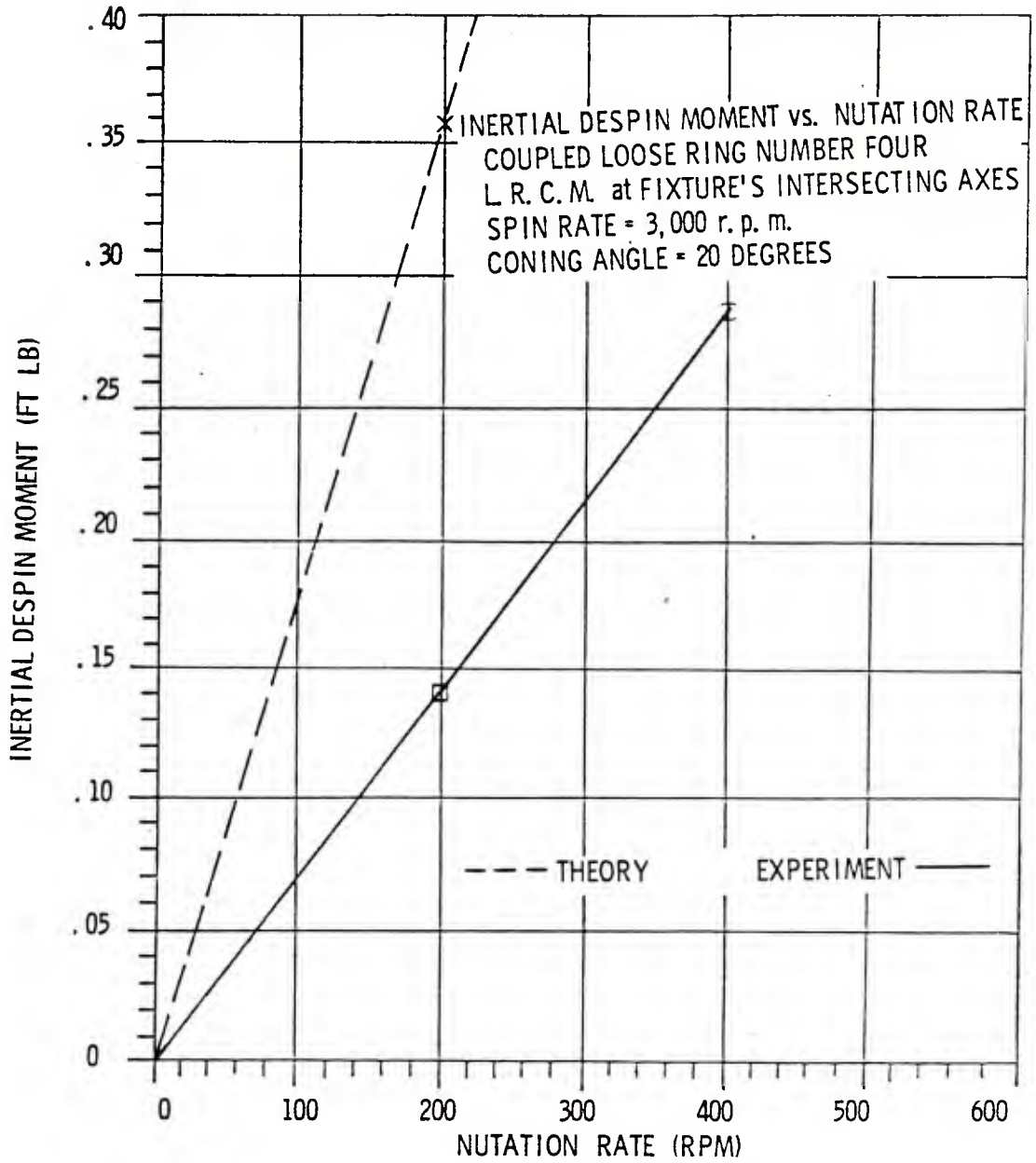


Figure 10d. Test Results from L.R. 4 at 20 Degrees Coning Angle

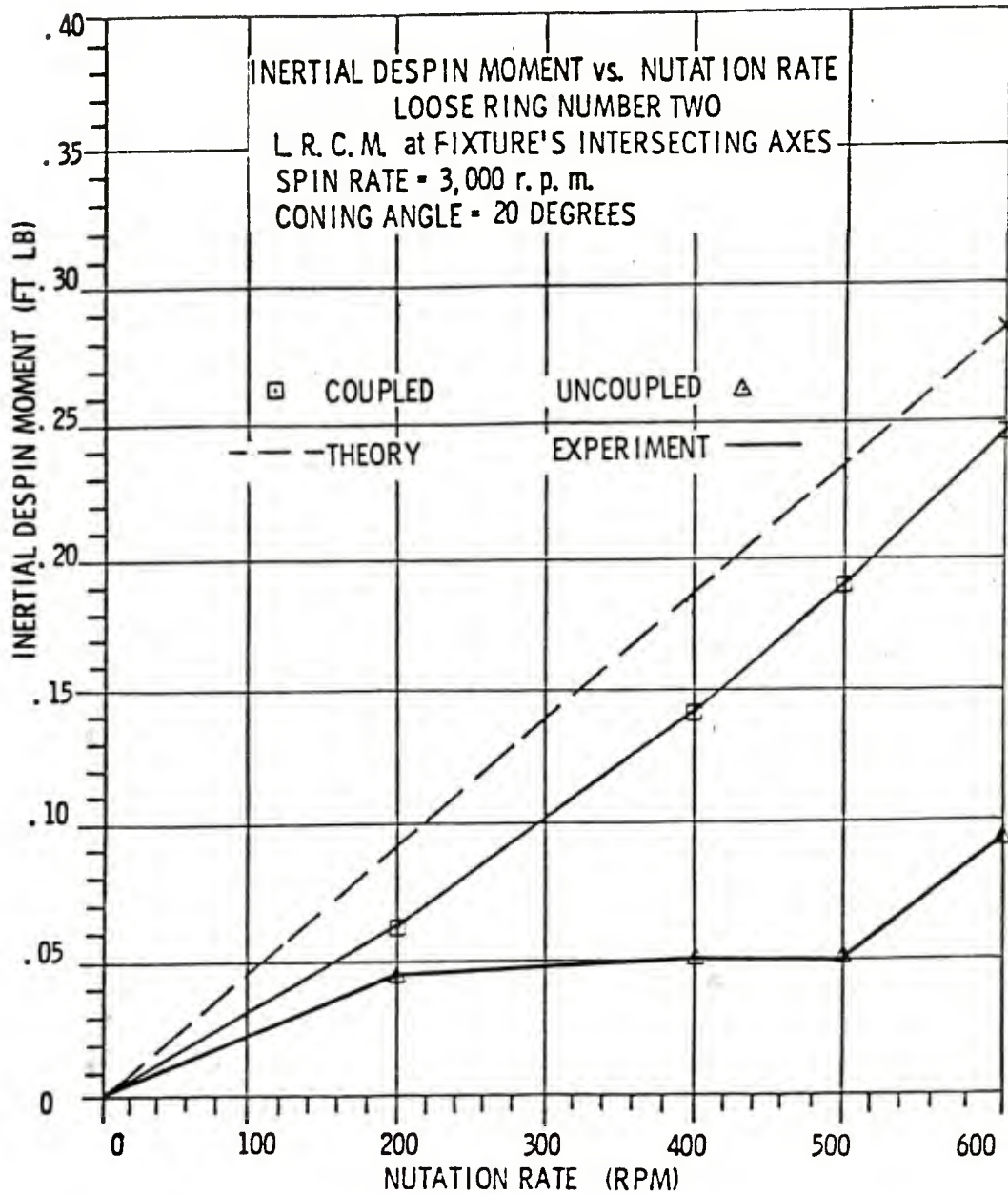


Figure 11. Example of Effect of Spin Coupling

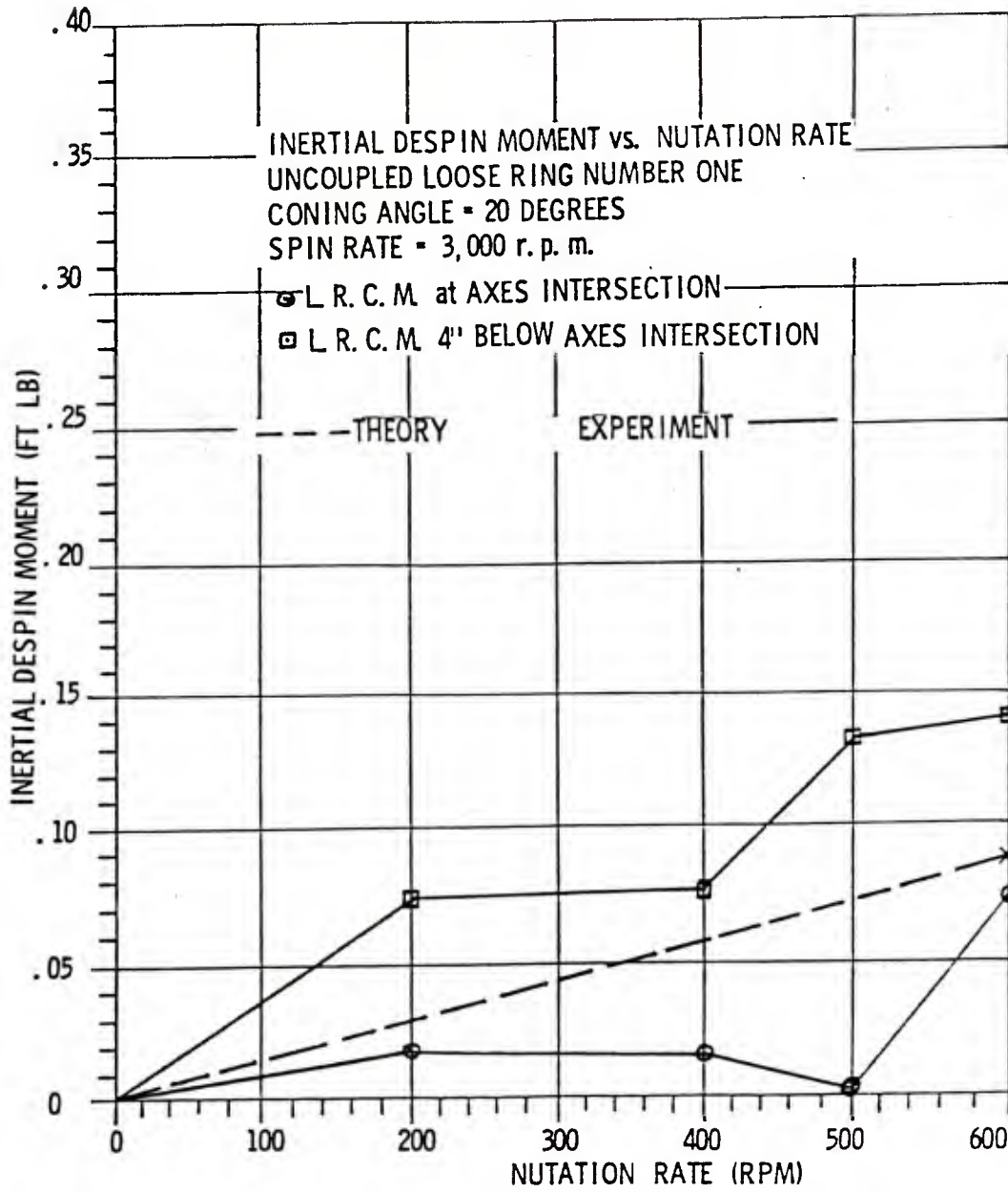


Figure 12. Example of Effect of Loose Ring Axial Position

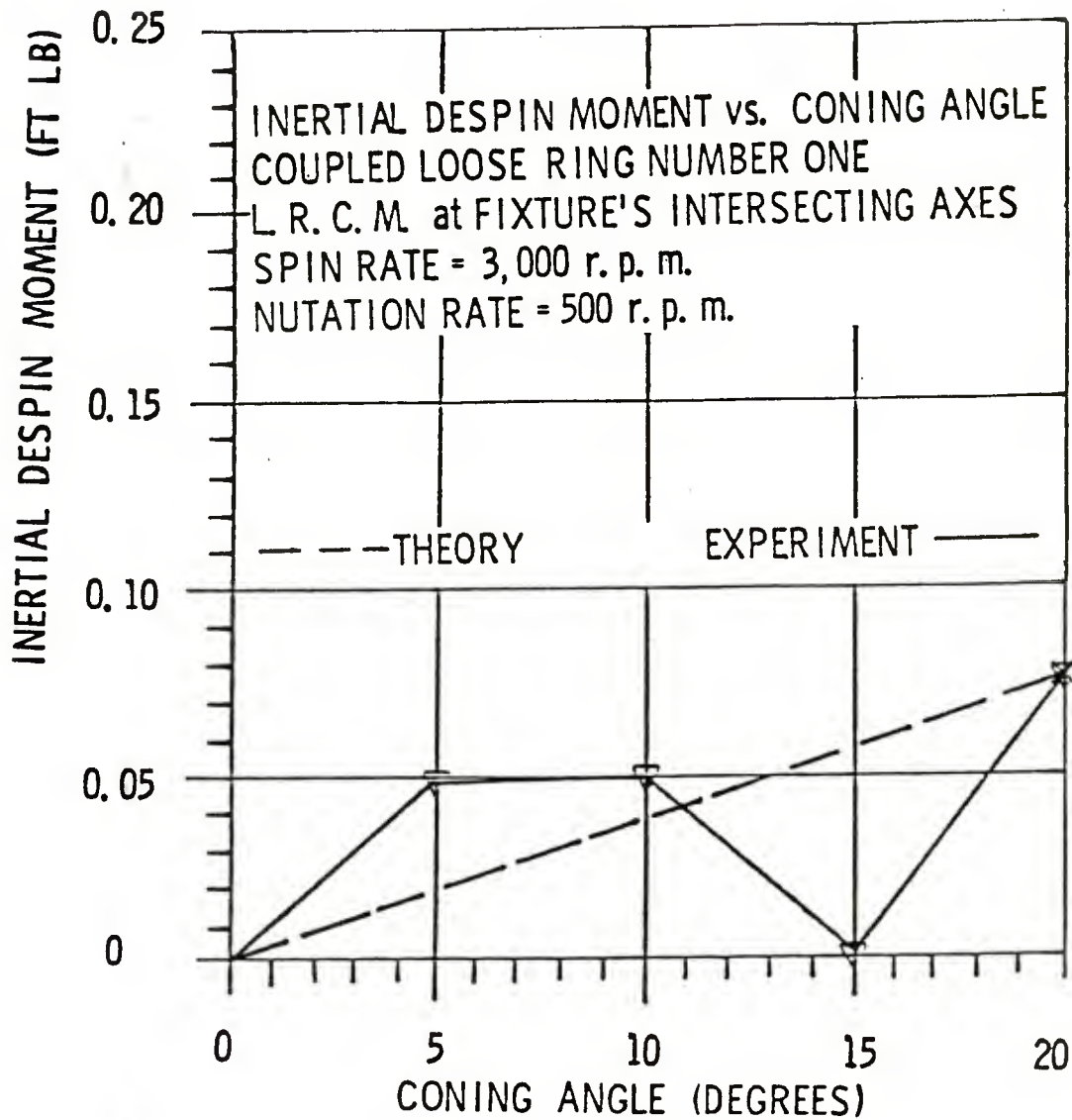


Figure 13. Example of Presumed Aberrant Test Results

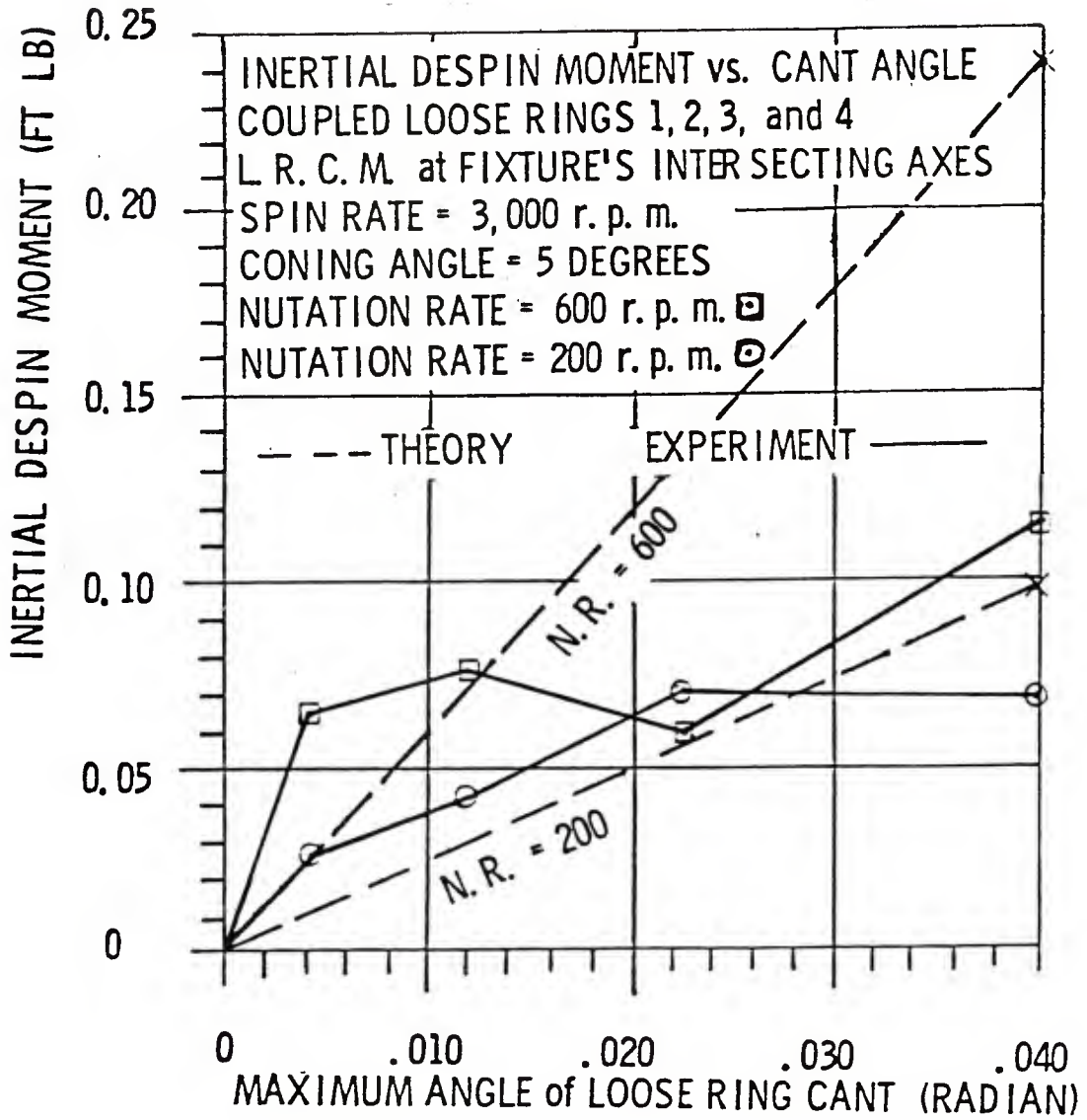


Figure 14. Example of Presumed Limitation of Combined Variables

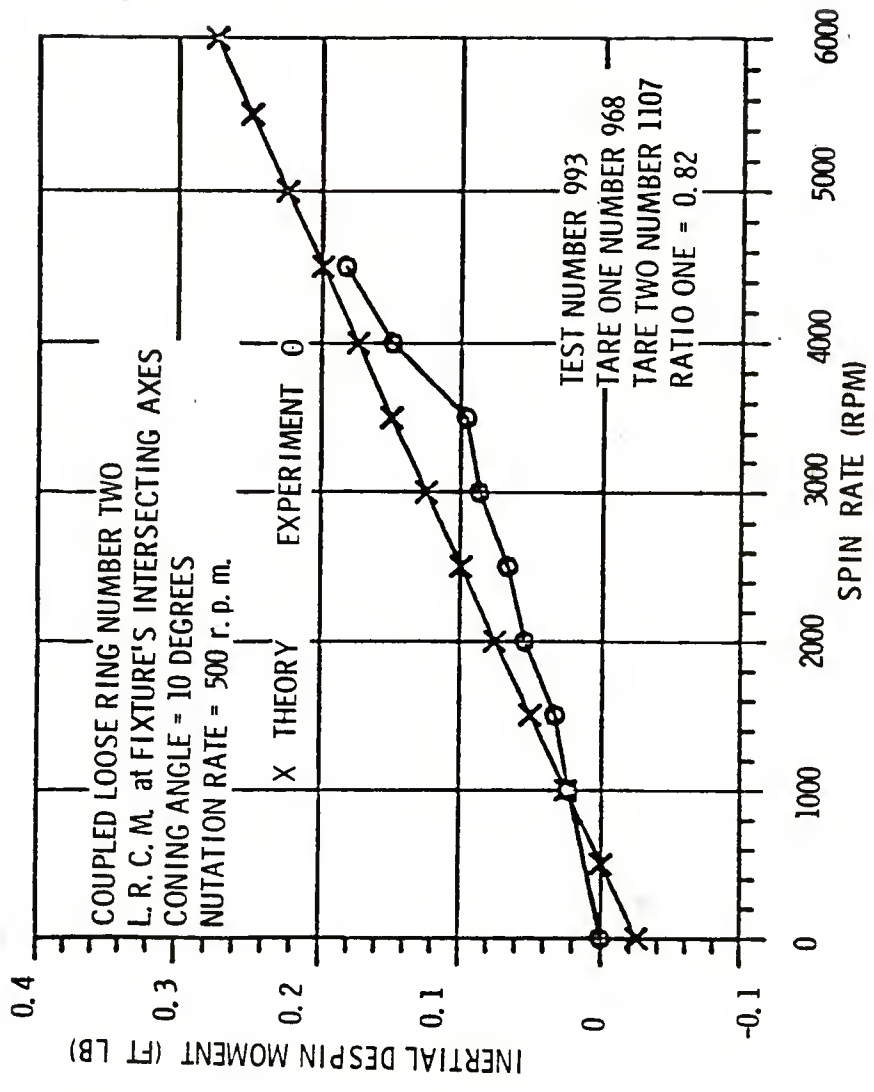


Figure 15. Example Spin-Down Showing Zero Spin Anomaly

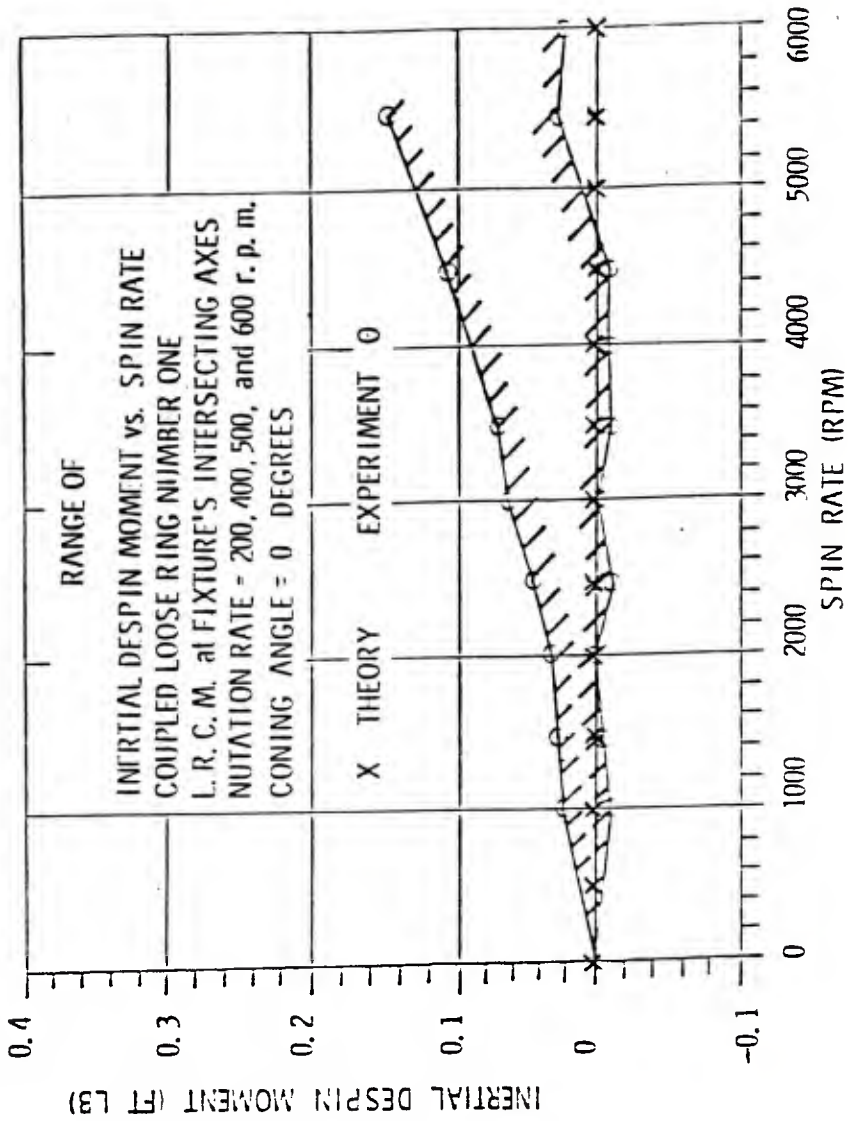


Figure 16a. Zero Coning Angle Test Results Conflict with Theory at Coupled L.R. 1

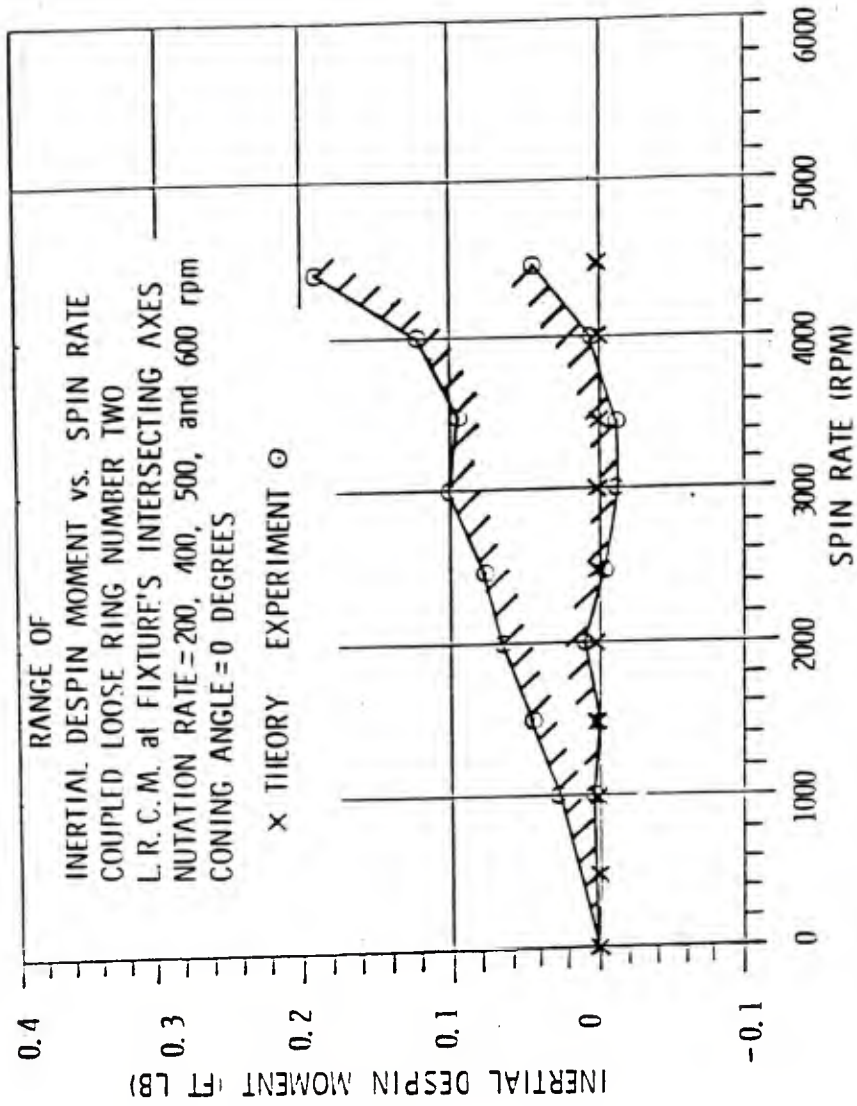


Figure 16b. Zero Coning Angle Test Results Conflict with Theory at Coupled L.R. 2

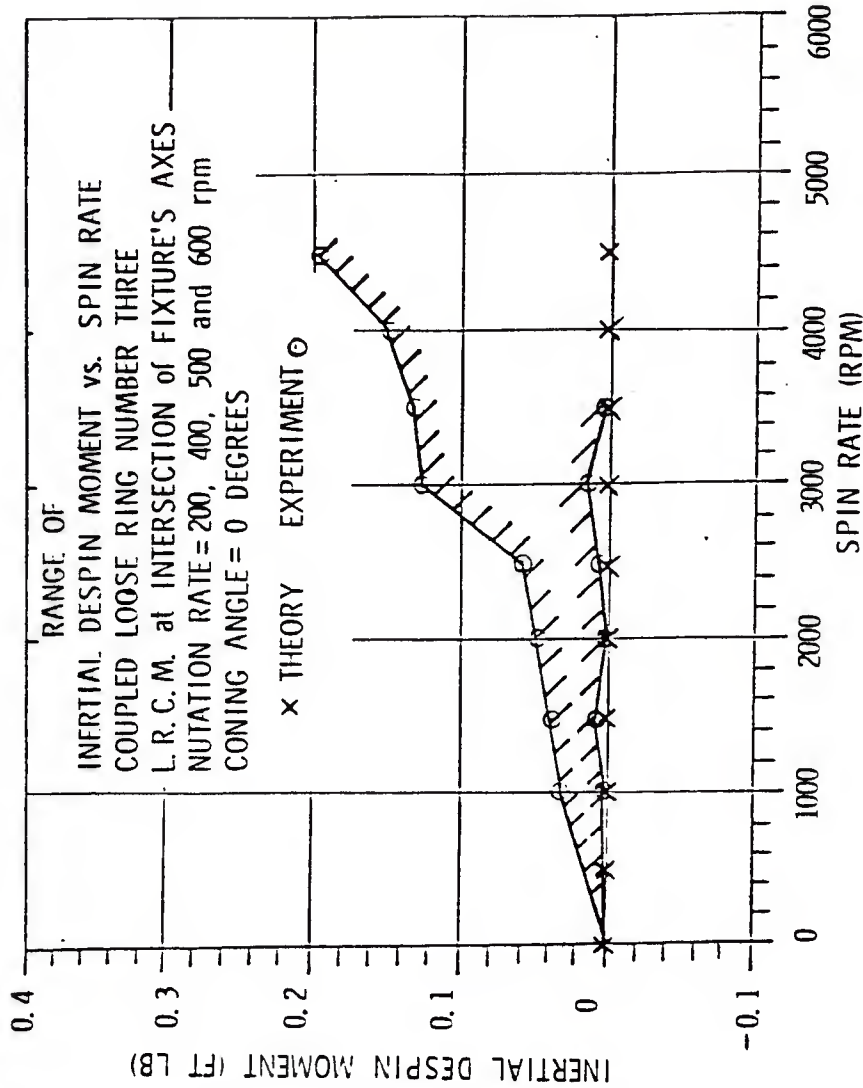


Figure 16c. Zero Coning Angle Test Results Conflict with Theory at Coupled L.R. 3

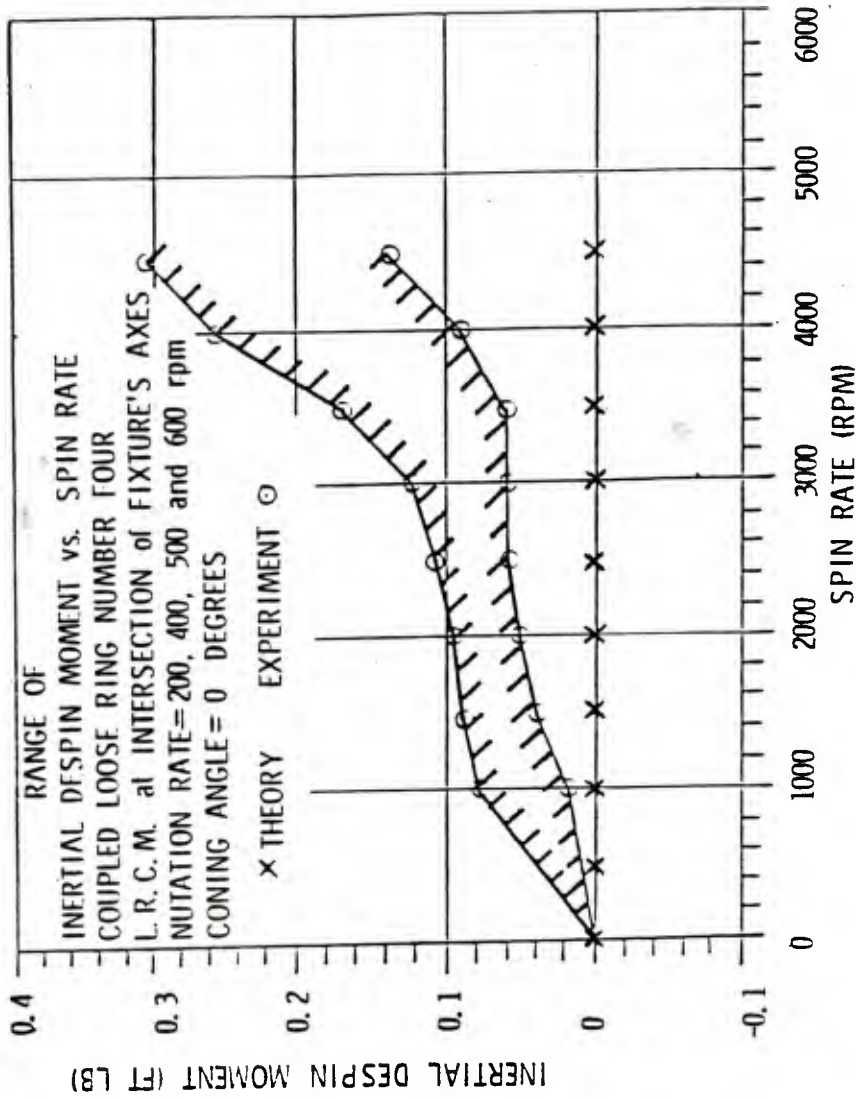


Figure 16d. Zero Coning Angle Test Results Conflict with Theory at Coupled L.R. 4

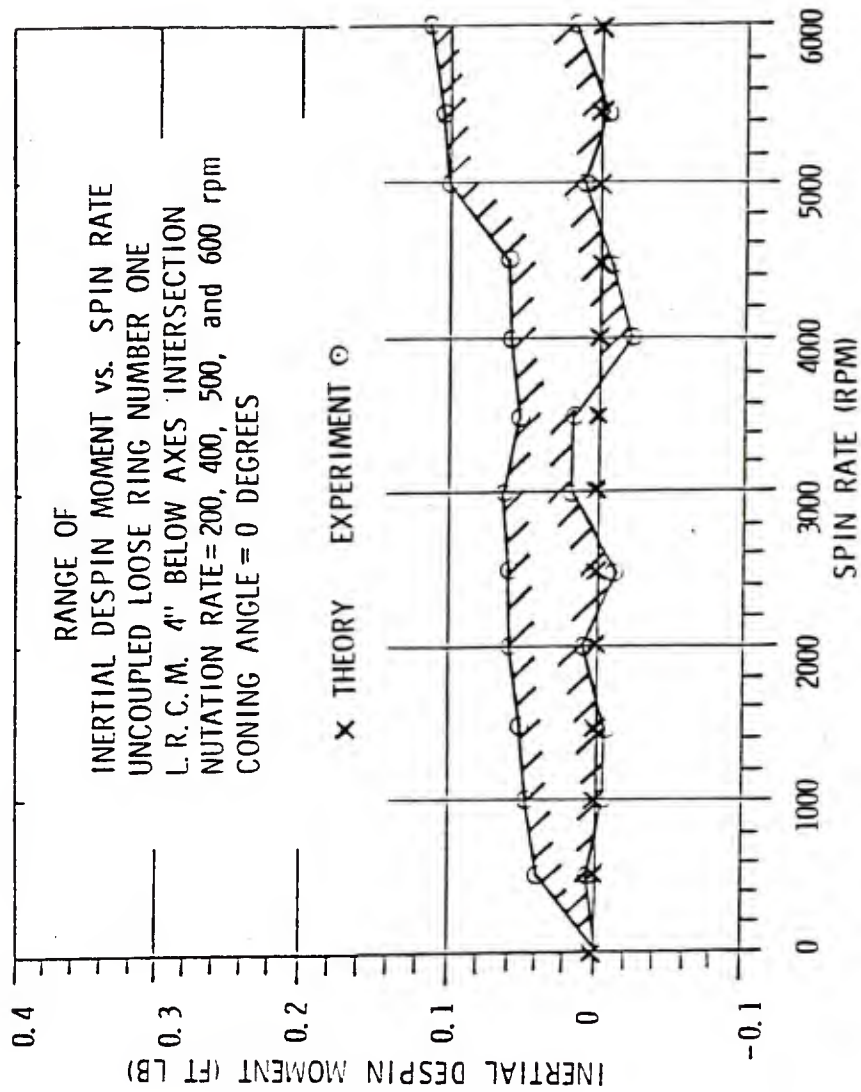


Figure 16e. Zero Coning Angle Test Results Conflict with Theory at Uncoupled L.R. 1 Positioned 4 Inches Below Intersection of Axes

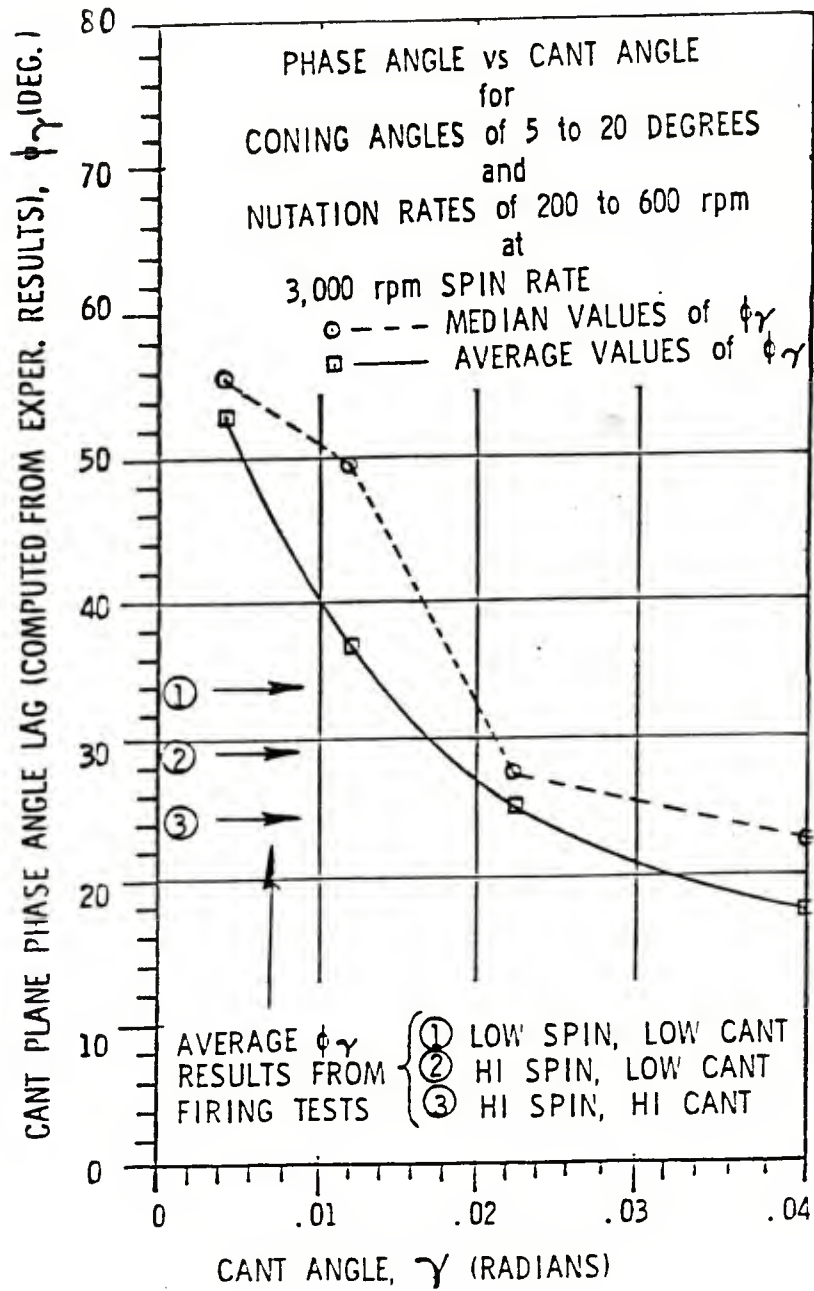


Figure 17. Computed Cant Plane Phase Angle vs. Cant Angle

Table 1. Aerodynamic Coefficients for T317

$I_x/I_t = 0.1352$	0.218	$M < 0.88$
	$C_D = -0.9612 + 1.34M$	$0.88 \leq M \leq 1.1$
	$0.6503 - 0.125M$	$M > 1.1$
$I_{xc}/I_t = 0.0472$		
$I_{tc}/I_t = 0.0251$		
	4.4	$M < 0.88$
	$C_{M_\alpha} = 1.32 + 3.5M$	$0.88 \leq M \leq 1.1$
	5.17	$M > 1.1$
$C_{D_{\delta^2}} = 3$		
$C_{l_p} = -0.012$		
	$C_{M_{p\alpha}} = -0.26 + 9\delta^2$	$\delta < 0.1$
	$-0.017\delta^{-1}$	$\delta \geq 0.1$
$C_{L_\alpha} = 2.0$		
$C_{M_q} + C_{M_\alpha} = -6.3$		

Table 2. Computed Flight Motions of T317

t, s	Round 1 ($\gamma = 0.0037$)			Round 2 ($\gamma = 0.0035$)			Round 3 ($\gamma = 0.0254$)		
	P_b , Hz	K_1 , deg	$\sin\phi_\gamma$	P_b , Hz	K_1 , deg	$\sin\phi_\gamma$	P_b , Hz	K_1 , deg	$\sin\phi_\gamma$
0	108			135			108		
5	105	4	0.48	133	3	0.44	79	24	0.46
10	99	6	0.62	127	5	0.44	52	31	0.41
15				120	9	0.47	35	40	0.40
20				113	13	0.55	26	42	0.38
25	78	20	0.62						
30	69	24	0.62	96	19	0.44			
35	62	27	0.50	88	20	0.43			
40	60	27	0.50	80	20	0.61			

Table 3. Physical Characteristics of Rings

<u>Ring (No)</u>	<u>Outside Diameter (Inches)</u>	<u>Inside Diameter (Inches)</u>	<u>Cant Angle (Deg)</u>	<u>Weight (lb)</u>	<u>Axial Moment of Inertia (ft lb sec²)</u>	<u>Trans. Moment of Inertia (ft lb sec²)</u>
Tare	3.994	2.000	0	10.576	.005760	.005980
1	4.000	2.016	.2922	10.593	.005745	.005926
2	4.015	2.050	.7162	10.560	.005903	.006001
3	4.039	2.092	1.3178	10.571	.005992	.006048
4	4.073	2.158	2.2632	10.560	.006116	.006109

Table 4. Physical Characteristics of Complete Spin Models

<u>Model (Configuration)</u>	<u>Weight (lb)</u>	<u>Axial Moment of Inertia (ft lb sec²)</u>
With Tare Ring	36.60	.01274
With L.R. No. 1	36.62	.01273
With L.R. No. 2	36.59	.01289
With L.R. No. 3	36.60	.01297
With L.R. No. 4	36.59	.01310

Table 5. Spin Rate vs Inertial Despin Rate and Moment

Coupled Ring No. 2		Test No. 993	Tare 1 No. 968	Tare 2 No. 1107		
Coning Angle = 10 deg		L.R.C.M. at Fixture's Intersecting Axes				
Nutation Rate = 500 rpm						
Spin (rpm)	Tare Despin Rate (rad/sec ²)	Tare Model Despin Moment (ft lb)	Test Despin Rate (rad/sec ²)	Test Model Despin Moment (ft lb)	Test Theory (ft lb)	Inertial Despin Moment Difference (ft lb)
6000					.274	
5500					.249	
5000					.224	
4500	15.05	.192	29.06	.374	.183	-.017
4000	12.71	.162	24.09	.310	.148	-.026
3500	11.00	.140	18.33	.236	.096	-.053
3000	10.22	.130	16.76	.216	.086	-.039
2500	9.13	.116	14.14	.182	.066	-.034
2000	8.13	.104	12.22	.157	.054	-.021
1500	7.36	.094	9.77	.126	.032	-.017
1000	6.28	.080	7.98	.103	.023	-.002
500					-.000	
0	0.00	0.000	0.00	0.000	-.025	.025

REFERENCES

1. C. H. Murphy, "Angular Motion of Projectiles with a Moving Internal Part", BRL Memorandum Report No. 2731, U.S. Army Ballistic Research Laboratory, Aberdeen Proving Ground, Maryland, February 1977. AD A037338.
2. M. C. Miller, "Flight Stability Test Fixture for Non-Rigid Payloads", presented at the Chemical Systems Laboratory Technical Conference, 23-24 May 1978.

LIST OF SYMBOLS

$A_{\ell p}$	$\frac{1}{2} \rho S \ell^2 V C_{\ell p}$
C_D	drag coefficient of projectile
$C_{D\delta^2}$	slope of drag coefficient vs square of projectile angle of yaw
$C_{L\alpha}$	slope of lift coefficient vs projectile angle of attack
$C_{\ell p}$	slope of rolling moment coefficient vs projectile roll rate
$C_{M\alpha}$	slope of pitching moment coefficient vs projectile angle of attack
$C_{M\dot{\alpha}}$	slope of pitching moment coefficient vs rate of change of projectile angle of attack
$C_{M_{p\alpha}}$	slope of Magnus moment coefficient vs projectile angle of attack
C_{M_q}	slope of projectile pitching moment coefficient vs pitch rate
$I_{A_{CLRM}}$	axial moment of inertia of complete loose ring model
$I_{A_{CTM}}$	axial moment of inertia of complete model (with tare ring)
I_t	projectile transverse moment of inertia
I_{tc}	transverse moment of inertia of loose internal component
I_x	projectile axial moment of inertia
I_{xc}	axial moment of inertia of loose internal component
K_1	nutation coning angle of projectile
ℓ	projectile length
LRCM	loose ring center-of-mass
M	Mach number

LIST OF SYMBOLS (Continued)

$M_{I_{LR}}$	inertial despin moment of the loose internal component
M_{LR}	despin moment of the complete model (with loose internal component), $\dot{\omega}_{LR} I_{A_{CLRM}}$
M_T	despin moment of the complete model (with tare ring), $\dot{\omega}_T I_{A_{CTM}}$
P_b	projectile roll rate
α	angle of attack of the projectile
γ	angle of cant of the loose internal component
δ	angle between the flight path and the axis of symmetry of the projectile
ρ	air density
ϕ_1	nutation angle
ϕ_γ	polar angle that the cant plane of the loose internal component makes with the projectile's angle of attack plane
ω	spin rate
ω_{LR}	model spin rate (with loose ring)
ω_T	model spin rate (with tare ring)
$(\dot{\quad})$	$d(\quad)/dt$

APPENDIX A: COMPUTED CANT PLANE PHASE ANGLES DURING SPIN-DOWNS

Because of the inability to measure the cant plane phase angle during the spin-down experiments, as stated earlier, it was not possible to verify the spin theory. However, it would be useful to use the spin theory in conjunction with the experimental results to make predictions of the variations in the cant plane phase angle to see how they might vary during a spin-down, as well as with coning angle and nutation rate.

The results are shown in Tables A1a through A1d. All the coupled loose ring results are given for the case where the center-of-mass of the loose rings is at the intersection of the fixture's spin and coning axes. Computations of the average value of the phase angle were made for each discrete spin rate of the tests and, although the average value was found to vary by as much as ± 5 degrees, it was determined to have a nominal level of approximately 30 degrees. If the zero spin rate, zero nutation rate, and zero coning angle conditions are omitted from the coupled loose ring tests, where the loose rings were positioned at the intersection of the fixture's axes, there remains 768 possible data points. The inability of the spin fixture to provide the high spin rates during many of the spin-downs precluded obtaining data at 311 points of the test agenda. This left 457 points where data were actually acquired. However, when the phase angles were computed, only 356 points provided phase angles between 0 and 90 degrees. Most of the other 101 points had indicated phase angles larger than 90 degrees. Only a few indications of phase angles less than zero existed and they were usually at the lowest spin rates, where the despin effect was small and somewhat indeterminate.

At this point, it is speculated that the phase angle does not necessarily have to fall between zero and 90 degrees. Figure 3 in the report shows a continually increasing magnitude of the computed (not observed) angular motion for a T-317 which had no looseness of its internal parts. However, Figure 4 indicates a more rapid growth in the magnitude of this angular motion followed by a reduction during the second half of the flight when a 4 milliradian angular motion was permitted in the rings. A traverse of the cant-plane phase angle from less than 90 degrees to more than 90 degrees is seen as a possible mechanism.

Figure A1 shows the computed phase angles that fall between zero and 90 degrees. The average value, computed for each spin rate, is seen to be quite constant at approximately 30 degrees even though the individual results vary widely.

Figures A2a through A2d show the cant-plane phase angle results computed for each loose ring. Four graphs are presented on each page to aid in the visualization. Each detailed plot includes the test results at a single coning angle and each curve of the family shows how the phase angle data at a specific nutation rate varies with spin. These results indicate a trend toward orderly patterns but typically indicate wide variations in the cant-plane phase angle with spin rate. Figure A2c for loose ring number three indicates a definite trend toward an orderly family of results for the coning-angles-of-five-degrees configuration. These curves not only indicate an organized trend with nutation rate but also have a fairly smooth variation with spin rate. The upsweep toward a large cant-plane phase angle at low spin rate is most pronounced in this set of data, but can also be observed in some of the other data sets, and is indicative of the kind of result that was anticipated.

Averaging of the results has been employed in Figure A3 to attempt to find a characteristic cant-plane phase angle from the ground-based tests. An average phase angle of approximately 30 degrees is indicated. It appears now that 30 degrees would have been much better than the 45 degrees that was assumed for the theoretical inertial despin moment computations; however, so much variation shows in the phase angle as to make doubtful the use of a constant value.

COMPUTED CANT PLANE PHASE ANGLES DURING SPIN-DOWNS

<u>Figure</u>		<u>Page</u>
A1	Cant Plane Phase Angle vs. Spin Rate	68
A2	Cant Plane Phase Angle vs. Spin Rate	69
	a. L.R. 1	69
	b. L.R. 2	70
	c. L.R. 3	71
	d. L.R. 4	72
A3	Phase Angle vs. Cant Angle	73

LIST OF TABLES

<u>Table</u>		<u>Page</u>
A1	Computed Experimental-Based Cant Plane Phase Lag Angle, ϕ_{γ} (Degrees)	74
	a. Cant Angle = .004 Radian	74
	b. Cant Angle = .012 Radian	75
	c. Cant Angle = .0225 Radian	76
	d. Cant Angle = .040 Radian	77

EXPERIMENTAL RESULTS, INCLUDING ALL CANT ANGLE, CONING ANGLE AND NUTATION RATE DATA WHEN RINGS WERE POSITIONED AT THE INTERSECTION OF THE FIXTURE'S SPIN AND CONING AXES. (ALL USEFUL RESULTS INCLUDE 356 TEST POINTS OUT OF A POSSIBLE 459)

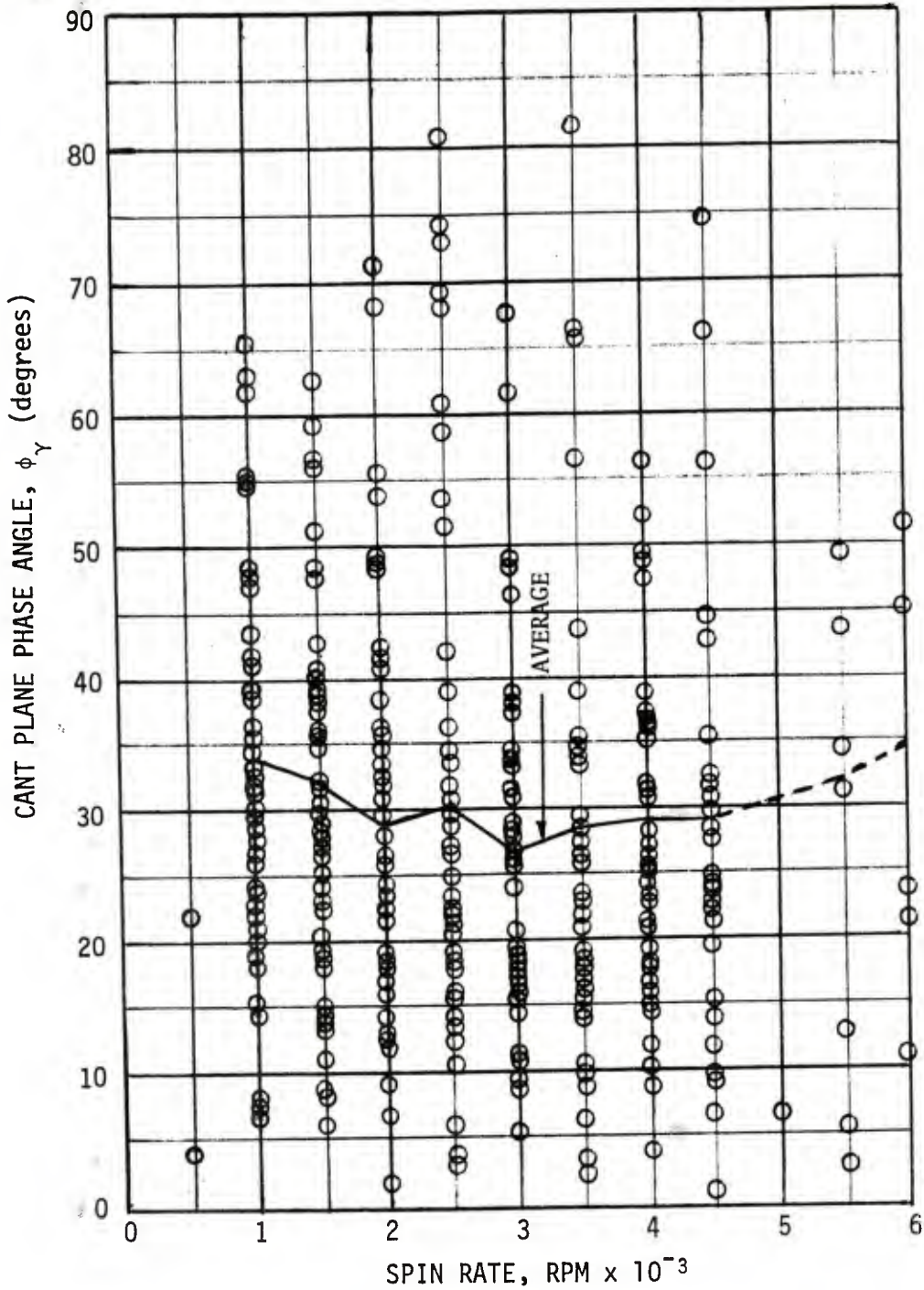


Figure A1. Cant Plane Phase Angle vs. Spin Rate

Cant Plane Phase Angle vs. Spin Rate
 Coupled Loose Ring Number One (Cant Angle, $\gamma = 0.004$ radian)
 Loose Ring Positioned at Intersection of Fixture's Axes

- | | |
|---|---|
| <p>○ Nutation Rate = 200 RPM
 + Nutation Rate = 400 RPM</p> | <p>◻ Nutation Rate = 500 RPM
 X Nutation Rate = 600 RPM</p> |
|---|---|

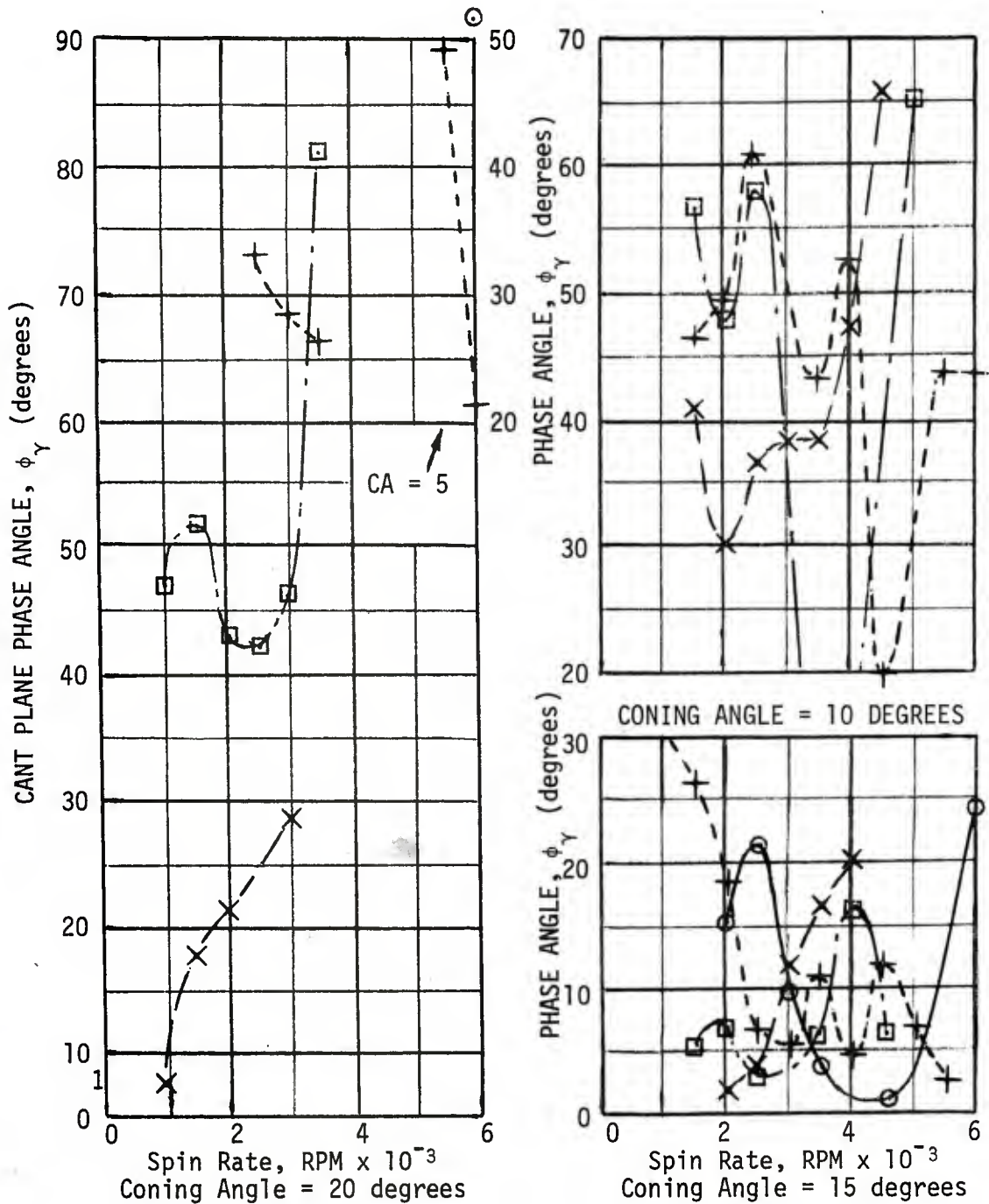
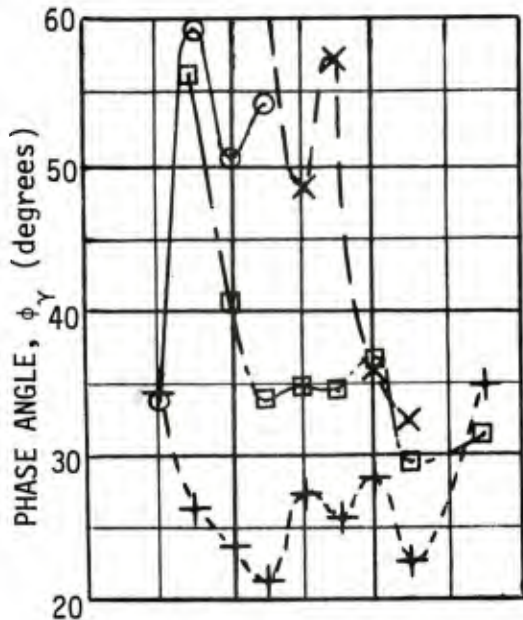


Figure A2a. Cant Plane Phase Angle vs. Spin Rate, LR 1

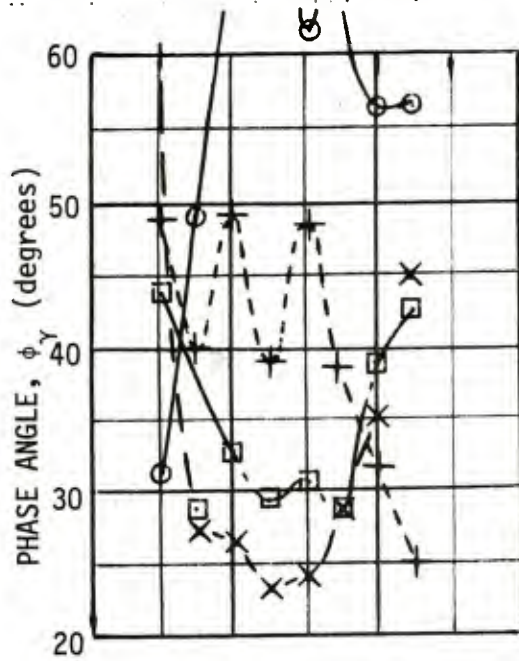
Cant Plane Phase Angle vs. Spin Rate
 Coupled Loose Ring Number Two (Cant Angle, $\gamma = .012$ radian)
 Loose Ring Positioned at Intersection of Fixture's Axes

○ Nutation Rate = 200 RPM
 + Nutation Rate = 400 RPM

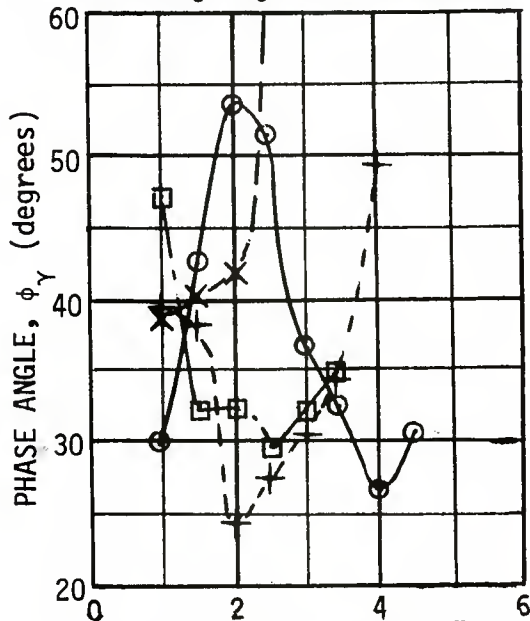
□ Nutation Rate = 500 RPM
 X Nutation Rate = 600 RPM



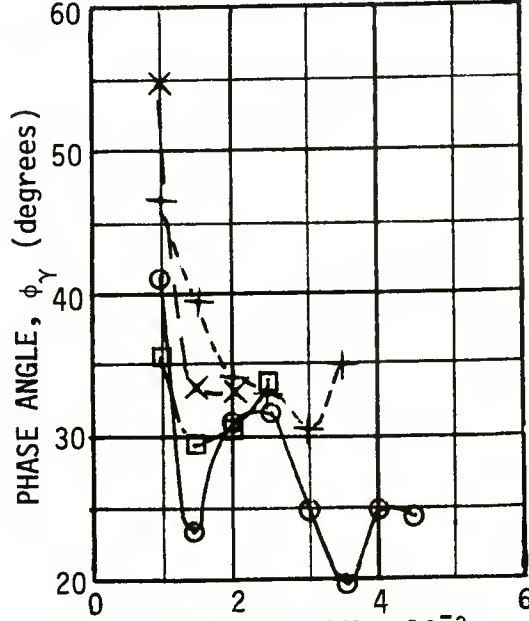
Coning Angle = 5 degrees



Coning Angle = 10 degrees



Spin Rate, $\text{RPM} \times 10^{-3}$
 Coning Angle = 15 degrees



Spin Rate, $\text{RPM} \times 10^{-3}$
 Coning Angle = 20 degrees

Figure A2b. Cant Plane Phase Angle vs. Spin Rate, L.R. 2

Cant Plane Phase Angle vs. Spin Rate
 Coupled Loose Ring Number Three (Cant Angle, $\gamma = .0225$ Radian)
 Loose Ring Positioned At Intersection of Fixture's Axes

○ Nutation Rate = 200 RPM
 + Nutation Rate = 400 RPM

□ Nutation Rate = 500 RPM
 X Nutation Rate = 600 RPM

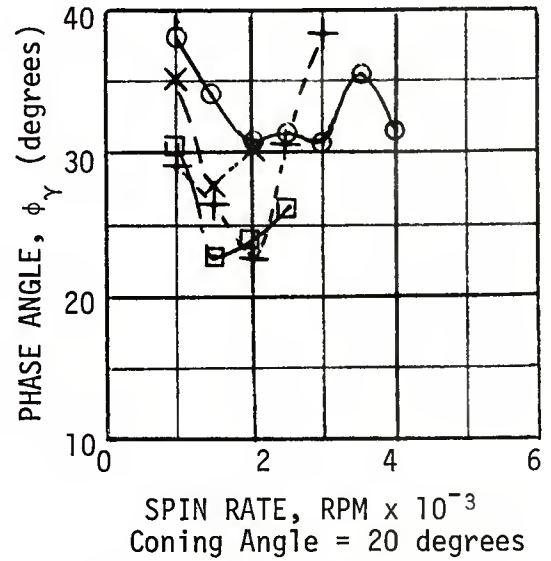
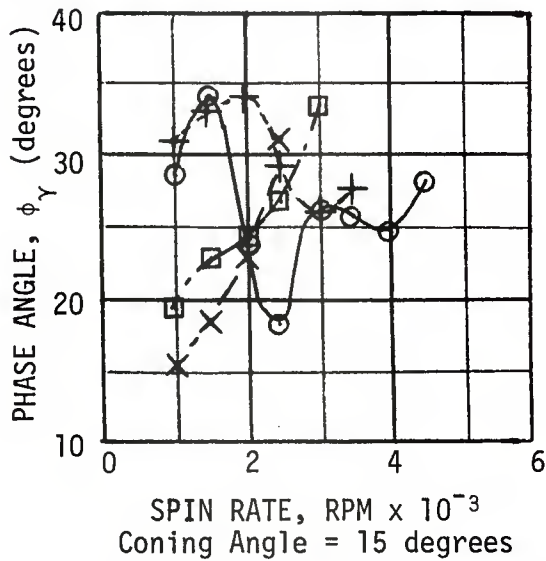
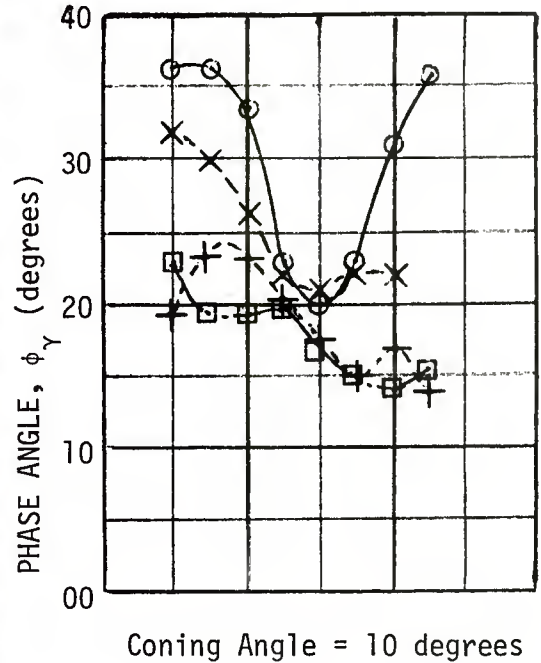
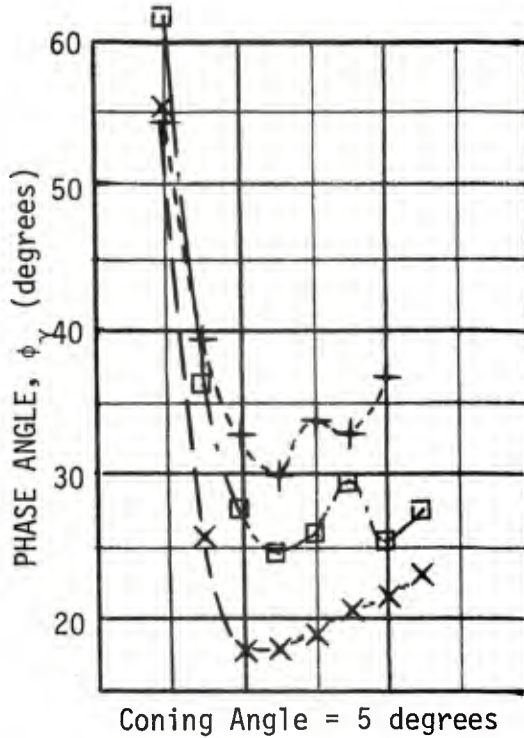
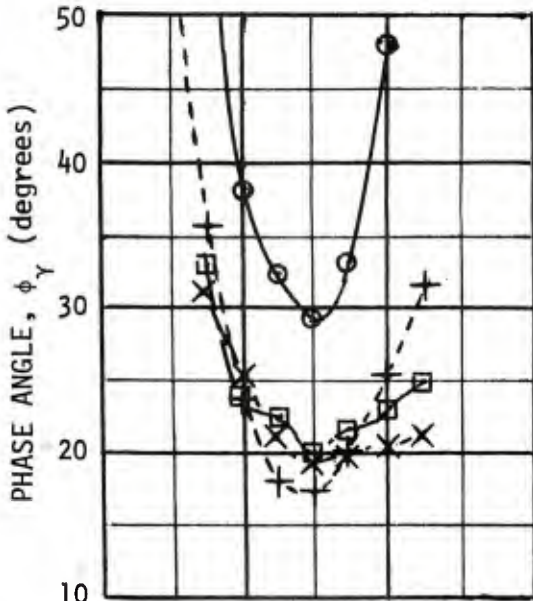


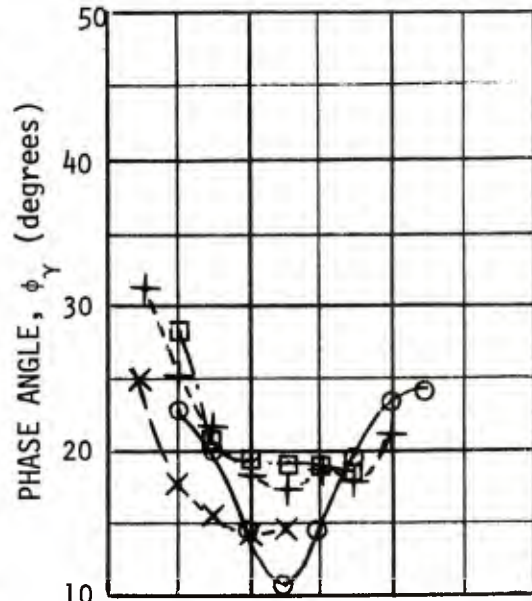
Figure A2c. Cant Plane Phase Angle vs. Spin Rate, L.R. 3

Cant Plane Phase Angle vs. Spin Rate
 Coupled Loose Ring Number Four (Cant Angle, $\gamma = .040$ Radian)
 Loose Ring Positioned at Intersection of Fixture's Axes

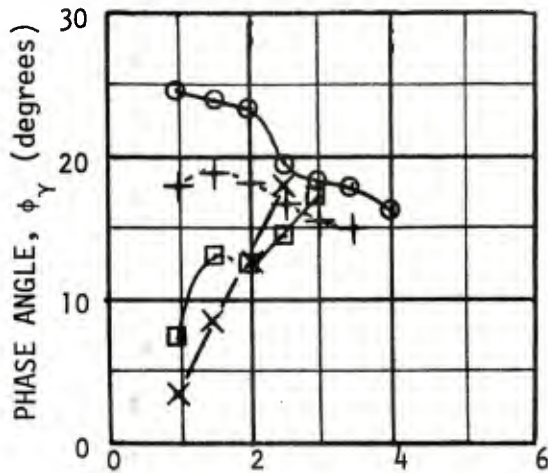
- | | |
|---|---|
| <p>⊙ Nutation Rate = 200 RPM
 + Nutation Rate = 400 RPM</p> | <p>□ Nutation Rate = 500 RPM
 X Nutation Rate = 600 RPM</p> |
|---|---|



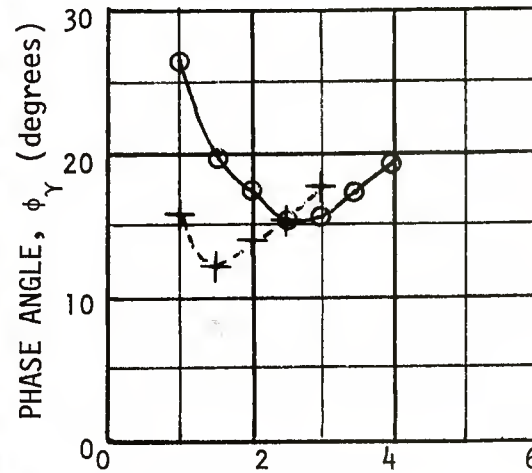
Coning Angle = 5 degrees



Coning Angle = 10 degrees



Spin Rate, RPM $\times 10^{-3}$
 Coning Angle = 15 degrees



Spin Rate, RPM $\times 10^{-3}$
 Coning Angle = 20 degrees

Figure A2d. Cant Plane Phase Angle vs. Spin Rate, L.R. 4

AVERAGE VALUES
of
PHASE ANGLE vs CANT ANGLE

SPIN FIXTURE RESULTS

- MEDIAN PHASE ANGLES } FROM 356 COMPUTED EXPERIMENTAL
 - AVERAGE PHASE ANGLES } POINTS OUT OF A POSSIBLE 457
- LOOSE RINGS 1,2,3 and 4 (CANT ANGLES FROM 0.004 to 0.040 RADIAN)
CONING ANGLE 5,10,15 and 20 DEGREES
NUTATION RATE = 200,400,500 and 600 RPM
SPIN RATE FROM MAXIMUM TO MINIMUM (APPROX. 4,000 to 1,000 RPM)

RANGE FIRING RESULTS

- △ $\gamma = .0037, 108 > p_b \text{ (Hz)} > 60, 4 < K_1 \text{ (DEG)} < 27$; Avg. $\phi_\gamma = 33.95$
- ▽ $\gamma = .0035, 135 > p_b \text{ (Hz)} > 80, 3 < K_1 \text{ (DEG)} < 20$; Avg. $\phi_\gamma = 28.97$
- ◇ $\gamma = .0254, 108 > p_b \text{ (Hz)} > 26, 24 < K_1 \text{ (DEG)} < 42$; Avg. $\phi_\gamma = 24.37$

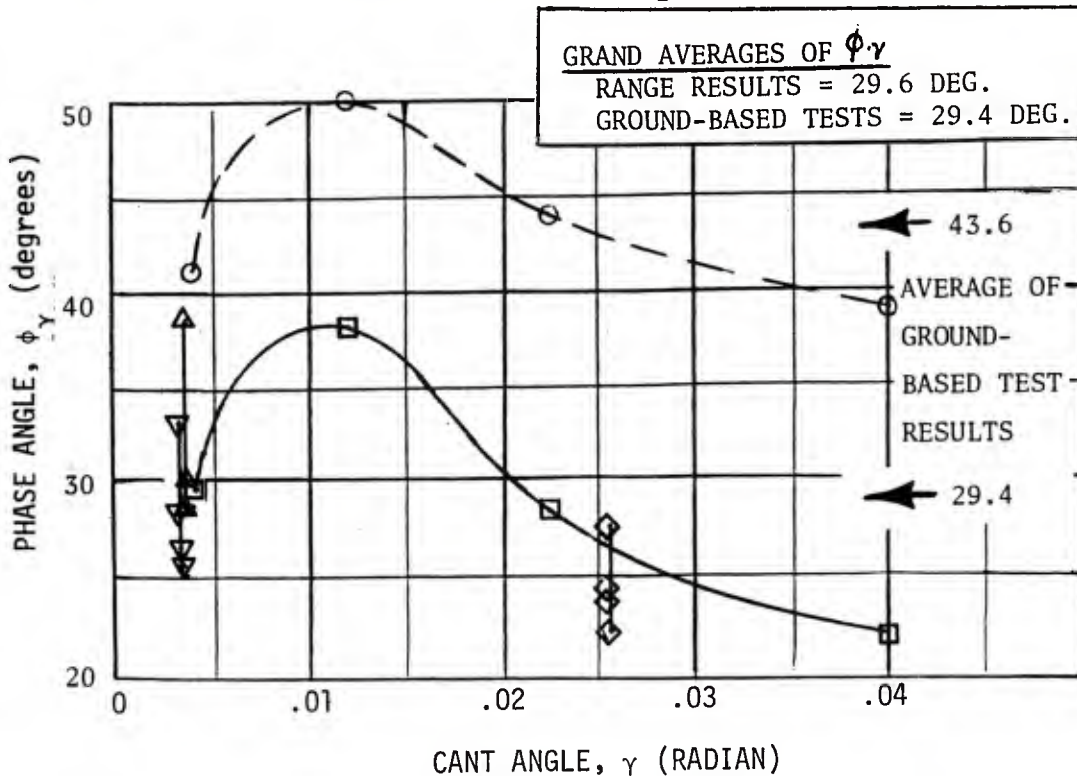


Figure A3. Phase Angle vs. Cant Angle

Table A1. Computed Experimental-Based Cant Plane Phase Lag Angle, ϕ_{γ} (Degrees)

a. Cant Angle = .004 Radian

L.R. (NO.)	SPIN (RPM)	CONING ANGLE = 5 DEGREES						CONING ANGLE = 10 DEGREES					
		NUTATION RATE (RPM)				MEDIAN AVERAGE		NUTATION RATE (RPM)				MEDIAN AVERAGE	
		200	400	500	600			200	400	500	600		
(CANT ANGLE = .004 RAD)	6000	51.4	21.4	-	-	36.4	40.7	-	43.8	-	-	34.3	39.3
	5500	-	-	-	-			-	43.9	-	-		
	5000	-	-	-	-			-	-	65.1	-		
	4500	-	-	-	-			-	19.5	-	65.9		
	4000	-	-	-	-			-	52.4	-	47.1		
	3500	-	-	-	-			-	43.1	2.6	38.4		
	3000	-	-	-	-			-	-	-	38.6		
	2500	-	-	-	-			-	60.7	58.7	36.0		
	2000	-	-	-	-			-	48.8	47.8	29.8		
	1500	-	-	-	-			-	47.1	56.8	40.7		
	1000	-	-	-	-			-	22.9	-	-		
500	-	-	-	-			-	-	-	-			
MEDIAN AVERAGE		51.4	35.3					-	40.1	33.9	47.9		
		51.4	35.3					-	37.6	46.2	42.4		
		CONING ANGLE = 15 DEGREES						CONING ANGLE = 20 DEGREES					
(CANT ANGLE = .004 RAD)	6000	24.1	-	-	-	16.3	11.0	-	-	-	-	44.4	45.4
	5500	-	2.6	-	-			-	-	-	-		
	5000	-	6.7	-	-			-	-	-	-		
	4500	1.0	11.9	6.2	-			-	-	-	-		
	4000	-	4.3	15.8	19.9			-	-	-	-		
	3500	4.0	10.7	6.5	16.5			-	66.5	81.2	-		
	3000	9.4	5.1	-	11.1			-	67.9	46.0	28.1		
	2500	21.4	6.3	3.5	3.9			-	72.9	41.9	21.1		
	2000	14.8	18.3	7.1	2.1			-	-	42.4	18.0		
	1500	-	27.2	5.4	-			-	-	51.3	7.6		
	1000	-	31.5	-	-			-	-	46.4	-		
500	-	-	-	-			-	-	-	-			
MEDIAN AVERAGE		12.6	17.1	9.7	11.0			-	69.7	61.6	17.9		
		12.5	12.5	7.4	10.7			-	69.1	51.5	18.7		
		COMPOSITE RESULTS FOR L.R. #1 (INCL. ALL NUTATION RATES, CONING ANGLES AND SPIN RPM'S)											
		MEDIAN AVERAGE		41.1 29.3									

Table A1. Continued

b. Cant Angle = .012 Radian

L.R.	SPIN	CONING ANGLE = 5 DEGREES				CONING ANGLE = 10 DEGREES									
		NUTATION RATE (RPM)				NUTATION RATE (RPM)				MEDIAN	AVERAGE				
		(NO.)	(RPM)	200	400	500	600	200	400			500	600		
(CANT ANGLE = .012 RAD)	2	6000	-	-	-	-	45.1	37.9	-	-	-	-	52.0	41.8	
	5500	-	39.4	31.4	-	-	-	-	-	-	-	-	-	-	
	5000	-	-	-	-	-	-	-	-	-	-	-	-	-	
	4500	-	22.2	29.7	32.1	-	-	-	56.1	24.9	42.8	44.8	-	-	
	4000	-	28.2	36.9	36.0	-	-	-	56.2	31.7	39.0	35.2	-	-	
	3500	-	25.4	34.2	56.5	-	-	-	65.8	38.5	28.4	28.3	-	-	
	3000	-	27.1	34.7	48.7	-	-	-	61.2	48.0	30.8	23.8	-	-	
	2500	53.8	20.6	34.3	69.6	-	-	-	80.8	38.9	29.5	23.1	-	-	
	2000	55.4	23.2	40.8	-	-	-	-	71.9	49.1	32.5	25.8	-	-	
	1500	59.0	26.0	56.4	-	-	-	-	48.2	40.1	28.6	26.4	-	-	
	1000	33.7	34.0	-	-	-	-	-	30.9	48.6	44.0	62.7	-	-	
	500	-	-	-	-	-	-	-	-	-	-	-	-	-	
MEDIAN		46.4	27.8	43.1	50.9	-	-	-	55.9	37.0	36.2	42.9	-	-	
AVERAGE		50.5	26.8	37.3	48.6	-	-	-	58.9	40.0	34.5	33.8	-	-	
		CONING ANGLE = 15 DEGREES				CONING ANGLE = 20 DEGREES									
(CANT ANGLE = .012 RAD)	2	6000	-	-	-	-	46.2	37.7	-	-	-	-	37.5	32.9	
	5500	-	-	-	-	-	-	-	-	-	-	-	-	-	
	5000	-	-	-	-	-	-	-	-	-	-	-	-	-	
	4500	30.7	-	-	-	-	-	-	24.3	-	-	-	-	-	
	4000	26.5	49.8	-	-	-	-	-	25.0	-	-	-	-	-	
	3500	32.4	33.9	34.2	-	-	-	-	19.7	35.1	-	-	-	-	
	3000	36.7	30.2	31.3	-	-	-	-	25.1	30.5	-	-	-	-	
	2500	51.3	27.2	29.7	67.8	-	-	-	31.7	32.6	32.5	-	-	-	
	2000	53.6	24.5	32.3	41.5	-	-	-	30.9	34.1	30.3	33.4	-	-	
	1500	42.3	38.7	32.1	40.0	-	-	-	24.0	39.5	29.6	33.4	-	-	
	1000	30.0	40.4	46.8	39.7	-	-	-	41.6	46.8	35.6	55.2	-	-	
	500	-	-	-	-	-	-	-	-	-	-	-	-	-	
MEDIAN		40.1	37.2	38.3	53.8	-	-	-	30.7	38.7	32.6	44.3	-	-	
AVERAGE		37.9	35.0	34.4	47.3	-	-	-	27.8	36.4	32.0	40.7	-	-	
		COMPOSITE RESULTS FOR L.R. #2 (INCL. ALL NUTATION RATES, CONING ANGLES, AND SPIN RPM'S)													
MEDIAN														50.3	
AVERAGE														38.0	

Table A1. Continued

c. Cant Angle = .0225 Radian

L.R. (NO.)	SPIN (RPM)	CONING ANGLE = 5 DEGREES						CONING ANGLE = 10 DEGREES					
		NUTATION RATE (RPM)				MEDIAN	AVERAGE	NUTATION RATE (RPM)				MEDIAN	AVERAGE
		200	400	500	600			200	400	500	600		
(CANT ANGLE = .0225 RAD) 5	6000	-	-	-	-	41.6	34.2	-	-	-	-	24.9	22.8
	5500	-	-	-	-	-	-	-	-	-	-	-	-
	5000	-	-	-	-	-	-	-	-	-	-	-	-
	4500	-	-	27.5	23.1	-	-	35.8	13.9	15.2	-	-	-
	4000	-	36.7	25.5	21.7	-	-	31.2	16.5	14.6	22.1	-	-
	3500	-	33.0	29.5	20.7	-	-	23.0	14.8	14.9	22.4	-	-
	3000	-	33.5	25.8	18.6	-	-	20.0	17.5	16.9	20.3	-	-
	2500	74.3	29.9	24.8	17.9	-	-	23.0	20.1	19.6	21.9	-	-
	2000	68.2	32.3	27.8	17.8	-	-	33.6	23.3	19.5	26.2	-	-
	1500	-	39.4	36.3	25.7	-	-	35.8	23.5	19.7	30.0	-	-
	1000	-	54.3	61.7	55.1	-	-	35.9	19.1	23.2	31.9	-	-
500	-	-	-	-	-	-	-	-	-	-	-	-	
MEDIAN AVERAGE		71.3	42.1	43.3	36.5			28.0	18.7	18.9	25.6		
		71.3	37.0	32.4	25.1								
		CONING ANGLE = 15 DEGREES						CONING ANGLE = 20 DEGREES					
(CANT ANGLE = .0225 RAD) 4	6000	-	-	-	-	24.6	26.2	-	-	-	-	30.6	30.4
	5500	-	-	-	-	-	-	-	-	-	-	-	-
	5000	-	-	-	-	-	-	-	-	-	-	-	-
	4500	28.1	-	-	-	-	-	-	-	-	-	-	-
	4000	24.6	-	-	-	-	-	30.7	-	-	-	-	-
	3500	25.6	27.6	-	-	-	-	35.6	-	-	-	-	-
	3000	26.1	26.6	33.6	-	-	-	30.4	37.8	-	-	-	-
	2500	18.6	29.5	27.1	31.0	-	-	31.4	30.8	26.4	-	-	-
	2000	24.0	33.8	24.4	23.6	-	-	31.5	22.8	24.4	30.7	-	-
	1500	34.4	33.2	23.2	18.7	-	-	34.4	26.2	23.4	28.1	-	-
	1000	28.4	31.0	14.7	15.4	-	-	38.4	28.7	30.8	35.3	-	-
500	-	-	-	-	-	-	-	-	-	-	-	-	
MEDIAN AVERAGE		26.5	30.2	24.2	23.2			34.4	30.3	27.1	31.7		
		26.2	30.3	24.6	22.2								
		COMPOSITE RESULTS FOR L.R. #3 (INCL. ALL NUTATION RATES, CONING ANGLES AND SPIN RPM'S)											
		MEDIAN		44.1									
		AVERAGE		28.0									

Table A1. Continued

d. Cant Angle = .040 Radian

L.R.	SPIN	CONING ANGLE = 5 DEGREES						CONING ANGLE = 10 DEGREES							
		NUTATION RATE (RPM)				MEDIAN AVERAGE		NUTATION RATE (RPM)				MEDIAN AVERAGE			
		(NO.)	(RPM)	200	400	500	600	200	400	500	600	200	400	500	600
(CANT ANGLE = .040 RAD)	4 6000	-	-	-	-	46.1	30.6	-	-	-	-	20.9	20.2		
	5500	-	-	-	-			-	-	-	-				
	5000	-	-	-	-			-	-	-	-				
	4500	74.6	31.6	25.0	21.5			24.3	21.5	-	-				
	4000	48.4	25.5	23.9	20.7			24.2	17.9	-	-				
	3500	33.4	20.2	21.9	19.8			19.8	18.4	19.0	-				
	3000	29.2	17.5	20.0	19.4			14.4	17.5	18.9	14.8				
	2500	32.6	18.1	22.6	21.6			10.5	18.3	19.6	14.5				
	2000	38.1	24.0	23.9	25.3			14.9	21.6	19.4	15.7				
	1500	62.5	35.6	33.2	30.9			24.9	25.1	20.9	17.6				
	1000	-	65.4	-	-			28.0	31.3	28.2	24.9				
500	-	-	-	-			-	-	-	-					
MEDIAN AVERAGE		51.9	41.5	26.6	25.2			19.3	24.4	23.6	19.7				
		45.5	29.7	24.4	22.7			20.1	21.5	21.0	17.5				
		CONING ANGLE = 15 DEGREES						CONING ANGLE = 20 DEGREES							
(CANT ANGLE = .040 RAD)	4 6000	-	-	-	-	14.0	16.0	-	-	-	-	19.3	17.3		
	5500	-	-	-	-			-	-	-	-				
	5000	-	-	-	-			-	-	-	-				
	4500	-	-	-	-			-	-	-	-				
	4000	16.1	-	-	-			19.5	-	-	-				
	3500	18.6	15.2	-	-			17.7	-	-	-				
	3000	18.4	15.3	-	-			16.0	17.9	-	-				
	2500	19.4	16.5	14.4	18.0			15.5	15.4	-	-				
	2000	23.3	18.1	12.2	12.2			17.8	14.4	-	-				
	1500	23.5	18.7	13.1	8.7			19.3	12.3	-	-				
	1000	24.5	18.2	7.6	3.4			26.3	15.3	-	-				
500	-	-	-	-			-	-	-	-					
MEDIAN AVERAGE		20.3	17.0	12.6	10.7			20.9	15.1						
		20.5	17.0	13.0	10.6			18.9	15.1						
		COMPOSITE RESULTS FOR L.R. #4 (INCL. ALL NUTATION RATES, CONING ANGLES AND SPIN RPM'S)													
		MEDIAN		39.0											
		AVERAGE		22.1											

APPENDIX B: CONCEPT TECHNIQUE FOR MEASURING THE CANT-PLANE PHASE ANGLE

Appendix B presents a concept for measuring the phase angle of the cant plane during spin-downs. Figure B1 indicates the major features of a model design that could be used. In addition to being able to measure the phase angle, the loose ring could be fabricated from materials that would have large mass density at the outer rim and low mass density at lesser radii. This composite construction would increase the ratio of axial moment of inertia to the mass of the loose ring and would improve the measurement accuracy of the despin moment.

An electrical commutator technique is indicated for measuring the cant-plane phase angle. The loose ring and tare ring spin-downs would remain the same as before with the exception that the phase angle of the cant plane of the loose ring would be tracked versus spin rate as the model despins. The tare ring, being rigidly fixed to the support shaft, would not have a phase angle associated with it so the phase angle measurement would only be made with a loose ring in place.

An electrically insulated commutator cage would surround the model. The complete commutator assembly would be keyed to spin precisely in phase with the support shaft. It would be constructed to be very rigid and relatively light in weight to optimize the measurement accuracy and to minimize its flywheel effect. However, this flywheel effect would only tend to extend equally the spin-down times of the tare and the loose ring runs, so there would not be a basic problem of measurement accuracy.

Seventy-two upper and 72 lower commutator strips would comprise the phase angle measurement capability. Electrical contact would be made diagonally through the fully canted loose ring or from above to directly below through the loose ring when the loose ring was "hula-hooping". For reference purposes, the commutator segments at zero and 180 degrees would be in the yaw plane. An angular measurement resolution of $\pm 2\text{-}1/2$ degrees would be possible when 72 commutator stations were used around the 360 degree periphery.

The phase-angle data could be recovered by an on-board telemetry link to ground-based instrumentation or, as shown, a series of slip-ring electrical connections could be utilized for the raw data acquisition. This slip-ring system would be composed of rings attached to the spinning model shaft with contacting riders mounted from the "stationary" nutation frame. A second slip-ring system, in series with the above system, would be required to bridge the gap from the nutating frame to the ground-based power supply and receivers. In the latter concept, the ground-based power would be rapidly and repeatedly directed sequentially to all the upper commutator segments and the lower segments would be similarly scanned, both in phase with the power distribution and 180 degrees out of phase with it. The completed circuit would take the commutator identification of the lower segment for the phase angle

measurement and the resulting in-phase or 180 degrees out-of-phase configuration of the scanning arrangement would differentiate between canting and "hula-hooping". The electrical circuit would remain open for any other loose ring activities.

CONCEPT TECHNIQUE FOR MEASURING THE CANT PLANE PHASE ANGLE

<u>Figure</u>		<u>Page</u>
B1	Proposed Model for Measuring Cant Plant Phase Angle . . .	82
B2	Details of Proposed Model	83
B3	Details of Proposed Model	84
B4	Descriptive Details of Proposed Model	85

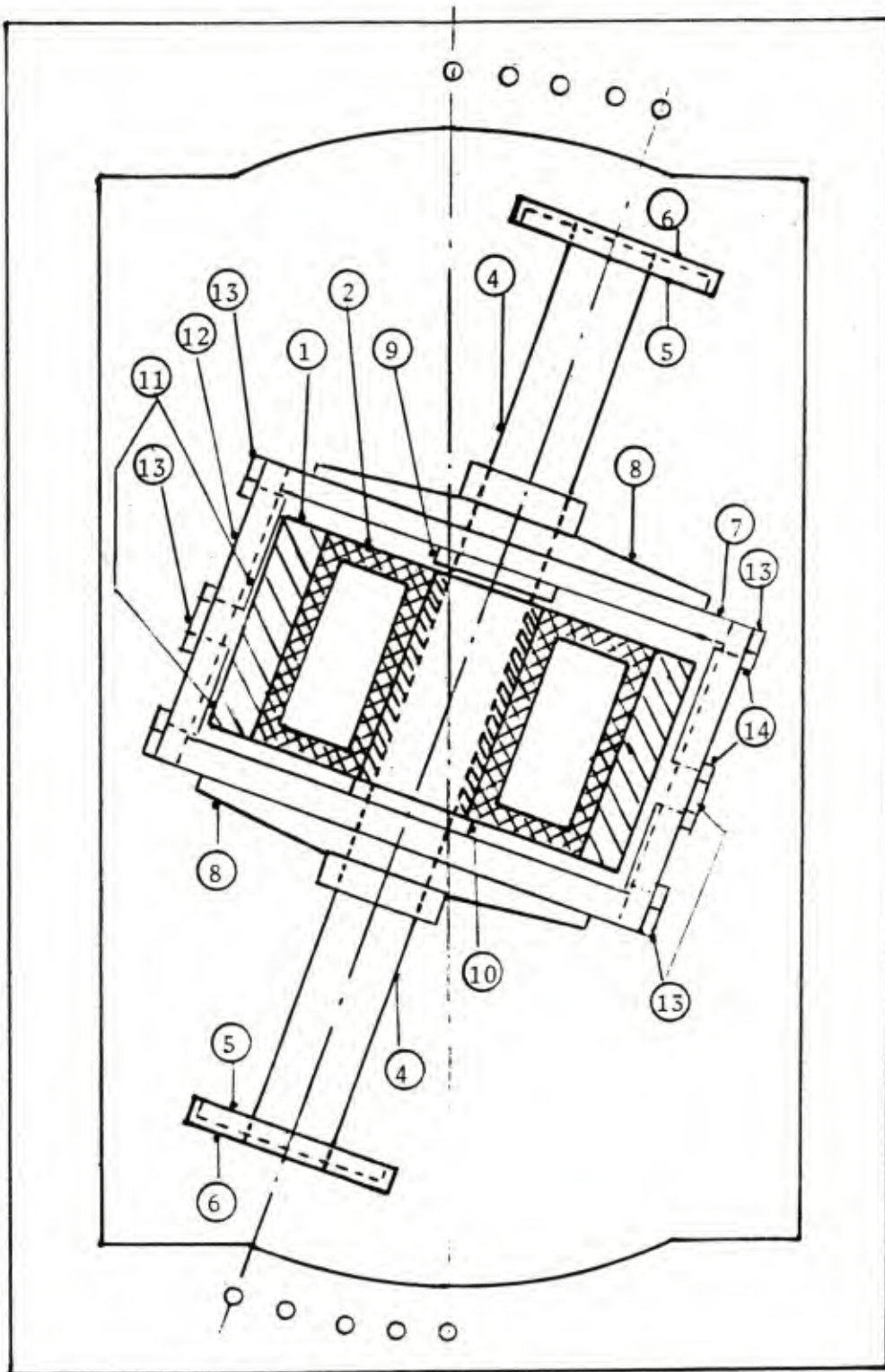
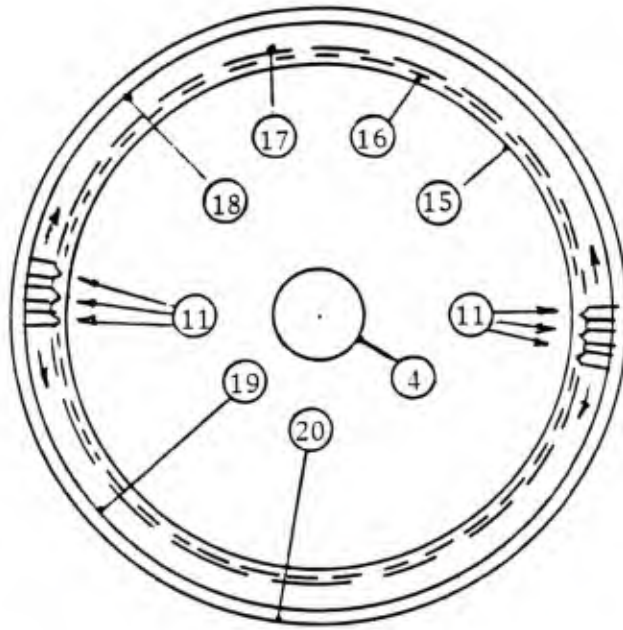
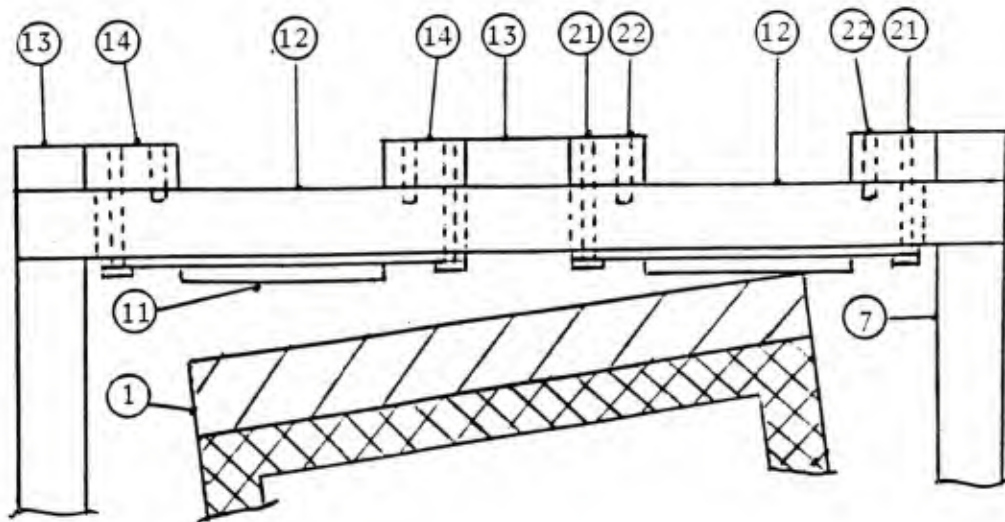


Figure B1. Proposed Model for Measuring Cant Plane Phase Angle



END VIEW OF PROPOSED MODEL



CANTED RING MAKING CONTACT (CANT ANGLE SHOWN EXAGGERATED)

Figure B2. Details of Proposed Model

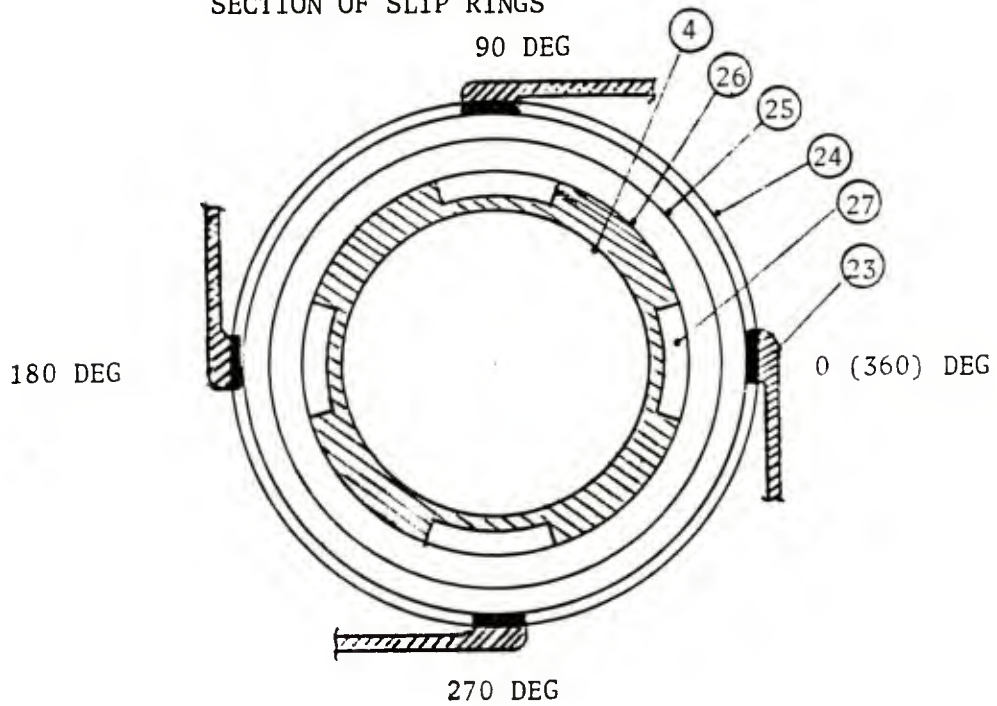
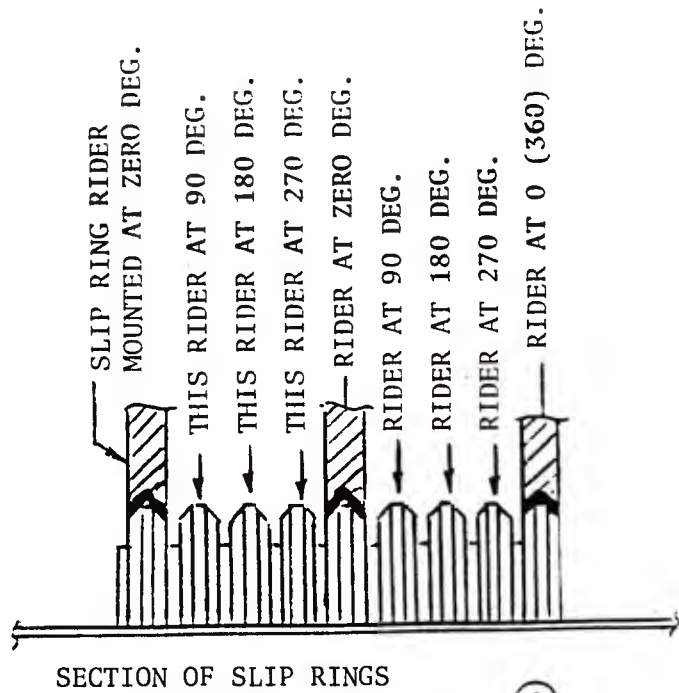


Figure B3. Details of Proposed Model

- ① HEVIMET RIM OF LOOSE RING
- ② HOLLOWED OUT LOOSE RING INTERMEDIATE STRUCTURE
- ③ HARDENED STEEL LOOSE RING BUSHING
- ④ SUPPORT SHAFT
- ⑤ END BELL
- ⑥ END BELL ELECTRICAL INSULATING COVER
- ⑦ HIGH IMPACT STRENGTH PLASTIC END OF COMMUTATOR FRAME
- ⑧ AL. ALLOY SUPPORT FOR ⑦ (FIXES COMMUTATOR RIGIDLY TO SHAFT)
- ⑨ ANTI-CLIMB STOP FOR LOOSE RING (WITH TYPICAL CLEARANCE FOR CANTING)
- ⑩ GRAVITY SUPPORT FOR LOOSE RING (WITH SAWTOOTH SPLINE TO MESH WITH LOOSE RING TO KEEP IT IN SPIN PHASE WITH THE SUPPORT SHAFT)
- ⑪ TYPICAL COMMUTATOR SEGMENT (BRASS)
- ⑫ SLOTTED SHELL OF COMMUTATOR FRAME FOR ACCEPTING ⑪
- ⑬ HIGH STRENGTH STEEL BANDS AROUND ⑫ TO PRECLUDE CENTRIFUGAL STRESS FAILURE OF ⑦ AND ⑫
- ⑭ THREADED PLASTIC BANDS FOR COMMUTATOR ADJUSTMENT SCREWS
- ⑮ EDGE OF LOOSE RING RIM ① (CENTERED NON-CANT CONDITION)
- ⑯ LOCUS OF COMMUTATOR CONTACTS
- ⑰ I.D. OF ⑫
- ⑱ O.D. OF ⑫
- ⑲ I.D. OF ⑬ AND ⑭
- ⑳ O.D. OF ⑬ AND ⑭
- ㉑ TENSION ADJUSTMENT FOR ⑪
- ㉒ COMPRESSION ADJUSTMENT FOR ⑪ (㉑ AND ㉒ COMBINE TO ELIMINATE HYSTERESIS IN ADJUSTED ⑪)
- ㉓ TYPICAL SLIP RING RIDER (MECHANISM ATTACHED TO NUTATION FRAME- DOES NOT SPIN WITH MODEL) BERYLLIUM COPPER OR MANGANESE BRONZE
- ㉔ TYPICAL SLIP RING (ELECTRICAL CONNECTIONS NOT SHOWN)
- ㉕ TYPICAL ELECTRICAL INSULATION BETWEEN ADJACENT ㉔ 's
- ㉖ ELECTRICAL INSULATION BETWEEN ④ AND ㉔
- ㉗ TYPICAL CHANNEL FOR WIRES

Figure B4. Descriptive Details of Proposed Model

DISTRIBUTION LIST

<u>No. of Copies</u>	<u>Organization</u>	<u>No. of Copies</u>	<u>Organization</u>
12	Commander Defense Technical Info Center ATTN: DDC-DDA Cameron Station Alexandria, VA 22314	1	Director US Army Air Mobility Research & Development Laboratory Ames Research Center Moffett Field, CA 94035
1	Commander US Army Materiel Development & Readiness Command ATTN: DRCDMD-ST 5001 Eisenhower Avenue Alexandria, VA 22333	1	Commander US Army Communications Research & Development Command ATTN: DRDCO-PPA-SA Fort Monmouth, NJ 07703
8	Commander US Army Armament Research & Development Command ATTN: DRDAR-TSS (2 cys) DRDAR-LCA-F Mr. D. Mertz Mr. E. Falkowski Mr. A. Loeb Mr. R. Kline Mr. S. Kahn Mr. S. Wasserman Dover, NJ 07801	1	Commander US Army Electronics Research & Development Command Technical Support Activity ATTN: DELSD-L Fort Monmouth, NJ 07703
1	Director US Army ARRADCOM Benet Weapons Laboratory ATTN: DRDAR-LCB-TL Watervliet, NY 12189	4	Commander US Army Missile Command ATTN: DRSMI-R DRSMI-YDL DRSMI-RDK Mr. R. Deep Mr. R. Becht Redstone Arsenal, AL 35809
1	Commander US Army Armament Materiel Readiness Command ATTN: DRSAR-LEP-L, Tech Lib Rock Island, IL 61299	1	Commander US Army Natick Research and Development Command ATTN: DRXRE, Dr. D. Sieling Natick, MA 01762
1	Commander US Army Aviation Research & Development Command ATTN: DRSAV-E P.O. Box 209 St. Louis, MO 63166	1	Commander US Army Tank Automotive Research & Development Command ATTN: DRDTA-UL Warren, MI 48090
		1	Commander US Army Research Office P.O. Box 12211 Research Triangle Park, NC 27709

DISTRIBUTION LIST

<u>No. of Copies</u>	<u>Organization</u>
1	Director US Army TRADOC Systems Analysis Activity ATTN: ATAA-SL, Tech Lib White Sands Missile Range NM 88002
1	Commander Naval Air Systems Command ATTN: AIR-604 Washington, DC 20360
1	Commander Naval Weapons Center ATTN: Technical Library China Lake, CA 93555
1	Director NASA Langley Research Center ATTN: MS-185, Tech Lib Langley Station Hampton, VA 23365
1	Director NASA Ames Research Center ATTN: MS-202, Tech Lib Moffett Field, CA 94035

Aberdeen Proving Ground

Director, USAMSAA
ATTN: DRXS-D
DRXS-MP, H. Cohen
Cdr, USATECOM
ATTN: DRSTE-TO-F
Dir, Wpns Sys Concepts Team
Bldg E3516, EA
ATTN: DRDAR-ACW
Mr. M. Miller
Mr. A. Flatau
CSL, Biophysics Lab.
ATTN: Dr.W. Sacco
Bldg E3160, EA

USER EVALUATION OF REPORT

Please take a few minutes to answer the questions below; tear out this sheet and return it to Director, US Army Ballistic Research Laboratory, ARRADCOM, ATTN: DRDAR-TSB, Aberdeen Proving Ground, Maryland 21005. Your comments will provide us with information for improving future reports.

1. BRL Report Number _____

2. Does this report satisfy a need? (Comment on purpose, related project, or other area of interest for which report will be used.)

3. How, specifically, is the report being used? (Information source, design data or procedure, management procedure, source of ideas, etc.) _____

4. Has the information in this report led to any quantitative savings as far as man-hours/contract dollars saved, operating costs avoided, efficiencies achieved, etc.? If so, please elaborate.

5. General Comments (Indicate what you think should be changed to make this report and future reports of this type more responsive to your needs, more usable, improve readability, etc.) _____

6. If you would like to be contacted by the personnel who prepared this report to raise specific questions or discuss the topic, please fill in the following information.

Name: _____

Telephone Number: _____

Organization Address: _____

